Identification of Factors Governing Chiral Resolution of 1-Phenylethylamine and Few Amino alcohols Using Metallo-organic Host

A
Thesis Submitted
In Partial Fulfilment of the Requirement
For the degree of

DOCTOR OF PHOLISOPHY

By

CHANDANI RANI DAS

Department of Chemistry
Indian Institute of Technology Guwahati
Guwahati- 781039
March 2015

Identification of Factors Governing Chiral Resolution of 1-Phenylethylamine and Few Amino alcohols Using Metallo-organic Host

A
Thesis Submitted
In Partial Fulfilment of the Requirement
For the degree of

DOCTOR OF PHOLISOPHY

By

CHANDANI RANI DAS

Department of Chemistry
Indian Institute of Technology Guwahati
Guwahati- 781039
March 2015

Dedicated to My Parents

INDIAN INSTITUTE OF TECHNOLOGY, GUWAHATI

Department of Chemistry

STATEMENT

I do hereby declare that the matter embodied in this thesis is the result of investigations carried out by me in the Department of Chemistry, Indian Institute of Technology Guwahati, India under the guidance of Dr. Manabendra Ray, Professor, Department of Chemistry, Indian Institute of Technology Guwahati, India.

In keeping with the general practice of reporting scientific observations, due acknowledgements have been made wherever the work described is based on the findings of other investigators.

January, 2016 (Chandani Rani Das)

I.I.T. Guwahati

INDIAN INSTITUTE OF TECHNOLOGY GUWAHATI

Department of Chemistry

CERTIFICATE

This is to certify that Chandani Rani Das has been working under my supervision since December, 2010 as a regular registered Ph. D. student. I am forwarding her thesis entitled "**Identification of Factors Governing Chiral Resolution of 1-Phenylethylamine and Few Amino alcohols Using Metallo-organic Host"** being submitted for the Ph. D. (Science) Degree of this Institute. I certify that she has fulfilled all the requirements according to the rules of this institute regarding the investigations embodied in her thesis and this work has not been submitted elsewhere for a degree.

January, 2016 (Dr. Manabendra Ray)

I.I.T. Guwahati Supervisor

INDIAN INSTITUTE OF TECHNOLOGY, GUWAHATI

Department of Chemistry

CERTIFICATE OF COURSE WORK

This is to certify that Chandani Rani Das has satisfactorily completed all the courses required for the Ph.D degree program. These courses include

CH 611:	Bioinorganic Chemistry
CH 623:	Chemistry of Biological Macromolecules
CH 632:	Chemical Applications of Group Theory
CH 639:	Principles and Applications of Molecular Fluorescence

Chandani Rani Das has successfully completed her Ph.D qualifying examination in November, 2011.

Prof. B.K. Patel
Head, Department of Chemistry
I. I. T. Guwahati

Dr. S. S. Bag
Secretary, DPPC
I. I. T. Guwahati

Acknowledgements

At the very outset I take opportunity to express my deep sense of gratitude to my Ph.D. supervisor Prof. Manabendra Ray, Department of Chemistry, IIT Guwahati for his able guidance, tireless efforts, constant encouragements and moral supports at each and every step of my research work, which enable me to complete my thesis work. I am fortunate enough to have his teaching about how to cultivate scientific thoughts.

I would like to acknowledge my sincere gratitude to all my doctoral committee members, Prof. Gopal Das, Prof. V.Manivannan and Dr. Chandan Mukherjee for their insightful advices and valuable suggestions.

I am grateful to Professor Prof. Arun Chatyopadhyaya and Prof. B.K. patel, Head, Department of Chemistry, IIT Guwahati for their valuable suggestions and providing good research environment.

I am thankful to the Institute, Indian Institute of Technology Guwahati for providing me with the state of the art infrastructure and facilities for advanced research.

I also express my sincere thanks to all faculty members, Department of Chemistry, IIT Guwahati for their help and encouragement.

I am grateful to all non-teaching staffs of the Department for their technical support.

I would like to thank DST under FIST program for providing single crystal XRD instrument facility and B. Das for mounting and solving the crystal.

My sincere thanks to Chandan Borgohain, K. Senapati and Shing of Central Instruments facility, IIT Guwahati for their help in all the characterizations (NMR , ESI-Ms, EPR, XRD) required during my research work.

I wish to show my gratitude to Prof. P. Banarjee (IACS) for celemental analysis (CHN).

I would like to thank my former and present group members Dr. Mrigendra Dubey, Dr. S. S. Faizi and C. M. Rajesh for their timely help, support and for the wonderful time we shared during this period.

I extend my sincerest special thanks to Sangeeta, Arghya Basu, Chirantan kar, Barun, Rajen and Samir and I also take this opportunity to thank aditidi, Pallabda, Hemanta, Najbul and Rituparna for their constant help, motivation, enthusiastic company and all the wonderful time we spent in various events.

I am thankful to all research scholars and M.Sc students, Department of Chemistry, IIT Guwahati for their help.

The financial support from Council of Scientific and Industrial Research (CSIR), New Delhi in the form of JRF and SRF is duly acknowledged.

I wish to express my sincere gratitude to my brothers and sisters for their constant unfailing support.

At last but not least, I want to express my sincere thanks to all of my family members, especially my parents, for their constant encouragements and moral supports during my research work. They are the main soul and inspiration for each and every step that I achieve in my life.

Chandani Rani Das

Abstract

In this thesis, we have attempted to isolate and estimate the contribution of individual factors responsible for chiral recognition of amine and amino alcohols using binuclear Ni(II) metalloorgaic host. During the course, by changing the host (histidine and methionine derived ligand) and guest (aryl amine and several amino alcohols) we have explored the effects on recognition pathway through crystallization. In this thesis, we have not only unraveled the relative contribution of crystallization, solution equilibrium and the diastereomer solubility but also been successful in effective separation of several biogenic amino alcohols.

The thesis has been divided into five chapters. Chapter wise summery of the work is given below.

Chapter 1. *Introduction*

In this chapter, we have discussed the general requirements for recognition, three point recognition model, other models and up-to-date literature on status of chiral recognition using organic and metallo-organic hosts, where structural characterization of host-guest adduct has been performed.

Chapter 2. *Crystallinity vs Solution equilibrium*

Earlier work from our group showed that a binuclear Ni(II) complex synthesized from a L-Histidine derivative, separates simple chiral amino alcohol during crystallization. As the separation was through crystallization we expected it to be influenced by both solution equilibrium favoring one enantiomer (recognition in solution) and properties of crystal such as solubility of one diastereoisomer over the other. We chose to explore the recognition of a chiral amine, 1-phenylethylamine, using the same L-histidine derived binuclear host. By using amine, lacking the H-bond capable alcoholic -OH, we thought to reduce the recognition in solution. We surmised that this would enable us to have better understanding of the effect of crystallization on the chiral recognition. The protocol used are the following: (a) Free amines were isolated from the crystals and were subjected to HPLC analysis using chiral column,

(b) The diastereoisomer distribution in the solution were estimated by first precipitating the host-guest complex without crystallization followed by isolation of free amine and determination of chiral distribution using HPLC. Results showed that both the enantiomer of amine were distributed as ~1:1 in amorphous precipitate whereas crystals contained 65:35 (30% enantiomeric excess of *S*-isomer). Thus crystallization indeed was responsible for the observed enhancement in this case. Structural characterization of the pure diastereoisomers and the crystals from racemic mixture were done and compared (Figure 2b). The solubility of the diastereoisomers was determined. Comparison of structural data along with the solubility differences led us to conclude that the difference in structural organization and the solubility difference played important role in the chiral enhancement.

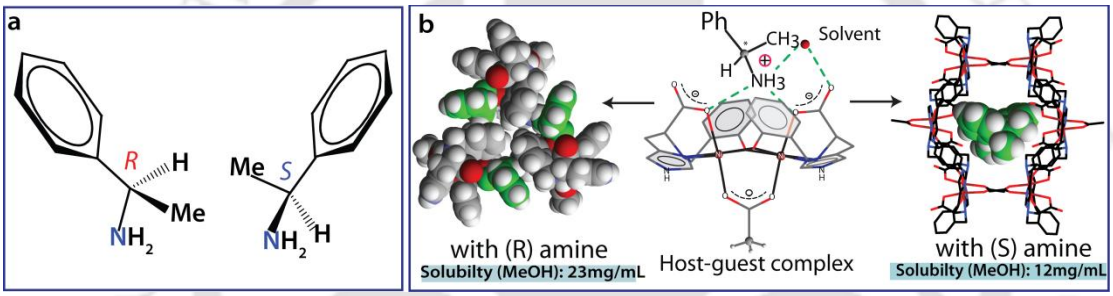

Figure 1. (a) 1-phenylethylamine used as guest amine. (b) Space-fill model of host-guest complex showing trinuclear assembly from *R*-amine and 1D channel from *S*-amine present in crystal lattice.

Chapter 3. *Change in crystallization pathway by modifying cavity*

In the previous chapter, we have concluded that the significant structural differences between diastereoisomers and difference in solubility played important role in the observed chiral enhancement. We have also noticed that stronger H-bond between imidazole (from histidine) and carboxylate in the host-guest adducts might have played major role creating the differences. In this chapter, we have used a newly synthesized binuclear complex with L-Methionine derived ligand as host and retained the same 1-phenylethylamine as guest. The new host, nearly identical in every way with the L-Histidine analogue, differs by the absence of imidazole group necessary to form strong H-bonding network (Figure 3a).

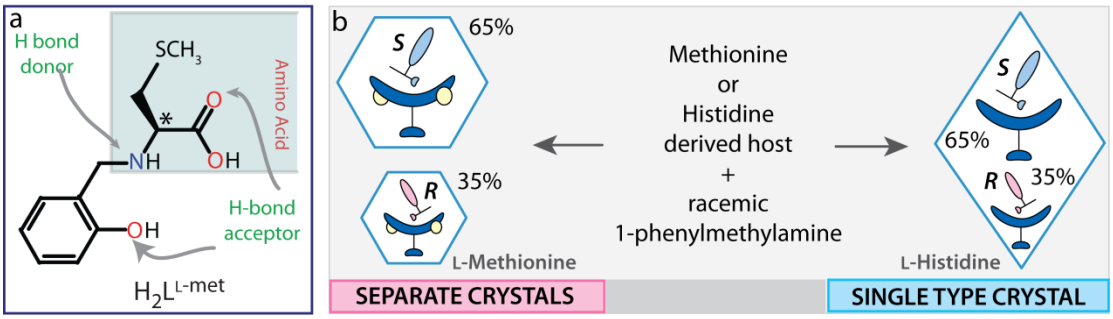

Figure 3. (a) L-methionine derived reduced Schiff base ligand used for synthesis of host. (b) Crystallization between two hosts showing major difference by two-dimensional cartoon representation.

Following the similar protocol used in the previous chapter, we found that the stronger imidazole-carboxylate H-bonded (length) network has been replaced by relatively weaker amine-carboxylate (length) network. Structural and solubility differences between diastereoisomer significantly were reduced.

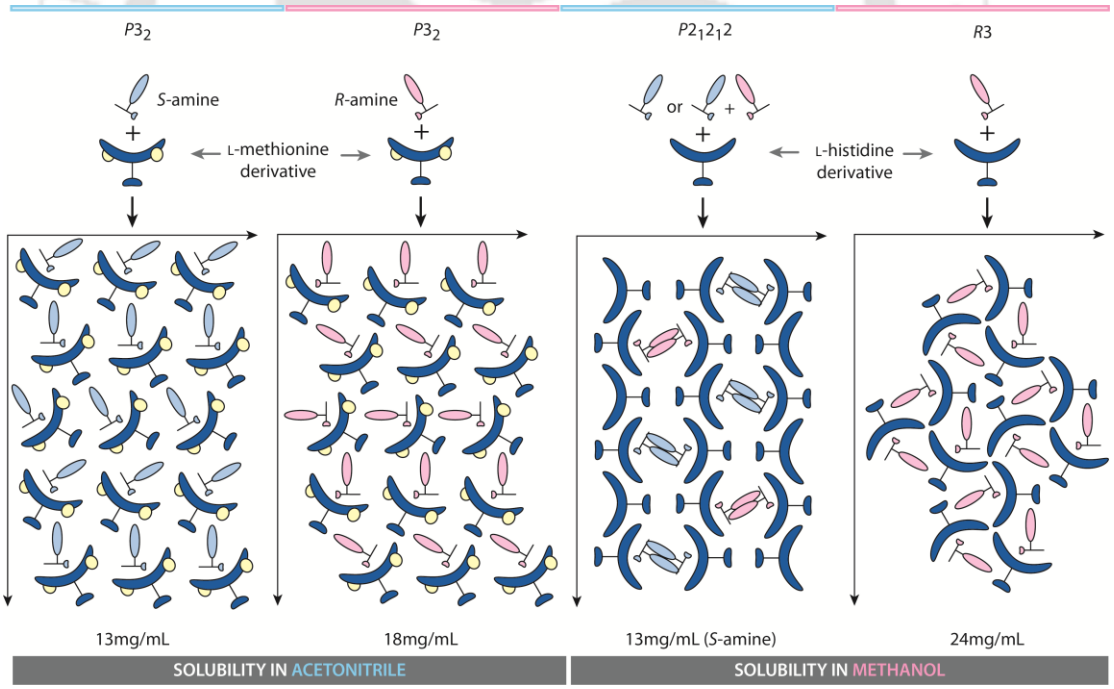

Figure 4. The differences and similarities between diastereomers for both the hosts are highlighted by two-dimensional cartoon representation of the crystal lattices.

While chiral enhancement remained same at 30% *ee*, few significant differences occurred in the crystallization process: (a) we observed formation of conglomerate *i.e.* both individual diastereoisomer in the isolated crystals instead of a single type of crystal (Figure 3b) and seeding effect observed earlier was absent.

The results in this chapter highlighted the intricate nature of the resolution through crystallization where a subtle change in the host can modify the crystallization pathway (Figure 4).

Chapter 4. *Separation of Biogenic amino alcohols*

In order to check the behavior of this new L-methionine derived host with amino alcohols and to evaluate the practicality of this method in chiral separation, we used two biogenic amino alcohols, 2-amino-1-phenylethanol and norfenefrine as guest. Both 2-amino-1-phenylethanol and norfenefrine are structurally related to noradrenaline (Figure 5a). Norfenefrine or 3-octopamine is an adrenergic agent. Previously, L-histidine derived host showed better resolution in case of two simple amino alcohols, namely 1-amino-2-propanol and 2-amino-1-propanol.[4] Use of L-histidine derived host did not resulted either crystal or well characterized solid with 2-amino-1-phenylethanol and norfenefrine. Results in this chapter: (*R*)-(−)-2-Amino-1-phenylethanol and (*R*)-Norphenylephrine were recognized and separated from racemic mixture with 92% *ee* (yield, 80%) and 94%*ee* (yield, 80%) respectively. Use of D-methionine derived ligand resulted in isolation of (*S*)-(+)-2-Amino-1-phenylethanol in 86% *ee* (yield, 86%) and (*S*)- norphenylephrine in 92% *ee* (yield, 85%) respectively (Figure 5b).

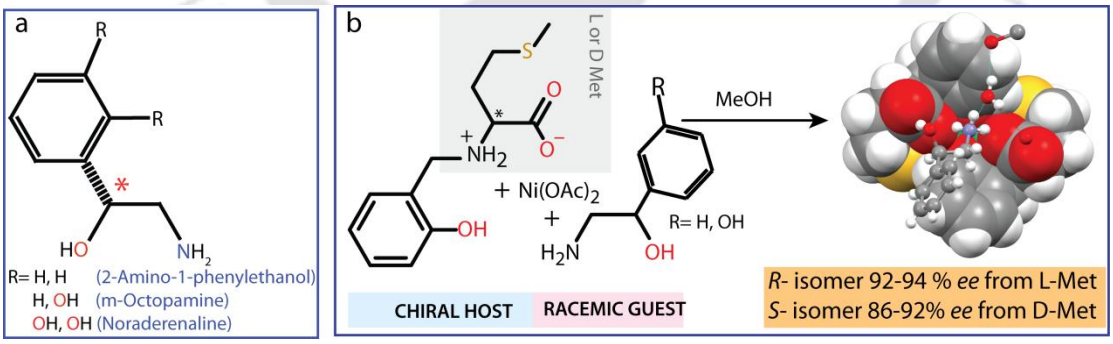

Figure 5. (a) Biogenic amino alcohols used as guest for chiral separation. (b) Schematic representation of direct synthesis of bi nuclear Ni(II) complex with guest amino alcohol.

Further, scalability of this method was tested by starting from 1 g of ligand and 0.568 g of racemic amine and we were able to isolate 0.144 g of the isomer (*R*, yield, 50%, 90% *ee*). We have compared the present metallorganic host design with known organic only design effective for these amino alcohols and found these

binuclear hosts are equally effective in terms of resolution and yield. All the host-guest adducts were structurally characterized.

Chapter 5. *Few more examples and identification of the factors*

In order to increase the number of examples in different categories, we have further tested the methionine host with few more amino alcohols following the same protocol from previous chapters. We then compared the structural features of all the isolated host-guest complexes and compared.

In general, chiral enhancement is contributed by both solution enhancement as well as crystallization. Solution enhancement has been estimated by forced precipitation of host-guest adducts followed by isolation of guest and subsequent HPLC experiments. (i) In 1-phenylethylamine, using both hosts, the solution enhancement was negligible (0-4% *ee*). Thus the enhancement of 30% *ee*, observed after crystallization was primarily occurred during crystallization (Scheme 1). (ii) In amino alcohols, solution enhancement is widely varied between 15-70%ee. Curiously, two amino alcohols with phenyl ring showed much higher solution enhancement (70% *ee*) than the three amino alcohols without phenyl ring (15-25% *ee*). However, all amino alcohols showed higher enhancement of 68-100% *ee* after crystallization compared to 1-phenylethylamine. Thus in case of amino alcohols, both solution enhancement and crystallization contributed to the final observed enhancement. (iii) Diastereomer solubility must have played an important role in chiral enhancement during crystallization. In seven out of eight cases tested with amino alcohols, very high solubility of one of the diastereoisomer prevented its isolation as solid, even when attempted with pure enantiomer. With 1-phenylethylamine, using both host and 2-amino-1-propanol with methionine derived host, both diastereomers could be isolated and crystallized using pure enantiomer of the guest. Solubility of diastereomer pairs was measured and compared. When these were tested with racemic guest, the isolated host-guest adduct showed chiral enhancement of the diastereoisomer having the lower solubility. Thus in almost all the case, diastereomer with lower solubility determined the chirality of the isolated amine.

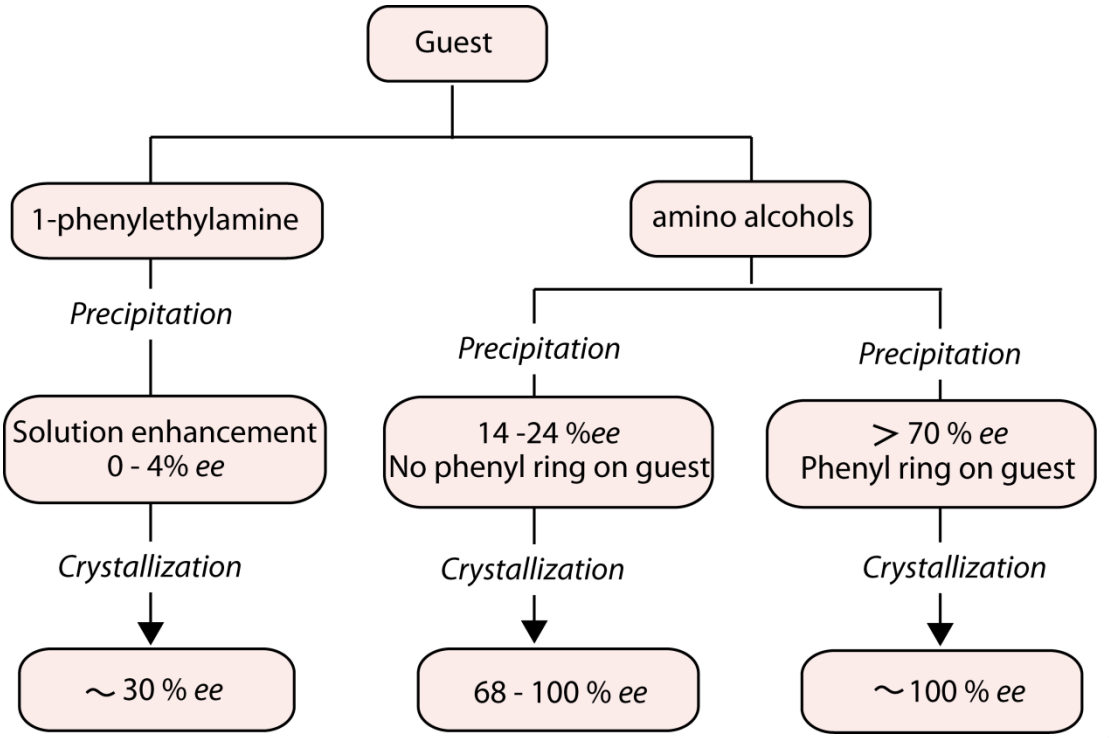

Scheme 1. Schematic representation of observations on chiral enhancement of amine and amino alcohols by two binuclear hosts.

This is true for both the binuclear host. (iv) The amino alcohols were chosen to have chiral centre either near amine or near alcohol group. In general, amino alcohols with chiral centre near alcohol group seems to show consistently better resolution (98-100% *ee*) compared to the ones with chiral centre near amine (68-90% *ee*). However, number of examples is still few thus difficult to make a generalization. This is just an observation. (v) The role of water was found to be assistive, used to fill the space between host and guest through H-bonding.

Contents

Chapter-1

Introduction

Chirality is "handedness," - that is, the existence of left/right opposition. The term Chiral apparently was coined by Lord Kelvin on Molecular Dynamics and the Wave Theory of Light in which he stated -"*I call any geometrical figure, or group of points, chiral, and say it has chirality, if its image in a plane mirror, ideally realized, cannot be brought to coincide with itself*".[1] Pair of molecule which are mirror images to each other but not super imposable with each other are called Enantiomer.[2] Chiral recognition is the preferential binding of one of the enantiomer over its mirror image isomer by a molecule or chemical entity functioning as molecular receptor. In living organisms, this process occurs frequently by proteins, enzymes and drug receptors.

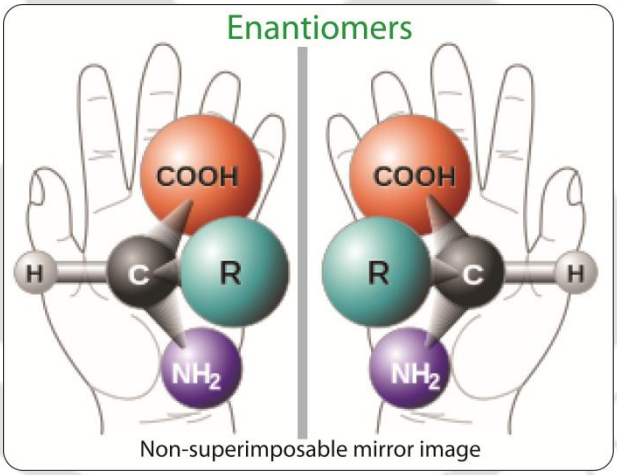

Figure 1.1 Example of chiral molecule showing two enantiomer of generic amino acid

Chirality of chemical substances is ubiquitous in nature, and the essential substances that form living organisms such as amino acids or sugars are chiral and usually exist as pure enantiomeric forms.[3] Chiral recognition utilizing non-covalent interactions is relevant for both biological recognition and resolution of chiral drugs as many of which show different biochemical activity depending on the particular enantiomer (Table 1.1).[4] Understanding of the chiral recognition of small molecule

with laboratory synthesized chiral host / receptor can be helpful in understanding the recognition process in living systems.

The chiral recognition efficiency is characterised by the selectivity with which a chiral host molecule can form a complex with a chiral guest, which involves a subtle balance between several intermolecular forces. Molecular recognition results because of the differences in Gibbs free energy between the two diastereoisomeric enantiomer-selector complexes.[5]

Table 1.1 Molecules showing different activity depending on chirality.

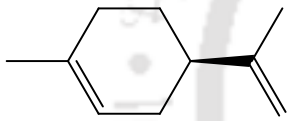 *R*-(+)-Limonene 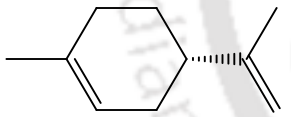 *S*-(-)-Limonene	Orange smell Lemon smell	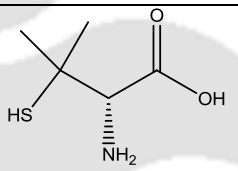 D-penicillamine 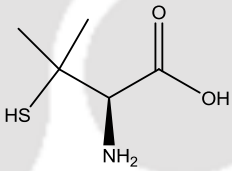 L-penicillamine	Anti-arthritic agent Toxic
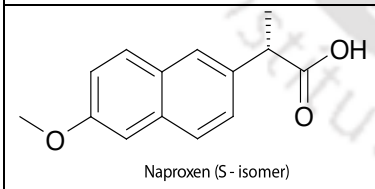 Naproxen (S - isomer)	Anti-inflammatory *S*-isomer is 28 times more active	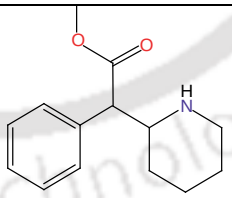 Methylphenidate	Attention deficiency disorder D-isomer is 13 times more active

Several models have been proposed to account for the selectivity of molecular recognition. Empirical models have been proposed first, like the ‘‘lock and key’’ (Figure 1.2a) image proposed by Fischer[6a] or the ‘‘induced fit’’ model[6b]. In this

model, the active site of the host moulds itself around the substrate for an effective fit. This target-assisted shape adjustment helps explain the specificity of enzymatic reactions or complex formation. In 1933, L. H. Easson and E. Stedman formulated the "three point contact rule" for chiral recognition.[6c-f] Simple chiral organic molecule must possess at least one chiral centre. The key points in the three-point interaction model are that at least three simultaneous interactions are required and they should occur with three different substituents attached to the stereogenic center. The model explains the differential binding of the two enantiomers to a chiral three-point site on the selector. Figure 1.2b shows that one enantiomer can present three substituents to match the selector's three-point site. No matter how its mirror image rotates, the enantiomer can match a maximum of only two sites (Figure 1.2b).[5a, 6g] Later on, for a π-complex selectors having large and rigid aromatic associations may discriminate between two similarly rigid chiral molecules through a pseudo-two point interaction model.[7]

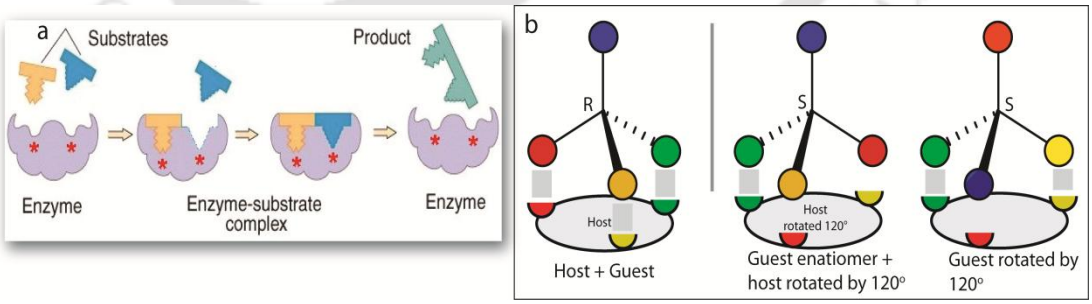

Figure 1.2 Cartoon representation of "lock and key" model (a) and "three point contact rule" model showing three point interactions with host for both enantiomers not possible (b).

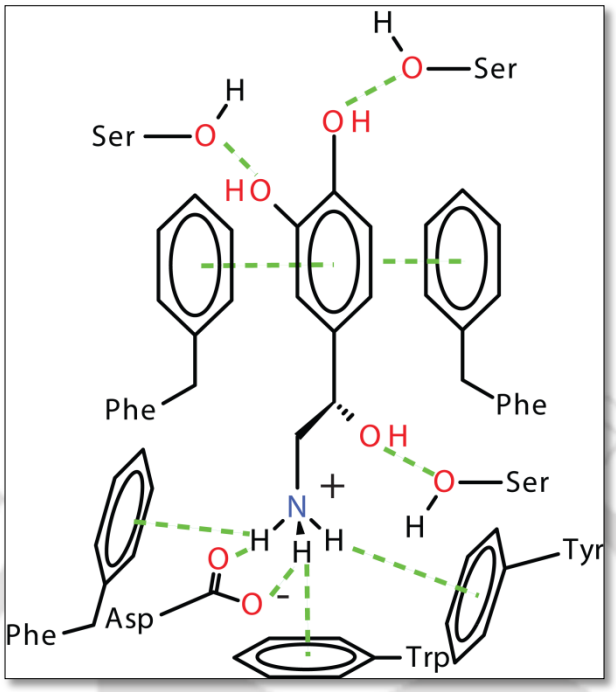

Figure 1.3 Non-covalent interactions between noradrenaline and the β-adregenic receptor

In host-guest complexation, there are four commonly mentioned types of non-covalent interactions.[8] hydrogen bonds, ionic bonds, van der Waals forces, and hydrophobic interaction which are responsible for the three-dimensional structure of large molecules, such as protein. Recognition of the groups in biological receptor often uses multiple non-covalent interactions as observed in case of adrenaline receptor (Figure 1.3).[9]

Utilizing the non-covalent interaction recognition and separation of enantiomers using synthesized hosts has been approached from diverse angle including macrocyclic receptor. (Table 1.2)[10]

While separation using chiral adsorbent as stationary phase[11] has been progressed substantially, the understanding of recognition at the molecular level is limited to molecular modelling due to the difficulty in structural characterization of large

organic. For example, in a notable work Kubo and co-workers showed chirality of an amino alcohol showed different colour upon addition to a large chiral host (Table 1.2, Figure B). While the receptor has been characterized using NMR, the mechanism of the recognition was proposed based on the molecular modelling.

In other examples, using few rigid metallorganic frameworks (MOF) having homochiral porous channel, chiral hydrophobic cavity or chiral capsule has been used for asymmetric catalysis reaction or recognition of one amino acid or peptide (Table 1.3).[12] In most cases, although stereo-selectivity has been enhanced due to the additional interaction with the cavity wall, structural characterization for understanding mechanism was not possible. Recently, Yong Cui and co-worker designed and structurally characterized a homochiral quadruple-stranded helicate cages from metallosalens (Table 1.3, figure **A**) and demonstrated the recognition ability of the cage towards chiral amine and alcohol, where % of resolution was limited up-to 25% *ee*.

Low-molecular weight rigid host would, in principle, facilitate structural characterization but it is challenging to accommodate three different recognition sites within a small host. Utilizing a chiral Co(III) complex, Kim and Co-workers showed for the first time that it was possible to study molecular recognition mechanism in a structurally characterized host-guest adduct owing to the rigidity. But in the isolated crystals of Co(III) complex with the tetradantate ligand, both D- and L-alanine was in ratio 70:30 (Table 1.4, Figure **A**). After that, there are very few examples where chiral recognition of small molecules has been obtained by formation of well characterized metal coordinated assembly (Table 1.4).[13]

Table 1.2 Selected examples of organic receptor used for chiral recognition.

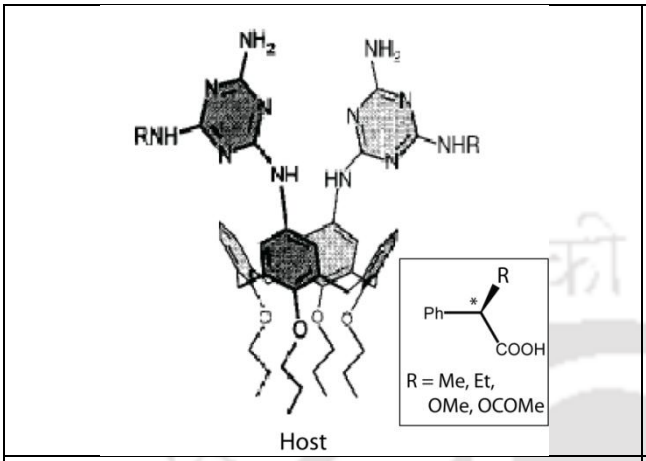	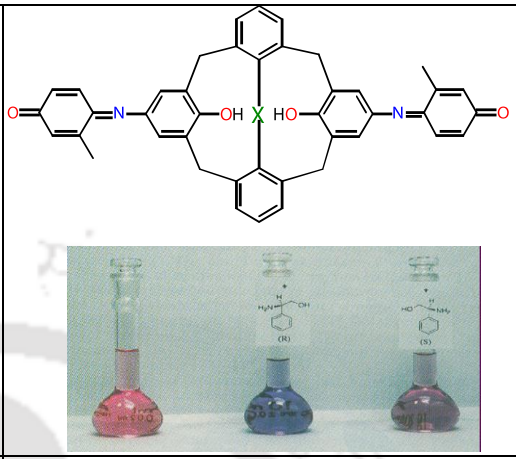
Angew. Chem. Int. Ed. **2002**, *41*, 1924. (**A**)	*Nature*, **1996**, 382.(**B**)
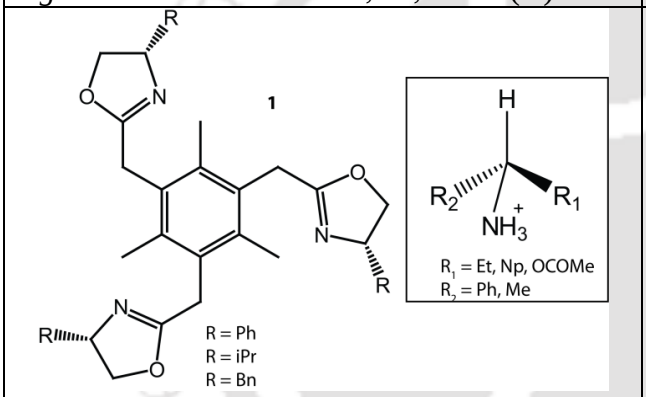	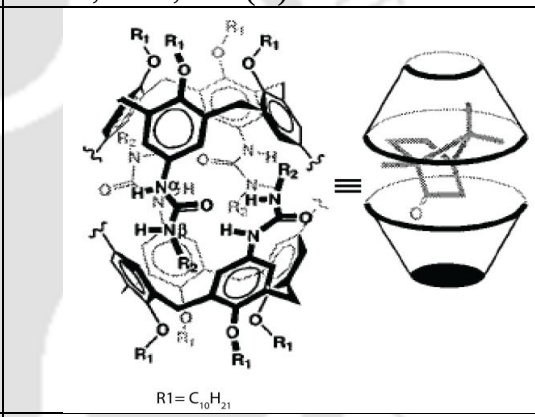
J. Am. Chem. Soc. **2002**, *124*, 591.(**C**)	*J. Am. Chem. Soc.* **1997**, 119, 12671.(**D**)
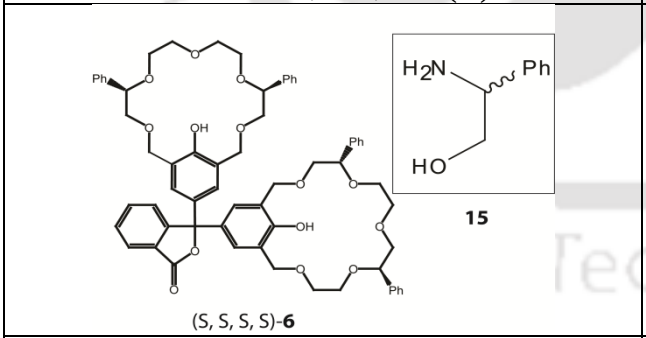	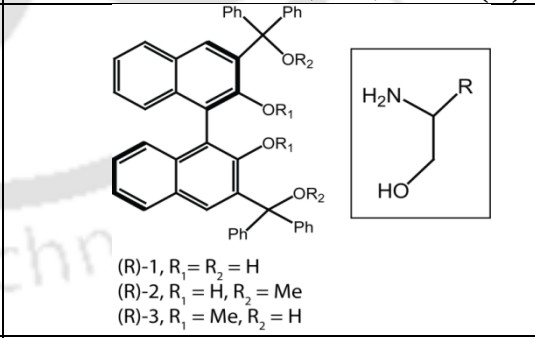
J. Org. Chem. **2005**, *70*, 4609.(**F**)	*J. Org. Chem.* **2007**, *72*, 97. (**G**)
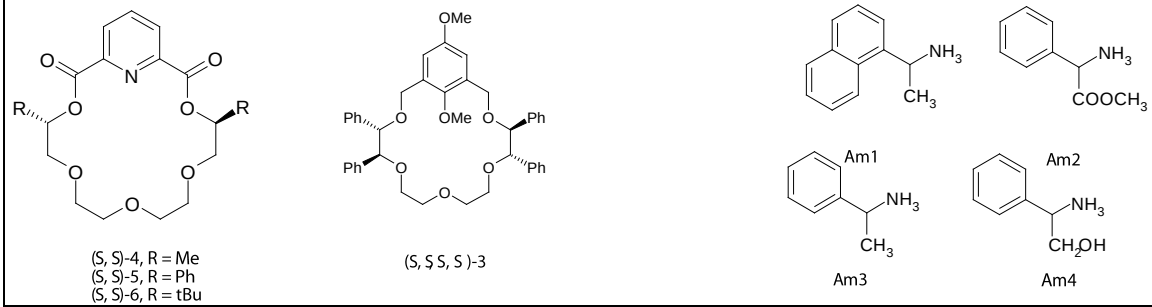	
Chem, Rev. **1997**, *97*, 3319. (**H**)	

Table 1.3 Selected Examples of MOF based receptor for chiral recognition.

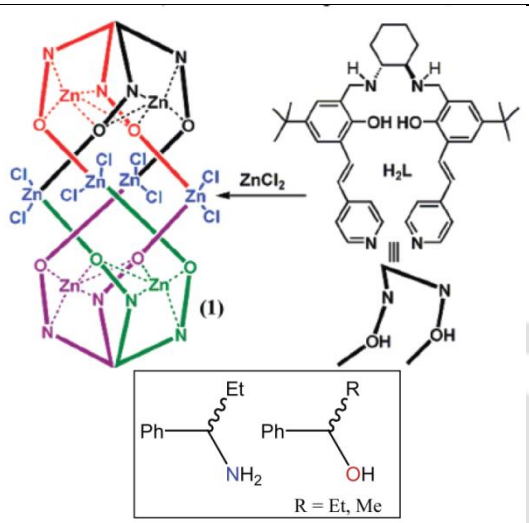

J. Am. Chem. Soc. **2012**, *134*, 6940.(**A**)

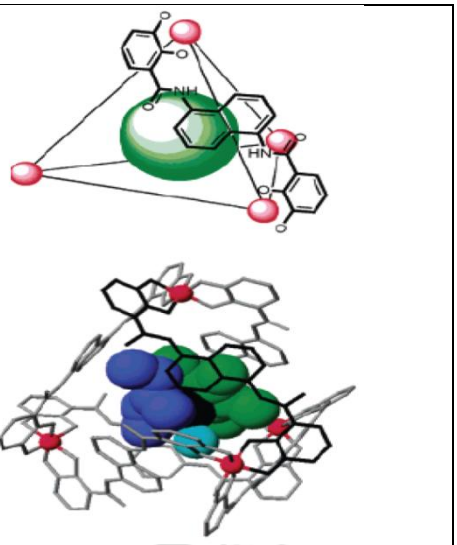

J. Am. Chem. Soc. **2004**, *126*, 3674.(**B**)

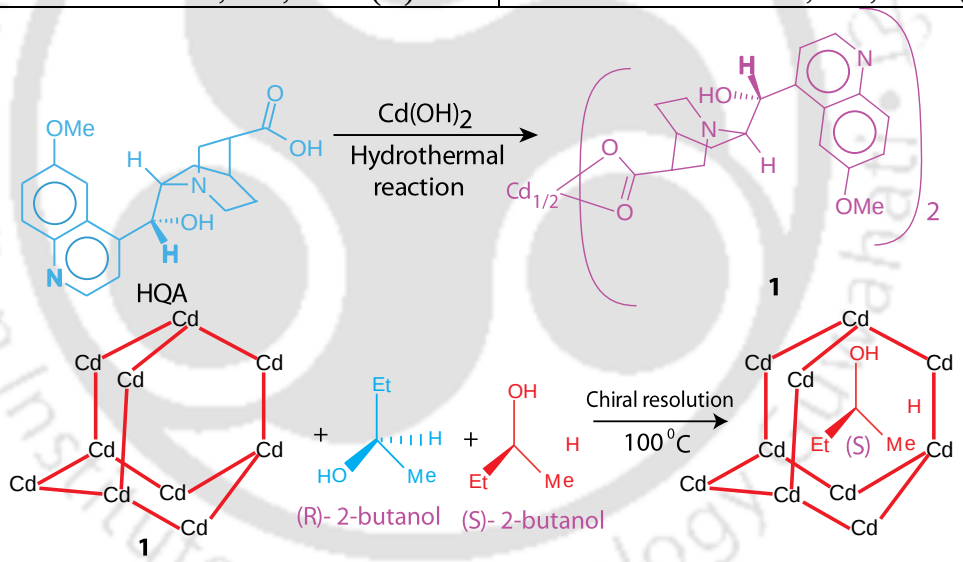

Angew. Chem. Int. Ed. **2001**, *113*, 4554. (**C**)

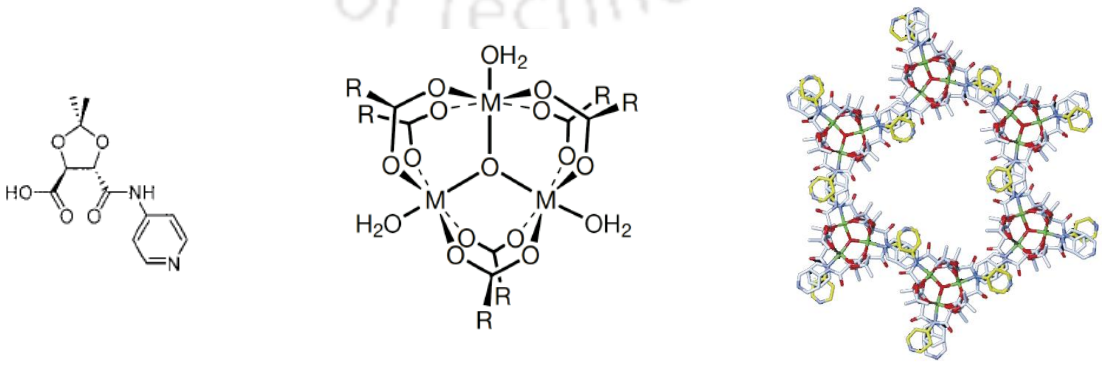

Nature **2000**, *404*, 982. (**D**)

In most of the discussed examples, information on chiral recognition mechanisms is obtained by measuring the binding energy of the two chiral-selector–enantiomer complexes by. Spectroscopic methods or the structural properties by can work with the chiral Circular Dichroism, optical rotatory dispersion method and NMR titration method. X-ray crystallography is a powerful technique for investigating the absolute configuration of diastereoisomeric complexes in the solid state.[5a]

Despite advent of multiple chromatographic techniques, chiral separation through crystallization[14] and co-crystallization[14e-f] remaining one of the more efficient techniques in terms of scale and practicality provided a chiral resolver exist for the purpose. At first, in the mid of 19th century L. Pasteur employed crystallization method for manual separation of tartaric acid as sodium ammonium-tatarate salt from racemic mixture.[15] Traditionally, limited numbers of organic chiral molecules as resolving agent are commercially available and have been used as chiral resolver (Table 1.5).[16] Choosing and screening of appropriate resolving agent for diastereomric salt formation through crystallization is time consuming, tedious and labour-intensive.

Table 1.4 Examples of chiral recognition utilizing co-ordinated metal complexes.

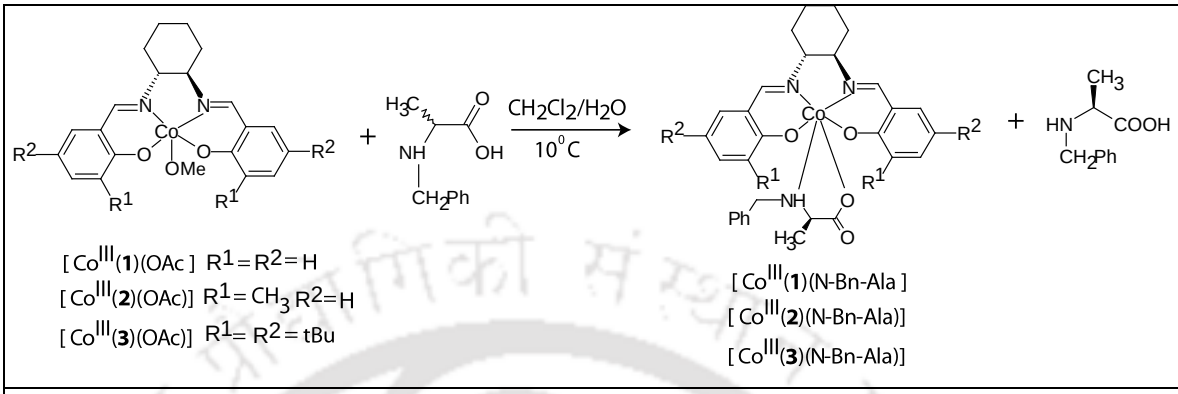

Angew. Chem. Int. Ed. **2006**, *45*, 2449. (**A**)

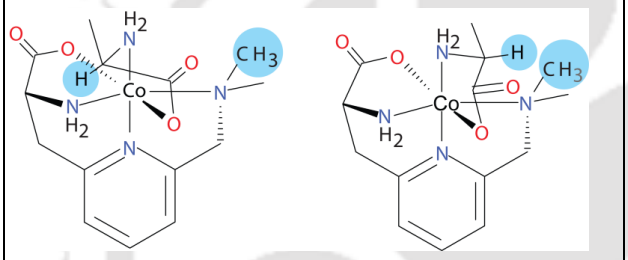

Nature 401, 254. (**B**)

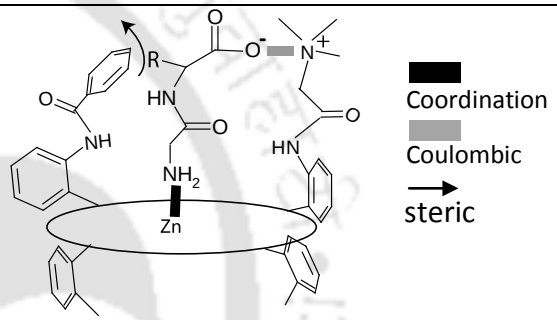

Inorg. Chem. **2004**, *43*, 1211. (**C**)

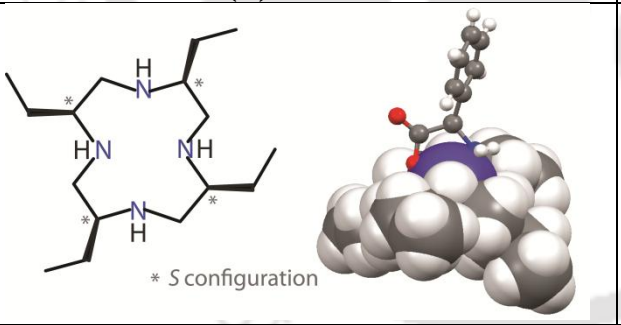

Inorg. Chem. **2011**, *50*, 4.(**E**)

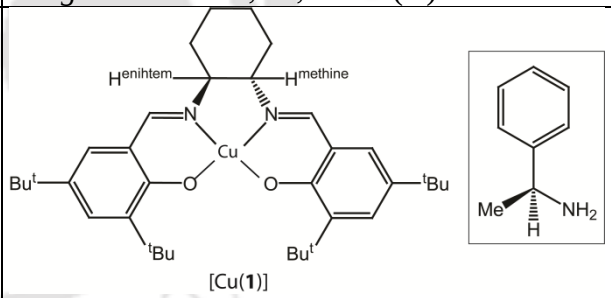

Inorg. Chem. **2011**, *50*, 6944.(**F**)

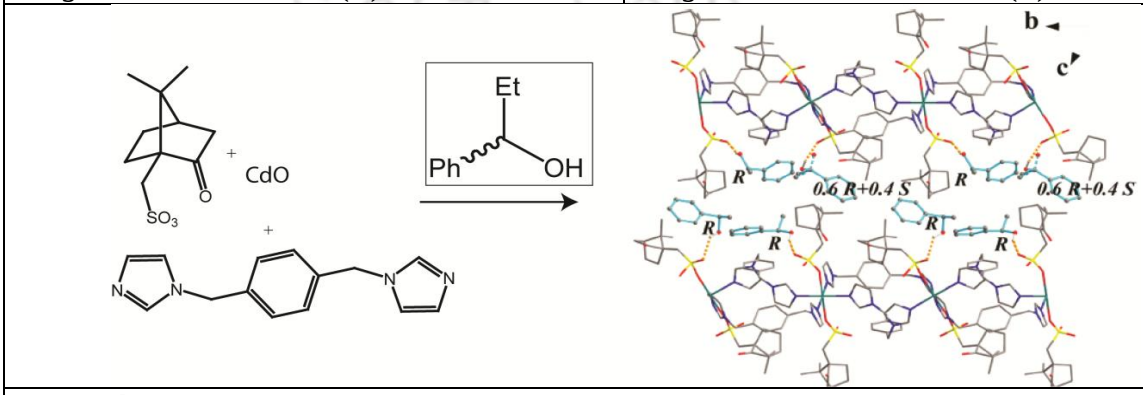

Inorg. Chem., **2013**, *52*, 11694.(**D**)

Table 1.5 Commonly used resolving agents.

Acids	Bases
Tartaric acid (+) (-)	1-phenylethylamine (+) (-)
Dibenzoyl tartaric acid (+) (-)	Ephedrine (+) (-)
Mandelic acid (+) (-)	2-amino-1-butanol (+) (-)
Camphoric acid (+) (-)	Quinine (+)
Malic acid (+) (-)	Quinidine (-)
1-camphor-10-sulphonic acid (+) (-)	Cinchonidine (-)
Pyroglutamic acid (+) (-)	Cinchonine (+)
α-methoxyphenylacetic acid (+) (-)	Brucine (-)
α-methoxy-α-trifluoromethylphenylacetic acid (+) (-)	Dehydroabietylamine (+)

The literature presented shows that recognition of enantiomer by laboratory synthesized receptors are mostly large relatively flexible organic molecules synthesized through multiple steps. While there are number of chiral inorganic metal complexes or assemblies (inherently rigid) reported in recent times, none could be structurally characterized along with chiral guest. Only the report by Chin and co workers was able to show the host guest interaction in structurally characterized complexes. Incidentally that lone set of complexes did not have enough steric interaction to bind one enantiomer exclusively. Thus opportunity in synthesizing small molecular weight chiral metallo-organic receptor exists. Small molecular weight and rigidity of metal complexes might yield structurally characterized host guest adduct which in turn can contribute to the understanding of the chiral recognition mechanism.

Earlier our group synthesized one host of binuclear Ni(II) complexes with L-histidine derived ligand and tested with two amino alcohol (Figure 1.4).[17]

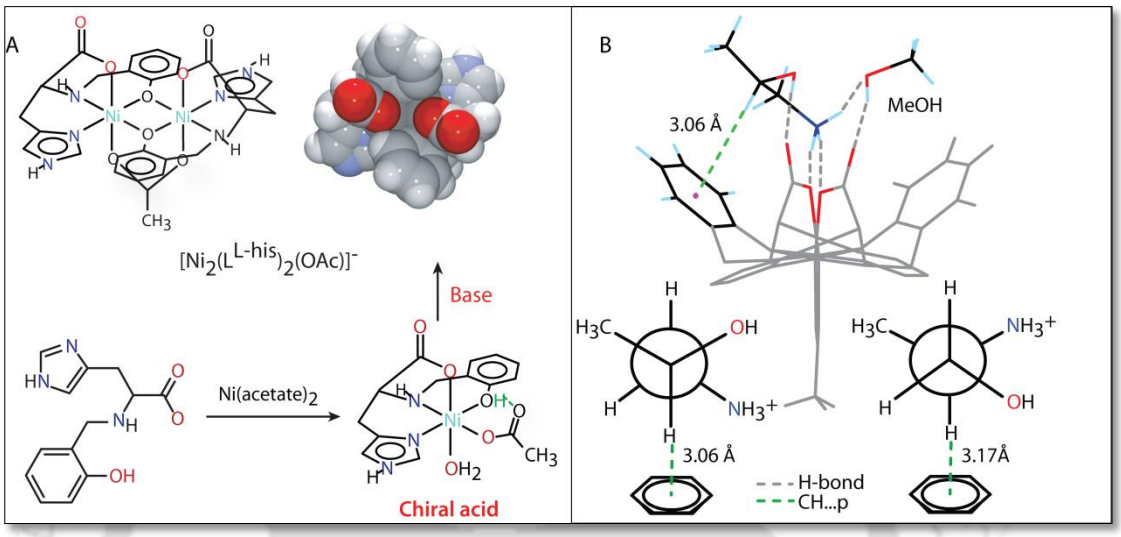

Figure 1.4 Synthesis of chiral anionic host (a), non-covalent interactions between host and guest (b).

In this thesis, we have one more host and tested on amines and amino alcohols to understand the recognition process in depth. We have attempted to isolate and estimate the contribution of individual factors responsible for chiral recognition within that host by systematic changes in both the guest (Chapter 2) and host (Chapter 3). In the process we not only unravelled the relative contribution of crystallization, solution equilibrium and the position of chiral centre but also been successful in effective separation of two biogenic amino alcohols, analogous to biologically recognized hormone nor-adrenaline by utilizing the modified host (Chapter 4). Lastly, we intend to extend the use of the host for few amino alcohols to indentify the trend of recognition and factors, mainly govern the chiral enhancement through crystallization (Chapter 5).

References

1. (a) Thomson, W. T. (Lord Kelvin) *Baltimore Lectures on Molecular Dynamics and the Wave Theory of Light*; Publication agency of the Johns Hopkins University: Baltimore, MD, **1904**.
2. (a) Eliel, E. L.; *Stereochemistry of Carbon Compounds*, **1962**, McGraw-Hill Book Company, Inc., New York. (b) Eliel, E. L.; Wilen, S. H.; *Stereochemistry of Organic Compounds*, **1994**,Wiley, New York.
3. (a) Rikken, G. L. J. A.; Raupach, E. *Nature*, **2000**, *405*, 932. (b) Maggiora, G. M.; Mao, B.; Chou, K. C. in *New Developments in Molecular Chirality*, ed. P. G. Mezey, Kluwer Academic Publishers, Dordrecht, **1991**, *5*, 93.
4. (a) Mustranta, A.; *Appl. Microbiol. Biotech.* **1992**, *38*, 61.(b) Cheng, H.; Rogers, J. D.; Demetriades, J. L.; Holland, S.; Seibold, J; Depuy, E. *Pharmaceutical Res.*, **1994**, *11*, 824. (c) Lioyd, L.G.; Davidson, L.; Hornykiewicz,O.; *J. Pharmacol Exp. Ther.* **1975**, *195*, 453. (d) Caner,H.; Groner, E.; Levy, L.; *Drug Discovery Today*, **2004**, *9*, 105.
5. (a) Berthod. A. *Anal.Chem*, **2006**,*78*, 2093. (b) Bernhardt, P.V.; Comba, P. ; Gyr, T. *Inorg. Chem.***1992**, *31*, 1220. (c) Carrillo, R.; Martin, V. S.; Martin, T. *Angew. Chen. Int. Ed*. **2009**, *48*, 7803. (d) Keurentjes, J. T. F.; Nabuurs, L. J. W. M.; Vegter, E. A. *J. Membr. Sci.* **1996**, *113*, 351.
6. (a) Fischer, E. *Ber. Dtsch. Chem. Ges.* **1894**, *27*, 2985. (b) Koshland, D. E. *Proc. Natl. Acad. Sci. U. S. A.* **1958**, *44*, 98. (c) Easson, L.Hz; Stedman, E. *Biochem*. J. **1933**, *27*, 1257. (d) Dalgliesh, C.E. *J. Chem. Soc.* **1952**, 3940. (e) Lochmiiller, C.H.; Souter, R.W. *J. Chrom.* **1975**, *113*, 283. (f) Dalgliesh, C.E.

J. Chem. Soc. **1952**, *137*, 3940. (g) Meyer, V.R.; Rais, M. A. *Chirality* **1989**, *1*, 167.

7. (a) Davankov, V. A.; Meyer V. R.; Rais, M. *Chirality* **1990**, *2*, 208.
8. (a) Nishio, M.; Hirota, M.; Umezawa, Y. 1998 The CH…π interaction; Wiley-VCH: New York (b) Desiraju, G.R.; Steiner, T.; **1999** in The weak hydrogen bond; Oxford University Press: New York (c) Desiraju, G. R. *Acc. Chem. Res* **2002**, *35,* 565.
9. (a) Ahlquist, R.P. *Am. J. Physiol.* **1948,** *153*, 586-600. (b) Nisoli, E.; Tonello, C.; Landi, M.; Carruba, *M. Mol. Pharmacol*. **1996**, *49*, 7. (c) Schrader. T, *J. Org. Chem*. **1998**, *63*, 264. (d) Schrader, T; *Angew. Chem. Int. Ed.* **1996***, 35*, 2649. (e) Strader, C.D.; Fong, T.M.; Tota, M.R.U. D. *Annu. Rev. Biochem.* **1994**, *63*,101.
10. Selected papaers: (a) Zhang, X. X.; Bradshaw, J. S.; Izatt, R. M. *Chem. Rev.* **1997**, *97*, 3313. (b) Kida, T.; Iwamoto, T.; Asahara, H.; Hinoue, T. Akashi, Mitsuru. *J. Am. Chem. Soc*. **2013**, *135*, 3371.(c) Akazaki, K.; Toshimitsu, F.; Ozawa, H.; Fujigaya, T.; Nakashima, N. *J. Am. Chem. Soc*. **2012**, *134*, 12700. (d) Wanderley, M. M.; Wang, C.; Wu, C.; Lin, W. *J. Am. Chem. Soc*. **2012**, *134*, 9050. (e) Maier, N. M.; Lindner, W. *Anal. Bioanal. Chem.* **2007**, *389*, 377. (f) Palmer, L. C.; Zhao, Y. L.; Houkb, K. N.; Rebek, *J. Chem. Commun*., **2005**, 3667. (g) Kim, S.; Kim, K.; Kim, Y. K.; Shin, Se. K., Ahn, K. H. *J. Am. Chem. Soc*. **2003**, *125*, 13819. (h) Kano, K. *J. Phys. Org. Chem*. **1998**, *11*, 286. (i) Castellano, R. K.; Kim, B. H.; Rebek, J. *J. Am. Chem. Soc.* **1997**, *119*, 12671.

11. Selected Reviews and papers: (a) Haginaka, J. *J. Pharm. Biomed. Anal*. **2002**, *27*, 357. (b) Gu. bitz, G.; Schmid, M.G. *Biopharm. Drug Dispos*. **2001**, *22*, 291. (c) Amini, A. *Electrophoresis* **2001**, *22*, 3107. (d) Schurig, V. *J. Chromatogr*. *A* **2001**, *906*, 275. (e) Boer, T.; Zeeuw, R.A.; Jong, G.J.; Ensing, K. *Electrophoresis* **2000**, *21*, 3220. (d) Francotte, E. *Chromatography as a separationtool for the preparative resolution of racemiccompounds*. *In Chiral Separations: Applicationsand Technology*; Ahuja, S., Ed.; AmericanChemical Society: New York, **1996**, 271. (f) Li, B.; Haynie, D.T. *Biomacromolecules* **2004**, *5*, 1667. (g) Rmaile, H.H.; Schlenoff, J.B. *J. Am. Chem. Soc.* **2003**, *125*, 6602. (h) Xiong, R. G.; You, X. Z.; Abrahams, B. F.; Xue, Z.; Che,.C. M. *Angew. Chem*. **2001**, *113*, 4554. (i) Gokel, G. W.; Leevy, W. M.; Weber, M. E. *Chem. Rev*. **2004**, *104*, 2723.

12. (a) Davis, M. E.; *Nature* **2002**, *417*, 813. (b) Kitagawa, S.; Kitaura, R.; Noro, S. *Angew. Chem. Int. Ed*. **2004**, *43*, 2334. (c) Xiong, R.; You, X.; Abrahams, B. F.; Xue, Z.; Che, C. M. *Angew. Chem. Int. Ed*. **2001**, *40*, 4422. (d) Wanderley, M. M.; Wang, C.; Wu, C.; Lin, W. *J. Am. Chem. Soc.* **2012**, *134*, 9050. (e) Kida, T.; Iwamoto, T.; Asahara, H.; Hinoue, T.; Akashi, M. *J. Am. Chem. Soc.* **2013**, *135*, 3371. (f) Xuan, W.; Zhang, M.; Liu, L.; Chen, Z.; Cui, Y. *J. Am. Chem. Soc.* **2012**, *134*, 6904. (g) Han, C.; Hou, X.; Zhang, H.; Wei Guo, W.; Li, H.; Jiang, L. *J. Am. Chem. Soc.* **2011**, *133*, 7644.

13. Examples of Metal complexes: (a) Seo, J. S.; Whang, D.; Lee, H.; Jun, S.; Oh, I. J.; Jeon, Y.; Kim, J. K. *Nature* **2000**, *404*, 982. (b) Ishi-i, T.; Calama, M. C.; Timmerman, P.; Reinhoudt, D. N.; Shinkai, S. *Angew. Chem. Int. Ed.* **2002**,

41, 1924. (c) Ishi-i, T.; Mateos-Timoneda, M. A.; Timmerman, P.; Calama, M. C.; Reinhoudt, D. N.; Shinkai, S. *Angew. Chem. Int. Ed.* **2003**, *42*, 2300. (d) Fiedler, D.; Leung, D.H.; Bergman, R. G.; Raymond, K. N. *J. Am. Chem. Soc*. **2004**, *126*, 3674. (e) Reeve, T. B.; Cros, J.; Gennari, C.; Piarulli, U.; Vries J. G. *Angew. Chem. Int. Ed*. **2006**, *45*, 2449. (f) Imai, H.; Munakata, H.; Uemori, Y.; Sakura, N. *Inorg. Chem*., **2004**, *43*, 1211. (g) Tashiro, S.; Ogura, Y.; Tsuboyama, S.; Tsuboyama, K.; Shionoya M. *Inorg. Chem*. **2011**, *50*, 4. (h) Li, Z. J.; Yao, J.; Tao, Q.;Jiang, L.; Lu, T.B. *Inorg. Chem*. **2013**, *52*, 11694.

14. (a) Siedlecka, R. *Tetrahedron* **2013**, *69*, 6331. (b) Querniard, F.; Linol, J.; Cartigny, Y.; Coquerel, G. *J. Therm. Anal. Calorim*. **2007**, *90*, 359. (c) Marchand, P.; Lefèbvre, L.; Querniard, F.; Cardinaël, P.; Perez, G.; Cournioux, J. J.; Coquerel, G. *Tetrahedron: Asymmetry* **2004**, *15*, 2455. (d) Jacques, J.; Collet, A.; Wilen, S. H. *Enantiomers, Racemates, and Resolutions*, Krieger Publishing Company, Malabar, FL, **1994**. (e) Springuel, G.; Collard, L.; Leyssens, T. *CrystEngComm* **2013**, *15*, 7951. (f) Springuel, G.; Robeyns, K.; Norberg, B.; Wouters, J.; Leyssens, T. *Cryst. Growth Des.* **2014**, *14*, 3996.
15. Pasteur, L. M. *C. R. Acad. Sci.,* **1848**, *26*, 535.
16. Vaidya, N. A. *Diastereomeric crystallisation - the "classical" chiral technology. Innovations in Pharmaceutical Technology*. **2000.**
17. Sahoo, S.C.; Ray, M. *Chem. Eur. J.* **2010**, *16*, 5004.

Chapter- 2

Crystallinity vs. Solution equilibrium

In the earlier report, it was demonstrated that two amino alcohols (1-amino-2-propanol and 2-amino-1-propanol) could be resolved with high efficiency (100% *ee* for 1-amino-2-propanol) where the guest (in the ammonium form) was bound inside the cleft of the binuclear Ni(II) complex through multiple non-covalent interactions.[1] The resolution efficiency was chiefly attributed to recognition of alcohol through ammonium, -OH group and C-H units (three point recognition) by the host. The effect of crystallization vis-à-vis host-guest interaction was outside the scope of investigation.

Here, we choose to explore the chiral recognition of aryl amine i.e., 1-phenylethylamine with the same binuclear Ni(II) host for two reasons. (a) The absence of an alcoholic group will reduce the energy difference between diastereomers as guest is losing one point interaction. Thus chiral enhancement, if at all observed, will be mainly due to solid-state interaction between the host-guest pair. (b) The reduced host-guest interaction (less than three points) might allow us to isolate both the diastereomer for better comparison of interactions.

The chiral recognition of amine and protonated amine compounds is important[2], since several of these compounds have significant biological activities[3] based on chirality. The resolution of enantiomers via the formation of a pair of diastereomers is the most practical method for obtaining enantiomerically pure compounds on both laboratory and industrial scales.[4] According to "three point contact rule"[5] formulated by L. H. Easson and E. Stedman for chiral recognition, ideally, recognition of three, out of four different groups around sp^3-hybridised carbon centre of an enantiomer, should facilitate complete separation through multiple non-covalent interactions.[6] Although recognition and resolution of enantiomers is possible by multiple means,[7]

our understanding of recognition mechanism is mainly based on molecular simulation studies.[5b] In this regard, our group designed reduced Schiff base ligand from simple starting material L-histidine and salicyldehyde (Scheme 2.1).[1] Using the ligand, a monomer of Ni(II) complex (**1**) as a monobasic acid was synthesized and further used for synthesis of binuclear Ni(II) complex as host in presence of chiral base.

Thus, in this Chapter, our attempt to synthesize and isolate the complex from the reaction with racemic 1-phenylethylamine as well as the complexes from the reaction with enantiopure 1-phenylethylamine as pure diastereomer by following the identical reaction procedure (Scheme 2.1). All the complexes are structurally characterized. Ratio of chiral distribution in the bulk crystals from racemic amine is measured through HPLC analysis.

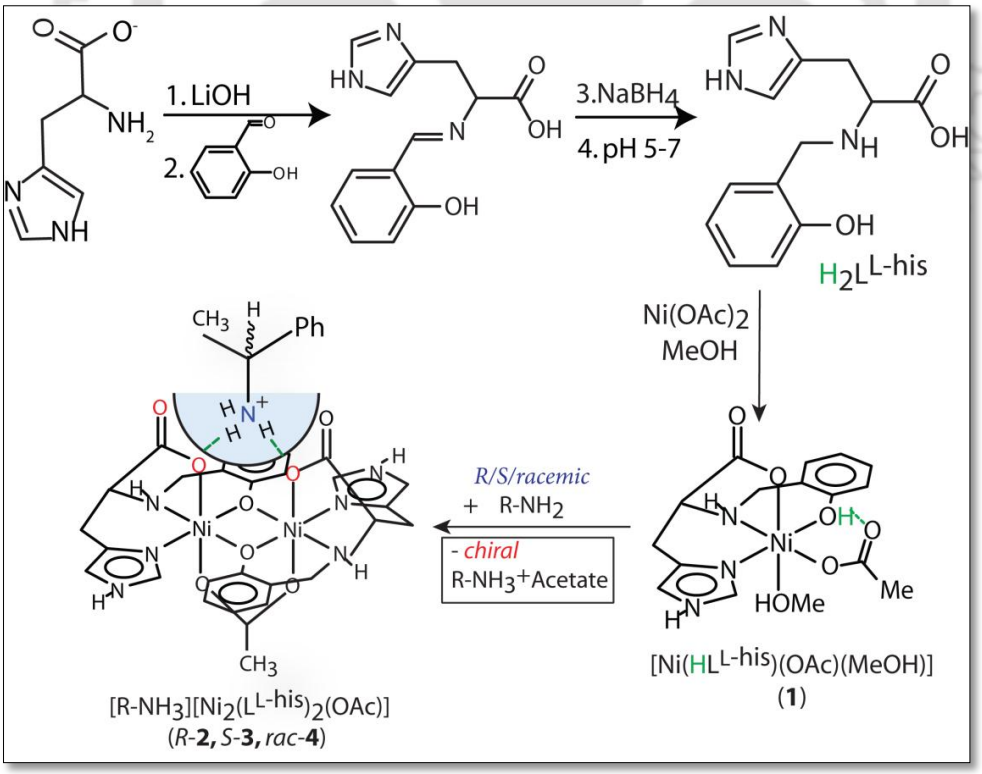

Scheme 2.1 Schematic representation of Synthesis of ligand, Ni(II) monomer and binuclear Ni(II) complex with guest amine.

2.1 Material and Methods

2.1.1 Solvents and reagents

Solvents were obtained from commercial sources and used without further purifications unless otherwise stated. o-Salicylaldehyde, (*R*)-(+)-(α)-1-phenylethylamine (96% *ee*) and (*S*)-(-)-(α)-1-phenylethylamine (98% *ee*) were purchased from Aldrich Chemical Co. and used as received. The amines were stored at +4 °C in the refrigerator when not used. The racemic 1-phenylethylamine was prepared by mixing equal volume of both enantiomers (measured $_{589}[\alpha]^{25}$ = -0.001°, c = 1g/100 mL(MeOH)). $NaBH_4$, amino acids and $Ni(OAc)_2{\bullet}4H_2O$ were purchased from Merck limited and used as received. Methanol (MeOH) was distilled over magnesium methoxide [$Mg(OCH_3)_2$]. The ligand $H_2L^{L\text{-}his}$ and the complex [$Ni^{II}(HL^{L\text{-}his})(OAc)(MeOH)$] (**1**) were prepared following reported procedures.[1]

2.1.2 Measurements

The IR spectra were recorded on Perkin-Elmer Spectrum One FT-IR spectrophotometer with KBr discs in the range 4000-400 cm^{-1} and electronic spectra on Perkin-Elmer Lambda 25 and Lambda 750 UV-vis spectrophotometers. The ^1H NMR spectra were recorded using a Varian Mercury plus 400 MHz instrument. The thermogravimetric analysis (TGA) of the compounds was performed using a TA instrument, SDT Q600 thermal analyzer with heating rate of 5-7 ^oC per min under a N_2 atmosphere using 5–10 mg sample per run. Powder pattern X-Ray diffraction were obtained using MAKE Bruker, D2 phaser with Cu-Ka radiation ((λ = 1.5418 Å) equipped with an integrated PC and DIFFRAC.SUITE software. Diffraction pattern were collected over 2θ range of 5- 40° at a step scan rate 0.02°. Optical rotations

were measured using a Perkin-Elmer 343 polarimeter. Solid-state magnetic susceptibility of the complexes at room temperature was recorded using Sherwood Scientific Magnetic balance MSB-1. Solution electrical conductivity was measured with Eutech Instruments CON 5/TDS 5 Conductivity Meter. The instrument was calibrated with standard solution. Elemental analyses were performed on a Carlo Erba 1108 and also by using a Perkin-Elmer series II 2400 instrument.

The crystals of complexes were mounted on glass fiber and on sealed quartz tube. All geometric and intensity data for the crystals were collected at room temperature using a Bruker SMART APEX CCD diffractometer equipped with a fine focus 1.75 kW sealed tube Mo-Ka (λ = 0.71073 Å) X-ray source, with increasing ω (width of 0.3º per frame) at a scan speed of either 3 or 5 s/frame. The SMART software was used for data acquisition and the SAINT software for data extraction. Absorption corrections were done using SADABS. After the initial solution and refinement with SHELXL, the final refinements were performed on WinGX environment using SHELX97. All non-hydrogen atoms in the complexes were refined anisotropically. Some Solvent molecules, methanol and water in few complexes were refined isotropically to avoid alert level A in checkcif. Wherever possible, the hydrogen atoms were located from the difference Fourier maps and were refined isotropically. Thus some of the C-H bonds will not be ideal and may vary. Some of C-C bonds have been restrained using DFIX, ISOR instruction in some complexes. Highly disordered solvent molecules (methanol, water), bridged acetate and cationic 1-Phenylmethylamine can be molded with positional disordered and treated with FVAR, PART command. Most of the hydrogen atoms attached to the solvent molecules could not be located or fixed, so the molecular weight may not match.

Crystallographic data and details of refinements are listed in Table 2.1, and selected bond distances and angles for are listed in Table 2.2a, b. Perspective views of the complexes were shown using ORTEP.

2.2 Syntheses

Detailed synthetic procedures along with characterization data has been provided below.

2.2.1 ((*R*)-1-phenylethylammonium)[$Ni_2(L^{L\text{-}his})_2(OAc)$](*R*-2). (*R*)-(+)-α-1-phenylethylamine (0.054 g, 0.450 mmol) was added to slurry [$Ni^{II}(HL^{L\text{-}his})(OAc)(MeOH)$] (**1**) (0.200 g, 0.450 mmol) in 5 mL of Methanol. Stirred for 2 min and volume was increased to a total of 10 mL. After 10 min stirring, the solution was quickly filtered through a sintered crucible. The transparent blue filtrate was placed in a 25 mL conical flask without stopper and kept in the refrigerator. Rod shaped crystals (Figure 2.1) appeared within 24 h. The crystals were isolated after 3 days, filtered and washed with distilled Acetonitrile. The crystals were ground and dried overnight inside a vacuum desiccator.Yield: 0.250g, 70%. Anal. Calcd. for $[Ni_2(C_{28}N_7O_8H_{29})(C_8NH_{12})].6H_2O$: C, 47.31; H, 5.90; N, 10.43; found C, 46.63; H, 5.54; N, 10.90; IR (KBr, cm^{-1}) $\upsilon(COO)_{asym}$ 1592(s), $\upsilon(COO)_{sym}$ 1480(m). μ_{eff}(powder, 298K)/Ni; 2.71 μ_B ,Λ_M (ohm^{-1} cm^2 mol^{-1}): 75 (MeOH).

2.2.2 ((*S*)-1-phenylethylammonium)[$Ni_2(L^{L\text{-}his})_2(OAc)$](*S*-3). This was prepared following the same procedure as described for *R*-**2** using (*S*)-(-)-(α)-1-phenylethylamine instead of (*R*)-(+)-α-1-phenylethylamine in same reaction scale. Rhombohedral shaped crystals (Figure 2.1) appeared within 12 h. Use of a 25 mL

beaker instead of a conical flask yielded smaller sized clusters of crystals within 2.5 h. The crystals were filtered after two days and washed with Acetonitrile. The crystals (0.265 g, 78%) were ground and dried overnight inside vacuum desiccators. Anal. Calcd. for $[Ni_2(C_{28}N_7O_8H_{29})(C_8NH_{12})].3H_2O.3CH_3OH$: C, 51.36; H, 5.65; N, 10.65; found C, 51.37; H, 5.14; N, 11.01; IR (KBr, cm^{-1}) $\upsilon(COO)_{asym}$ 1569(s), $\upsilon(COO)_{sym}$ 1480(m). μ_{eff}(powder, 298K)/Ni; 2.73 μ_B .Λ_M (ohm^{-1} cm^2 mol^{-1}): 50 (MeOH).

2.2.3 ((*Rac*)-1-phenylethylammonium)[$Ni_2(L^{L\text{-}his})_2$(OAc)](*rac*-4). This was prepared following the same procedure as described for *R*-**2** using racemic (α)-1-phenylethylamine instead of (*R*)-(+)-α-1-phenylethylamine, in same reaction scale. The rhombohedral shaped crystals that resemble with *S*-**3** (Figure 2.1) appeared after 3days. The crystals were filtered after four days and washed with Acetonitrile. The crystals (0.220 g, 61%) were ground and dried overnight inside vacuum desiccators. Anal. Calcd. for $[Ni_2(C_{28}N_7O_8H_{29})(C_8NH_{12})]$. $H_2O.3CH_3OH$: C, 50.36; H, 5.96; N, 10.64; found C, 50.87; H, 5.64; N, 10.49; IR (KBr, cm^{-1}) $\upsilon(COO)_{asym}$ 1556(s), $\upsilon(COO)_{sym}$ 1474(m). μ_{eff}(powder, 298K)/Ni; 2.69 μ_B .Λ_M (ohm^{-1} cm^2 mol^{-1}): 52 (MeOH).

2.3 Estimation of enantiomeric separation through HPLC.

Chiral amines were extracted from reaction mixture and extent of chiral separation was measured by HPLC using Chiralcel OD-H coloumn attached with UV detector at a flow-rate of 1mL /min. Hexane and isopropanol in 93:7 ratio was used as eluent. The extraction procedure and organic derivative preparation (necessary for HPLC) have been provided below.

2.3.1 Procedure of recovery of amine from metal complexes as crystal

The crystals of host-guest complex (0.192 g, 0.24mmol) were dissolved in 10 mL methanol. KNO_3 (0.094 g, 0.96mmol) in minimum water-methanol (v/v, 1:1) was added to solution and further stirred for 6h leaving a light blue precipitate. The solvent was evaporated to dryness and stirred with 6 mL of acetonitrile, filtered. Filtrate was evaporated. Free Amine was extracted from Na_2CO_3 in water-ethylacetate and the organic part was separated, dried and evaporated to dryness. The free amine was subjected to derivatization with benzoyl chloride following the above procedure. The derivative amide was analyzed by HPLC.

The guest amines from the crystals were also recovered by decomposition of the metal complex with dil. HCl followed by extraction of the amine from aqueous solution using ethylacetate. The extracted amine was derivatized using the procedure described in the preceding section. HPLC results using both recovery methods were identical. However, the acidification method produces ligand fragments, which gives extra peaks in the HPLC traces.

2.3.2 Procedure of recovery of amine from amorphous metal complexes

Monomer complex (0.200 g, 0.45mmol) was stirred in 10 mL methanol. 1equivalent of racemic-1-phenylethylamine (0.055 g, 0.45mmol) was added and stirred for 8h. The mixture was evaporated to dryness and 5 mL of acetonitrile was added and filtered. From the residue free amine was recovered and derivatized by following above procedure.

2.3.3 Derivatization of chiral amine With Benzoyl Chloride

As the chiral column (Chiralcel OD-H) was not suitable to separate chiral amines, we have derivatized the chiral amines to corresponding amide derivative

before subjecting it to HPLC run. All the derivatives were prepared identically and the derivatives were characterized using IR, ESI-Mass and proton NMR spectroscopy. Detailed procedure and characterization data for one representative derivative is provided below

Racemic-1-phenylethylamine by mixing of equal volume of (*S*)-(-)-α-1-phenylethylamine and (*R*)-(+)-α-1-phenylethylamine (0.1452 g, 1.2mmol) and triethylamine (0.136 g, 1.25mmol) was stirred in 5mL of dichloromethane at ice bath for 15 min. Benzoyl Chloride (0.168 g, 1.2mmol) in 1 mL of dichloromethane was added drop wise. The reaction mixture was stirred for 3-4h at 0° and stirred another 2h at room temperature. The compound was extracted from dichloromethane and water in presence of saturated sodium chloride. The organic layer was separated and evaporated resulting in a white solid. The white solid was washed with Diethyl ether and dried under vacuum. Yield: 75%. IR (KBr, cm^{-1}): 1633(s), 3357(s). (ESI-Mass, +ve) m/z 226.095 (cal. 226.113) ($[M+H]^+$), 248.055 ($[M+Na]^+$). ^1H NMR ($CDCl_3$, 400MHz): 7.76 (2H, d, o-C_6H_5(benzoyl)), 7.47-7.25 (8H, m, C_6H_5 (benzoyl and benzyl), 6.44 (1H, b, -N**H**),5.33(1H, m, -C**H** (benzyl)), 1.58(3H, d, -C$\mathbf{H}_3$).

Table 2.1 Crystallographic data and refinement parameters of Complexes.

	R-**2**	*S*-**3**	*rac*-**4**
empirical formula	$C_{120}H_{123}N_{21}Ni_6O_{40}$	$C_{78}H_{82}N_{14}Ni_4O_{27}$	$C_{76}H_{85}N_{14}Ni_4O_{19}$
fw	2851.53	1882.34	1733.34
T (K)	296(2)	296(2)	296(2)
wavelength (A°)	0.71073	0.71073	0.71073
crystal system	Trigonal	Orthorhombic	Orthorhombic
space group	*R3*	$P2_12_12$	$P2_12_12$
a, A°	34.5876(9)	19.1309(6)	19.1159(7)
b, A°	34.5876(9)	20.0808(7)	19.8690(8)
c, A°	11.2474(6)	12.8654(4)	12.6674(5)
V, Å ^{3}	11652.6(10)	4942.4(3)	4811.3(3)
z/ρ	3/1.219	2/1.265	2/1.196
μ	0.788	0.825	0.835
coll.reflns	12672	9934	10987
indep reflns	6336	5492	6056
FLACK para.	-0.003(15)	-0.01(2)	-0.02(3)
GOF	1.036	1.069	0.951
R1 [a]	0.0612	0.0541	0.0903
wR2 [a]	0.1433	0.1391	0.2474
R1[b]	0.1061	0.0777	0.1350
wR2[b]	0.1696	0.1606	0.2897

[a] $I > 2\sigma$. [b] All data.

Table 2.2a Selected bond distances (Å) and angles (°) of *R*-**2** and *S*-**3**.

	R-**2**	*S*-**3**
Ni1 -O1	2.101(3))	2.103(4)
Ni1-O3	2.046(4)	2.065(4)
Ni1-O3A	2.041(4)	2.023(4)
Ni1-O4	2.101(4)	2.067(4)
Ni1-N1	2.085(5)	2.073(2)
Ni1-N2	2.050(6)	2.063(2)
Ni2- O1A	2.104(4)	2.110(4)
Ni2-O3	2.045(4)	2.025(4)
Ni2-O3A	2.037(4)	2.054(4)
Ni2-O5	2.092(4)	2.085(4)
Ni2-N1A	2.074(4)	2.066(2)
Ni2-N2A	2.053(6)	2.064(2)
N1-Ni1-N2	87.0(2)	87.95(8)
O3-Ni1-O3A	83.02(16)	82.66(15)
N1- Ni1-O1	80.50(16)	80.34(12)
N2-Ni1-O4	90.8(2)	91.89(13)
O1-Ni1-O4	173.18(15)	171.55(18)
N1A-Ni2-N2A	85.23(19)	88.57(8)
O3A-Ni2-O3	83.16(16)	82.89(15)
N1A-Ni2-O1A	80.54(16)	80.08(12)
N2A-Ni2-O5	92.9(2)	93.41(13)
O1A-Ni2-O5	171.37(18)	170.76(18)

Table 2.2b Selected Bond length (Å) and bond angle (°) in complex *rac*-**4**.

Ni1 – O4B	1.84(3)	N4A – C17A	1.20(5)
Ni1 – O3A	2.041(5)	C16A –C17A	1.494(10)
Ni1– N2	2.055(6)	C17A- C18A	1.504(10)
Ni1 – O3	2.059(6)	C18A –C19A	1.3900
Ni1 – N1	2.071(7)	C18A C23A	1.3900
Ni1 - O1	2.096(6)	C19A – C20A	1.3900
O3 – Ni2	2.027(5)	C20A – C21A	1.3900
Ni2 –N2A	2.039(7)	C21A – C22A	1.3900
Ni2 – O3A	2.070(6)	C22A C23A	1.3900
Ni2 – N1A	2.093(7)	N4B – C17B	1.54(4)
Ni2 – O1A	2.106(6)	C16B –C17B	1.501(10)
Ni2 – O5B	2.20(4)	C17B - C18B	1.504(10)
O4A – C14A	1.24(4)	C18B – C19B	1.3900
O5A – C14A	1.34(5)	C18B – C23B	1.3900
C14A - C15A	1.43(4)	C19B – C20B	1.3900
O4B – C14B	1.43(9)	C20B – C21B	1.3900
O5B – C14B	1.10(9)	C21B – C22B	1.3900
C14B – C15B	1.63(8)	C22B – C23B	1.3900
O4B - Ni1 - O3A	91.6(14)	C9 - O3 - Ni2	135.9(5)
O4B - Ni1 - N2	95.4(15)	Ni2 - O3 - Ni1	95.8(2)
O3A - Ni1 - N2	97.2(2)	O3 - Ni2 - N2A	98.4(3)
O4B - Ni1 - O3	87.7(15)	O3 - Ni2 - O3A	83.2(2)
O3A - Ni1 - O3	83.1(2)	N2A - Ni2 - O3A	177.7(3)
N2 - Ni1 - O3	176.9(3)	O3 - Ni2 - N1A	174.6(3)
O4B - Ni1 - N1	86.9(14)	N2A - Ni2 - N1A	86.9(3)
O3A - Ni1 - N1	174.4(2)	O3A - Ni2 - N1A	91.6(2)
N2 - Ni1 - N1	88.3(3)	O3 - Ni2 - O1A	100.1(2)
O3 - Ni1 - N1	91.5(2)	N2A - Ni2 - O1A	86.5(3)
O4B - Ni1 - O1	167.2(14)	O3A - Ni2 - O1A	91.6(3)
O3A - Ni1 - O1	100.6(2)	N1A - Ni2 - O1A	81.1(3)
N2 - Ni1 - O1	87.1(3)	O3 - Ni2 - O5B	89.6(9)
O3 - Ni1 - O1	89.8(2)	N2A - Ni2 - O5B	94.5(8)
N1 - Ni1 - O1	80.5(3)	O3A - Ni2 - O5B	87.1(9)
C1 - O1 - Ni1	112.7(6)	N1A - Ni2 - O5B	89.0(9)
C9 - O3 – Ni1	116.5(5)	O1A - Ni2 - O5B	170.0(9)

2.4 Result and Discussion

2.4.1 Syntheses and isolation host-guest complexes

Following the previous protocol[1] host-guest adducts have been synthesized (Scheme 2.1). The addition of chiral amine acting as a base, to mononuclear $[Ni^{II}(HL^{L\text{-}his})(OAc)\ (MeOH)]$ (**1**) which acts as a monobasic acid, produces the chiral ammonium salt of binuclear $[Ni_2(L^{L\text{-}his})_2(OAc)]^{1-}$ (equation 1). This binuclear complex anion acts as chiral host to the chiral ammonium cation.

$$2\ [Ni^{II}(HL^{L\text{-}his})(OAc)(MeOH)]\ (\mathbf{1}) + 2\ \text{Chiral amine} \rightarrow (\text{Chiral ammonium})[Ni_2(L^{L\text{-}his})_2(OAc)] + (\text{Chiral ammonium})(OAc) + MeOH \quad \text{----------} \quad (1)$$

Good quality crystals in 60-75% yield were obtained from the methanolic solution kept at 10°C (refrigerator) between 24 h to 36 h for *R* and *S* isomer of 1-phenylethylamine. Crystals from racemic amine took considerably longer time to form (2-3 days). Crystals of *R*-**2**, S-**3** and *rac*-**4**, isolated using *R*, *S* and racemic form of 1-phenylethylamine respectively, had distinctive shapes. While *R*-**2** is rod shaped, the *S*-**3** and *rac*-**4** both are rhombohedral plates (Figure 2.1).

The complexes *R*-**2**, *S*-**3** and *rac*-**4** are further characterized using FTIR, UV-Vis, conductance, magnetic moment and elemental analysis. Data is commensurate with values earlier obtained for analogus complexes.[8]

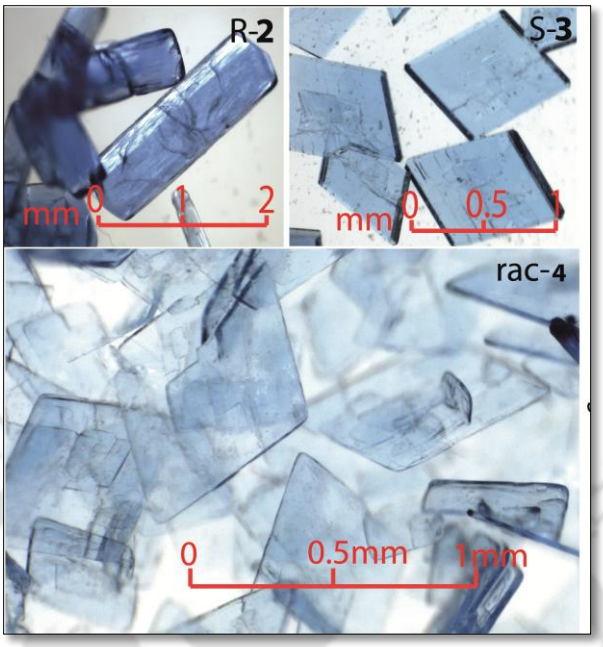

Figure 2.1 Crystal morphology of the complexes.

2.4.2 X-Ray Structure of ((*R*)-1-phenylethylammonium)[$Ni_2(L^{L\text{-}his})_2(OAc)$](*R*-2)

Complex *R*-**2** is crystallized in chiral space groups of *R*3. The asymmetric units contains one anionic $[Ni_2(L^{L\text{-}his})_2(OAc)]^{1-}$ unit, one cationic form of chiral amine, four methanol and two water molecules. The $[Ni_2(L^{L\text{-}his})_2(OAc)]^{1-}$ unit contains two octahedral Ni(II) centers, each ligated with one tetradentate $(L^{L\text{-}his})^{2-}$, a bridging phenolate oxygen and one bridging bidentate acetate ligand (Figure 2.2a). Geometry around each nickel is slightly distorted from perfect octahedron as evident from the deviation of angles from ideal 90° and 180° (Table 2.2a). Comparing bond lengths and angles within first coordination sphere, both Ni(II) centers are nearly identical. The chiral carbon in $(L^{L\text{-}his})^{2-}$ has *S* conformation as L-histidine (*S*-conformation) was used during the ligand synthesis. Both the coordinated amine N atoms, N1 and N1a, have *R* conformation. This has been observed in all previous complexes with this ligand.[7] In $[Ni_2(L^{L\text{-}his})_2(OAc)]^{1-}$, two carboxylates oriented next to each other, flanked

on both sides by the aromatic rings form a molecular cleft suitable for guest binding through non-covalent interactions.[9]

The complex *R*-**2** contains large number of fairly strong H-bonds as well as weaker non-covalent interactions (Table 2.3). Two out of three NH of the $-NH_3^+$ in *R*-**2** is H-bonded to carboxylate oxygen atoms O1 and O1A (Figure 2.2b). The third NH is bound to methanol oxygen (O9), which is part of a chain of H-bonds provided by two intervening methanol oxygen, O8 and O9 terminating on carboxylate oxygen (O2A). The relatively shorter C17…C10 (3.477 Å) & C17…C11 (3.531Å) lengths indicate C17-H29 is interacting with the C10-C11 bond.

The low angle (~58°) between -CH and aromatic ring containing C8-C13 atoms, rules out a CH…π type of interaction. The methyl group (C16) of the guest amine participates in an inter-molecular CH…π interaction with the neighboring aromatic ring (C8-C13) atoms. Three molecule of binuclear complex along with bound chiral ammonium cations form a very compact triangular assembly through inter-molecular CH…π interaction between C17 and C10-C11 bond and H-bonding between imidazole-carboxylate (N3A…O2A) (Figure 2.4c). Incidentally, water oxygen (O11) at the centre of this triangle is not H-bonded to any neighboring atom. The triangular assemblies, situated on top of each other, form a columnar structure utilizing C2A…O2 and C2…O7…O5 interactions. The space between the columns form narrow (6-8 Å) one-dimensional empty channels along *c*-axis with total 498 $Å^3$ solvent accessible void spaces in the lattice (Figure 2.2d).

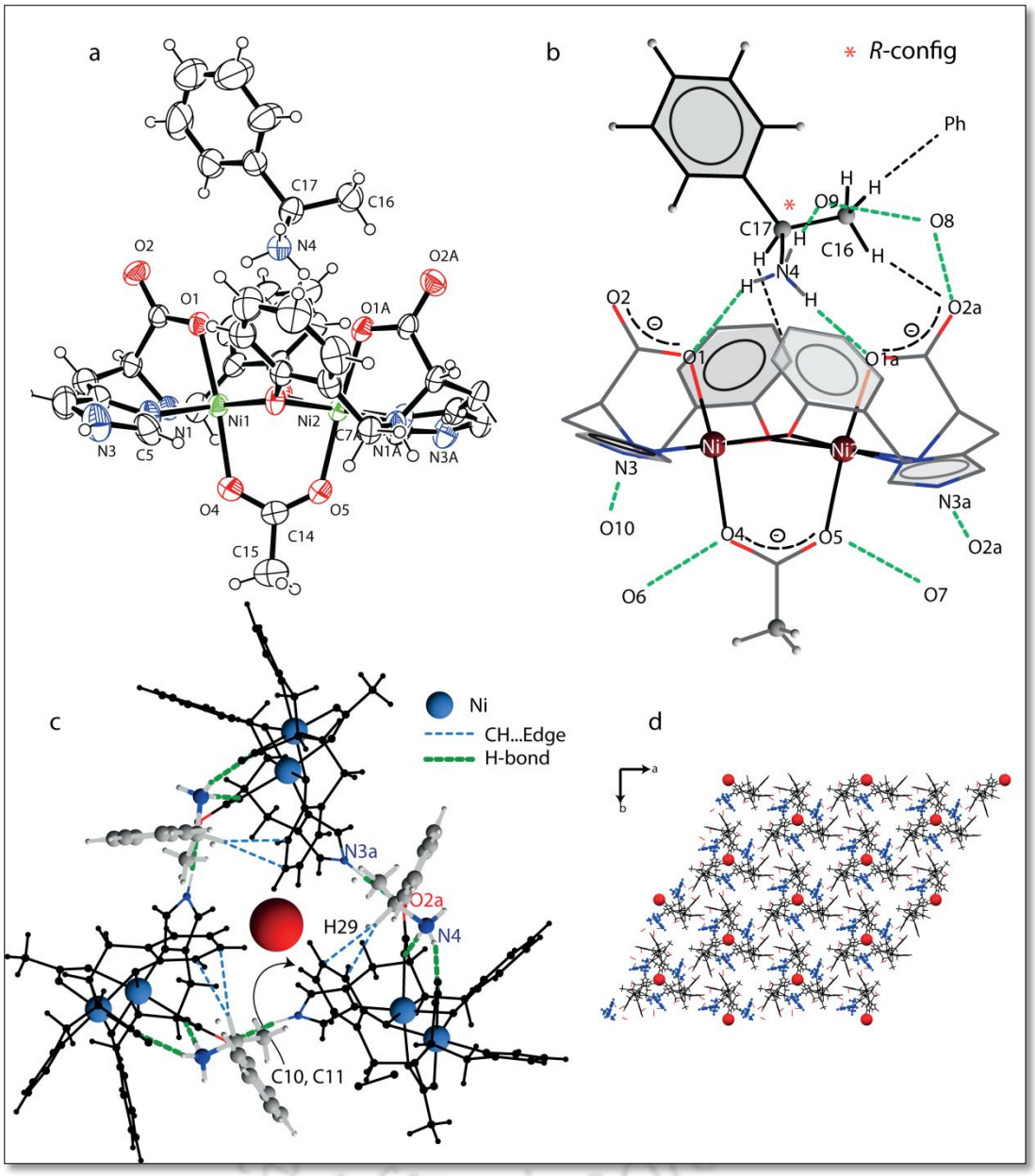

Figure 2.2 ORTEP diagram of complex *R*-**2** with 40% ellipsoid probability (a), molecular structure of host-guest complex showing non-covalent interaction between host and guest amine (b), trinuclear assembly between three host-guest adduct (c) and crystal lattice of complex *R*-**2** (d).

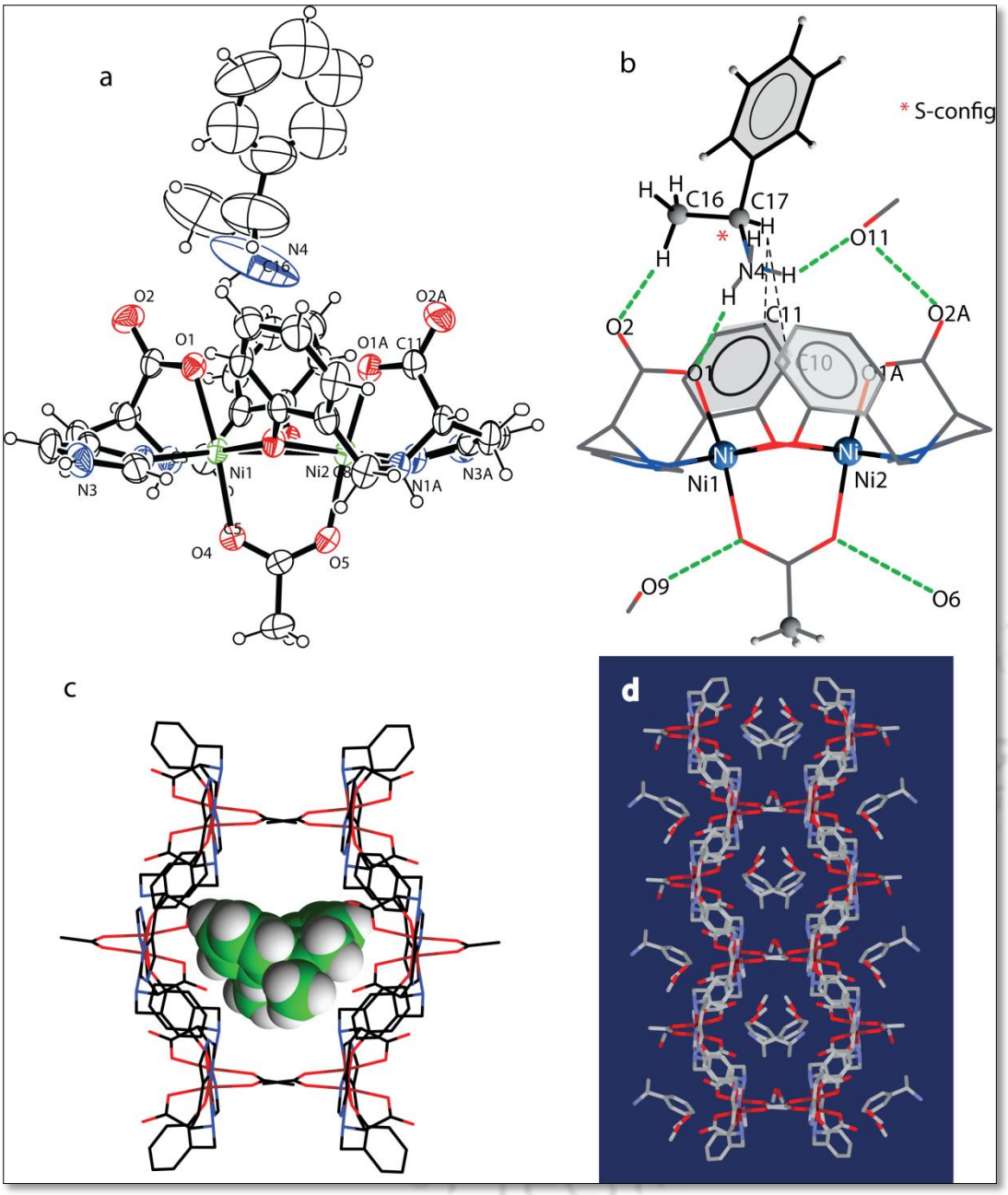

Figure 2.3 ORTEP diagram of complex *S*-**3** with 40% ellipsoid probability (a), molecular structure of host-guest complex showing non-covalent interaction between host and guest amine(b), one dimensional channel along c-axis encapsulated with guest amine (c) and crystal lattice of complex *S*-**3** (d).

2.4.3 X-ray Structureof ((*S*)-1-phenylethylammonium)[$Ni_2(L^{L\text{-}his})_2(OAc)$](*S*-3)

The complex *S*-**3**, the diastereomer of *R*-**2**, was crystallized in orthorhombic space group $P2_12_12$ (Table 2.1). Beside the binuclear Ni(II) anion and 1-Phenylmethylammonium cation, the unit cell contains three methanol and three water molecules in the asymmetric unit. The molecular structure of the binuclear Ni(II) anion is nearly identical with that in *R*-**2**.

The major differences lies with the way of chiral ammonium cation, interacted with binuclear anion and the non-covalent interactions within the lattice (Figure 2.3b). Unlike in *R*-**2**, the $–NH_3^+$ formed H-bonds with only one carboxylate oxygen (N4…O1) and solvent oxygen (O11) (Figure 2.2b & Figure 2.3b). The O11 is also H-bonded to another carboxylate oxygen (O2A). Inter-molecular H-bonding between imidazole and carboxylate (O2A…N3 & O2…N3A) form a two-dimensional (2D) network. This network is further strengthened by H-bonds between bridging carboxylate and solvent molecules (O5…O6 and O4…O9, Table 2.3). Stacking of the 2D networks form one-dimensional channels along *a* axis (O2-O2A = 10.79 Å) which is filled with guest ammonium ions (Figure 2.5c & d).

Additionally, an inter molecular weak CH…π interaction (C7H…π (C18 –C22) = 3.681 Å) has been observed between phenyl ring of neighbor guest amine and the host binuclear moiety.

2.4.4 X-ray Structure of ((*rac*)-1-phenylethylammonium)[$Ni_2(L^{L\text{-}his})_2(OAc)$] (*rac*-**4**).

The crystals of *rac*-**4** were isolated from the racemic amine in ~60% yield. Crystals are uniform in shape.

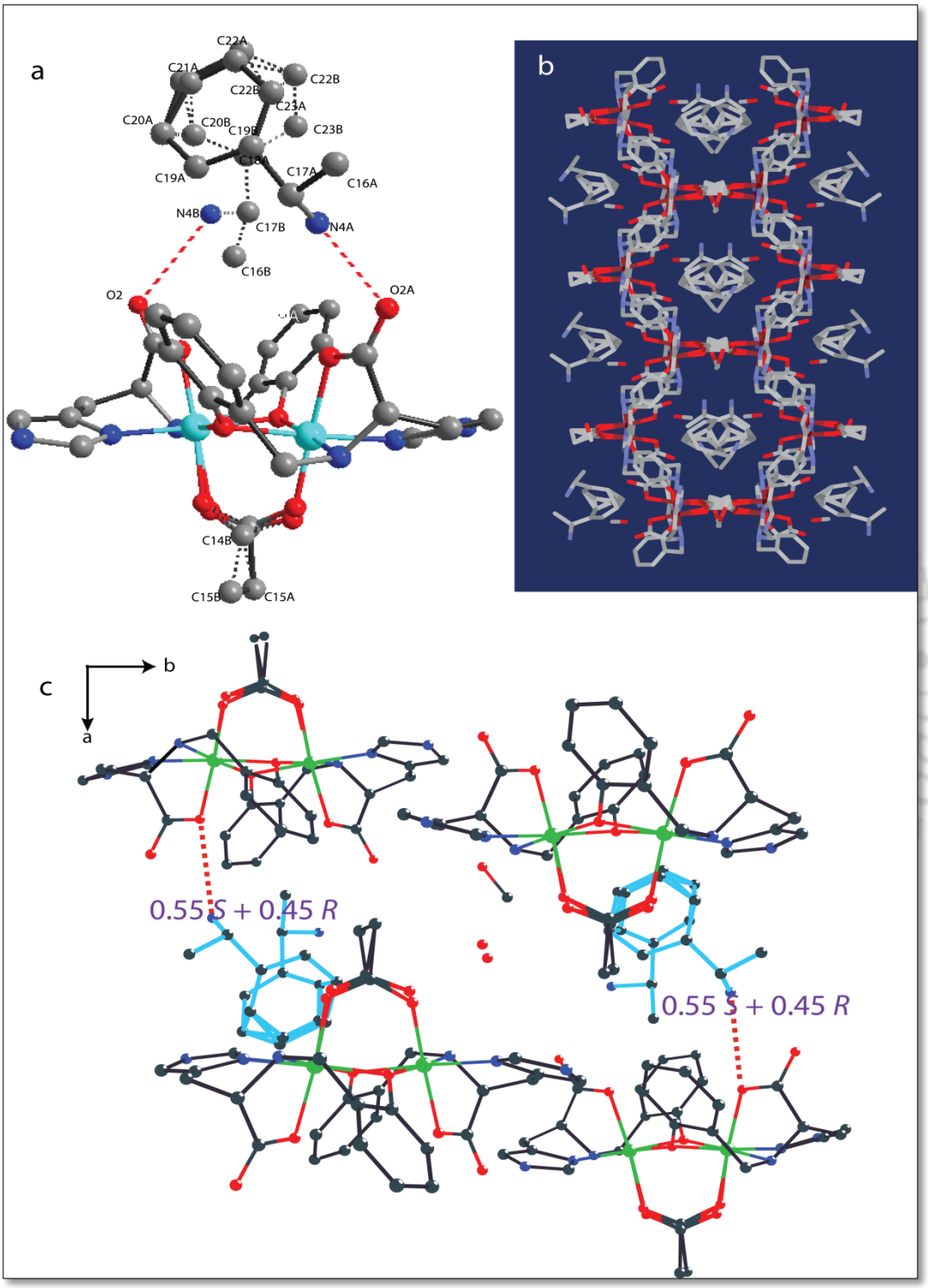

Figure 2.4 Molecular structure of complex *rac*-**4** in ball and Stick model (a), one dimensional channel encapsulated with both R-amine and S-amine (b) and guest amine is disordered with 55:45 ratio of S:R isomer in the crystal lattice of complex *rac*-**4** (c).

Table 2.3 Hydrogen bond and other non-covalent bond distances (Å) present in complexes.

	D-H···A	D-H (Å)	H···A(Å)	D···A(Å)	DHA(°)
***R*-2**	Direct Host-Guest interaction				
	N4 - H4B···O1	0.89	2.01	2.823(7)	151
	N4 - H4A···O1A	0.89	2.01	2.895(6)	174
	C17-H29···π	0.98§	3.092§	3.987§	153§
	Other non-covalent interactions				
	O9···O8			2.587§	
	O10···O2			2.630§	
	O5···O7			2.685§	
	N3 -H6···O10	0.86	1.92	2.748(17)	158
	N3A- H7···O2A	0.86	1.93	2.790(9)	174
	N1 - H1···O6	0.91	2.40	3.25(3)	154
	N1A - H2···O7	0.91	2.51	3.329(7)	150
	C2- H10···O7	0.98	2.59	3.479(8)	150
	C16-H22A···π	0.97§	2.686§	3.644§	175§
***S*-3**	Direct Host-Guest interaction				
	N4 - H4C···O1	0.89	2.07	2.920(17)	158
	C16-H16C···O2	0.96	2.35	3.19(2)	145
	Other non-covalent interactions				
	O4…O9			2.747§	
	N3-H10···O2A	0.86	1.90	2.748(6)	168
	N3A-H44C···O2	0.86	1.90	2.759(6)	173
	N4-H4B···O11	0.89	2.23	2.780(3)	119
	O5···O6			2.837§	
	O11···O2A			2.859§	
	N1 – H4A···O9	0.90	2.40	3.230(10)	155
	C7 – H7B···π	0.97§	2.78§	3.768§	154§

§ distance measured from Mercury view

Crystals bear the distinctive rhombohedral shape of *S*-**3** (Figure 2.1). The space group and other crystal parameters of *rac*-**4** resemble those of *S*-**3** (Table 2.1). The chiral ammonium cations occupy the channels along *c* axis as in *S*-**3** (Figure 2.4b). The gross structure is identical with that of *S*-**3** except the disorder at bridging carboxylate and the chiral cation. The disordered cations were modeled and refined using PART and free variable (FVAR) options. The model fits well with 55:45 ratio

of *S* and *R* enantiomer of the chiral cation respectively (Figure 2.4c). T. B. Lu and co-workers previously reported similar results where chiral 1-Phenylethanol was disordered within a chiral polymer with ratio of *R*:*S* is 60:40.[10] The uniform nature of the crystals and consistency of chiral enhancement within the crystal and bulk, suggest a distribution of both *R* and *S* isomer within a single type of crystal. The lack of rod shaped crystals of *R*-**2** support this observation.

2.4.5 Thermogravimetric analysis of complexes

To determine the number of solvent molecules in the bulk material thermogravimetric analyses were performed.

Thermogravimetric analysis of *R*-**2** was performed from 25 to 600 °C at 7°/min heating rate (Figure 2.5a). The weight loss of 10.6 % is observed from 25° to 120 °C. Crystal structure showed presence of five methanol and one water molecule as solvents of crystallization. Removal of solvent of crystallization as per structure requires weight loss of 18.7%, far higher than observed. The observed value could be accounted for six water molecules (cald. 10.8%). The crystals show desolvation upon exposure to air. Thus it is possible that water from air might have replaced the more volatile methanols on the crystals. The structure show (next section) formation of compact triangle shaped assembly of three host-guest adducts where solvents of crystallization are on the surface of those triangles, which could be removed with relative ease. The formula, (1-phenylethylammonium)$[Ni_2(L^{L\text{-}his})_2(OAc)](H_2O)_6$ for the bulk material of *R*-**2** is supported by elemental analysis. The complex decomposes above 250 °C.

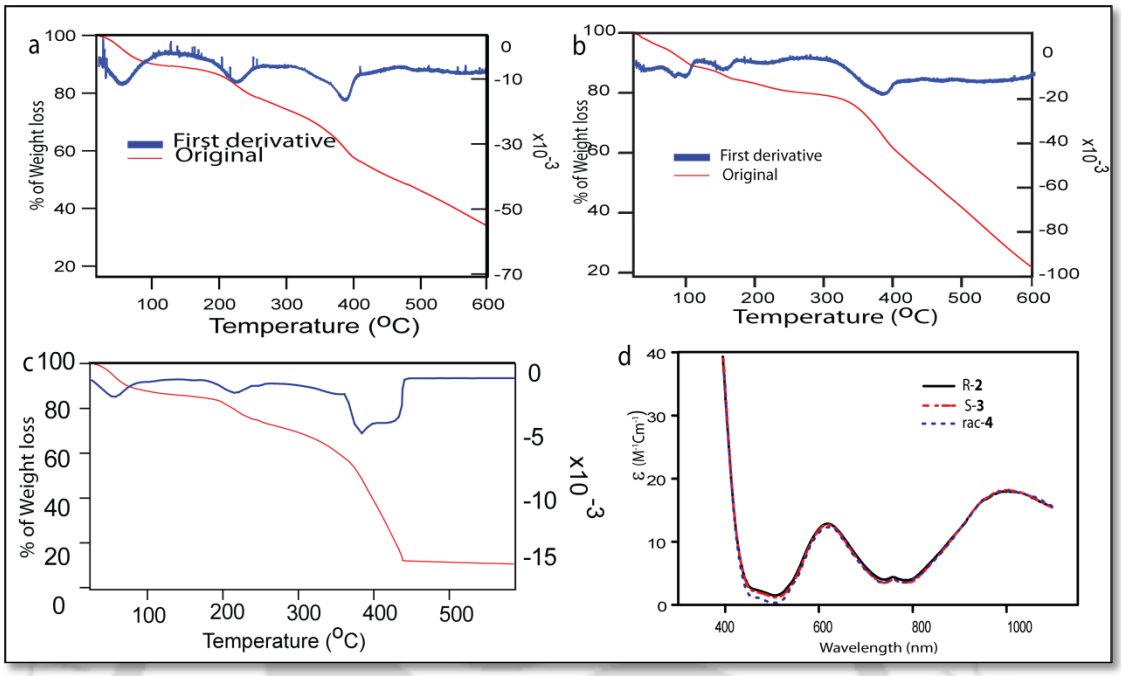

Figure 2.2 TGA plot of Complexes *R*-**2**. *S*-**3**, *rac*-**4** (a, b, c) and UV-Vis spectra of complexes in MeOH (d).

Thermogravimetric analysis of *S*-**3** was performed from 25 to 600 °C at 5°/min with heating rate (Figure 2.5b). An observed weight loss of 15.6 % between 25 - 175 °C can be accounted for three methanol and three water molecules (cald. 15.5%). This is consistent with crystal structure. First derivative plot of TGA showed that the removal of solvent of crystallization occurred in multiple steps: weight loss of 4.9% from 25 - 67 °C, 6.8% from 67 to 116 °C, 4.2 % from 116 to 175 °C. This could be explained as loss of one methanol & one water (cald. 5.1%), followed by two methanol (cald. 6.7) and finally loss of two water molecules (cald. 3.8%). The complex decomposes above 300 °C. The formula, (1-phenylethylammonium)[$Ni_2(L^{L\text{-}his})_2(OAc)](H_2O)_3(CH_3OH)_3$ for the bulk material of *S*-**3** is supported by the elemental analysis as well.

Thermogravimetric analysis of *rac*-**4** was performed from 26 to 600 °C at 7°/min heating rate (Figure 2.5c). The weight loss of 12.4 % was observed from 25 to 150

°C. Crystal structure showed presence of three methanol and one water molecule as solvents of crystallization. Removal of solvent of crystallization as per structure requires weight loss of 12.2%, which is consistent with observed value. The weight loss between 150- 280 °C is 14.4% which can account for the removal of 1-phenylethylamine (cald. 14.9%). The complex decomposes above 300 °C. The formula, (1-phenylethylammonium)$[Ni_2(L^{L\text{-}his})_2(OAc)](H_2O)(CH_3OH)_3$ for the bulk material of *rac*-**4** is supported by elemental analysis.

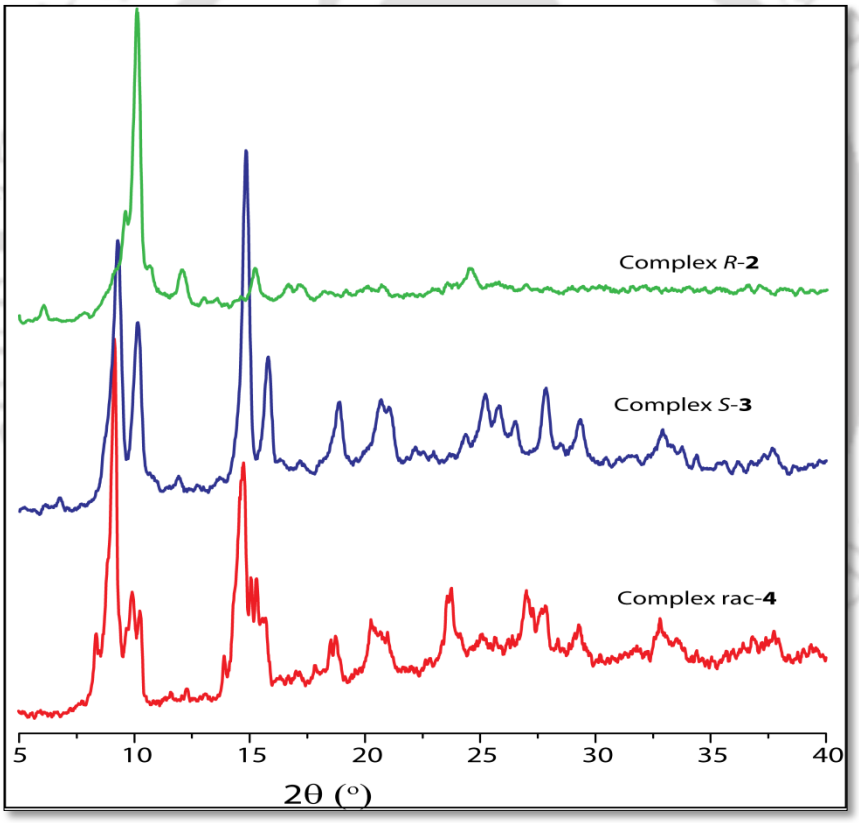

Figure 2.6 Powder X-Ray diffraction (PXRD) patterns of complexes (corresponding naming with respect to complexes given).

2.4.6 Powder X-ray diffraction analysis of complexes

Phase purity of the complexes has been further checked by Powder X-ray diffraction (PXRD) pattern (Figure 2.6). The diffraction pattern for complex *rac*-**4** is

different with *R*-**2**, but resemble with *S*-**3**, which is consistent with the single crystal X-ray result.

2.4.7 Recovery of the chiral guest amine and determination of enantiomeric enhancement through HPLC

From our ealier report[1], recovery and isolation of the recognized guest amine has been accomplished by metathesis reaction with a potassium salt, as the binding constant with potassium ion is high. The structural data of the host-guest adducts *rac*-**4** showed that, in crystal, (*S*)-isomer of the amine was recognized preferentially (~10% *ee*). To determine the distribution of *R* vs. *S* amine in the bulk of the crystals, the free amine was isolated by releasing the guest from the host-guest adducts. Isolation was followed by derivatization necessary for detection in high-pressure liquid chromatography (HPLC). The detailed method of isolation and derivatization has been provided in section 2.1.

HPLC results showed that bulk crystals of *rac*-**4** contained *S* and *R*-isomer in the ratio 65:35 i.e., enantiomeric enhancement (*ee*) of 30% has occurred (Table 2.4). This closely resembles the results of structural analysis. Identical analysis were also performed with *R*-**2** and *S*-**3** as reference. Complexes *R*-**2** and *S*-**3** show presence of pure isomers as these were synthesized using enantiopure amine. As we do not have any direct tool to measure the ratio of distribution of both diastereomer in solution, rapid precipitation of *rac*-**4** without crystallization is expected to closely represent the chiral distribution present in the solution. The chiral distribution in the amorphous powder isolated by rapid precipitation showed negligible *ee* for 1-phenylethylamine (Table 2.4). This indicates that the chiral enhancement observed is a result of crystallization. Seeding (addition of few crystal of pure diastereomer to the solution

mixture of rac-amine) crystallization with a specific diastereomer is known to influence the chiral distribution in the resulting crystals.[11]

Table 1.4 Chiral distributions in bulk complexes either as crystals or amorphous solid determined by HPLC analysis.[1]

Guest	Isolated yield (%)	R	S	% ee
Condition: Guest isolated from Crystals washed with MeCN				
R-(-)-(α)-1-phenylethylamine	70	99	1	98
S-(+)-(α)-1-phenylethylamine	75	0	100	100
Racemic-1-phenylethylamine	60	35	65	30
2-amino-1-propanol	65	90	10	80
1-amino-2-propanol	75	0	100	100[2]
Condition: Guest isolated from amorphous precipitate[3]				
Racemic-1-phenylethylamine	85	48	52	4
2-amino-1-propanol	85	58	42	16
1-amino-2-propanol	85	40	60	20
Condition: Guest isolated from crystals washed thrice with MeCN:MeOH (3:1)				
Racemic-1-phenylethylamine	45	26	74	49
	filtrate from washing	71	29	42
*Condition: Crystal formation was seeded with one crystal of (S)-***3,** *washed with MeCN.*				
Racemic-1-phenylethylamine	50	26	74	49
*Condition: Crystal formation was seeded with one crystal of (R)-***2,** *washed with MeCN.*				
Racemic-1-phenylethylamine	45	46	54	8

[1] Each experiment were performed with 200 mg of **1** and guest amine in 1:1 ratio in 10 mL of MeOH. [2] Ref.1. [3]MeCN was used as precipitant.

The chiral distribution in the present case was found to be dependent upon seeding as well as method of washing. Seeding with crystal of *S*-**3** results enhancement of *ee*

upto 49%. Seeding with opposite diastereomer results reduction of the *ee* to merely 8%. Washing of the crystals with methanol/acetonitrile mixture increases *ee* value from 30 to 49% (Table 2.4). This can be due to partial solubilization of the *R*-amine. Seeding experiments strongly suggest that crystallization played prime role in enhancing chiral resolution of 1-phenylethylamine. However, none of the controls could enhance *ee* value beyond 49%.

To compare, we performed similar analysis on two amino alcohols (Table 2.4). The recognition for amino alcohols, unlike 1-phenylmethylamine, in the crystalline state could reach well above the 80% *ee* mark. However, analysis of precipitated complex as amorphous solid showed recognition in solution varies widely. The 1-amino-2-propanol showed 20% *ee* in precipitated solid, which reached 100% *ee* after crystallization. Recognition of 2-amino-1-propanol in amorphous state showed 16%*ee* enhancement, but reaches to 80% *ee* in the crystalline state. In general, amino alcohols showed higher enhancement in the crystalline state than 1-phenylmethylamine.

2.4.8 Effect of the solubility and crystalization on chiral enahancement

The results presented above showed that crystallization played important role in chiral enhancement. Seeding with *S*-**3**, during crystallization of *rac*-**4** (Table 2.4) considerably increases the value of *ee* of *S*-isomer from 30% to 49%, which establishes that the initial nucleation of *S*-**3** guide the crystallization to the observed chiral enhancement in the isolated bulk. The ratio and type of crystal seeding depend on both solubility and solution equilibrium favoring a particular diastereomer. Upon checking, the solubility of *S*-**3** (13mg/mL) is found to be lower than *R*-**2** (24mg/mL) in methanol. This lower solubility of *S*-**3** perhaps help enhancement of *S*-isomer

despite the poor excess in solution equilibrium (4% *ee*). In case of 1-amino-2-propanol, higher initial excess of *S*-isomer (20%) leads to highest chiral enhancement of 100%. Thus chiral enhancement, in the present cases, is a result of shift in solution equilibrium enhanced further by crystallization.

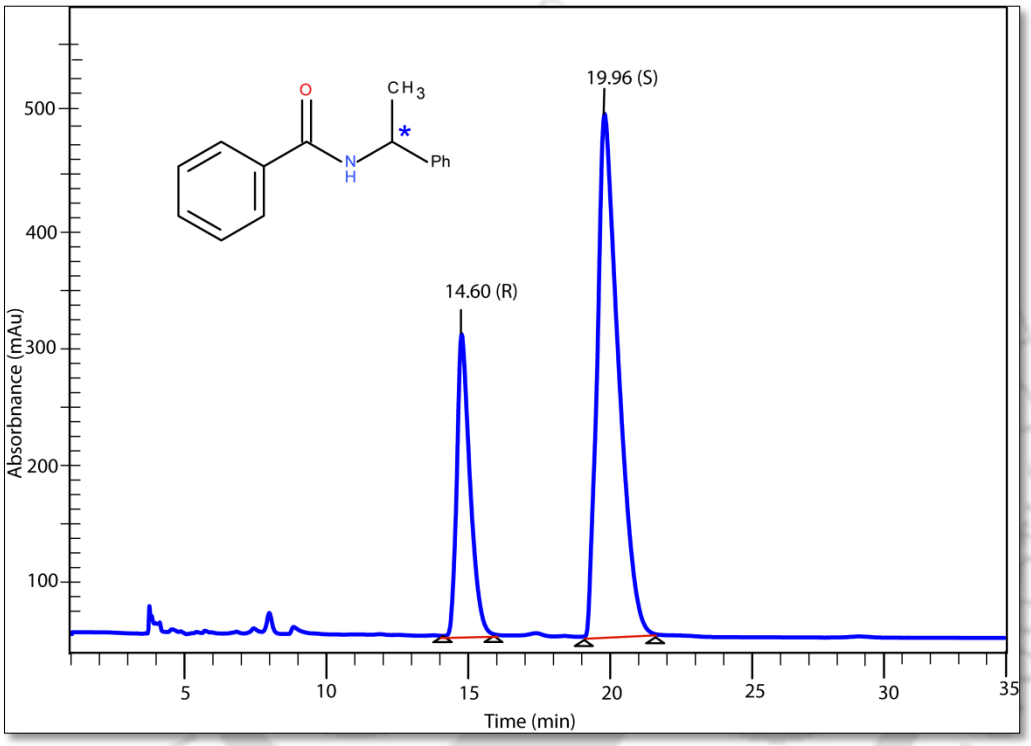

Figure 2.7 HPLC trace of devatized amine recovered from the crystals of *rac*-**4**.

This lead to two questions: (a) what are the factors that determine initial equilibrium in solution? And (b) what are the factors that improve the enhancement during crystallization? Ideally, chiral recognition is more efficient when three out of four groups around the chiral centre are recognized by the host (three point recognition). Stronger the host-guest interaction, one enantiomer will fit better (lower in energy) resulting in a shift of equilibrium. Comparing structures of 1-phenylethylamine with 1-amino-2-propanol, we observed that host-guest interactions are stronger in case of amino alcohol due to the alcoholic –OH. Further, complex

with 1-amino-2-propanol is the only one where ideal three point recognition (three out of four group around chiral centre, $-NH_3^+$, -OH through H-bonding and chiral hydrogen through CH…π) occurred. This is perhaps the reason for considerable chiral enhancement present in solution for 1-amino-2-propanol. In case of 1-phenylethylamine, except the ammonium ion, interactions are through weaker CH…π type, which is inherently susceptible to the interference by solvent. In case of 2-amino-1-propanol, the chiral center is on a different carbon than 1-amino-2-propanol. This might have affected its solution equilibrium due to the lack of enough chiral discrimination between enantiomer by the host.

For indentifying the factors responsible for chiral enhancement during crystallization, we compared the structures. The structures of *R*-**2** and *S*-**3** remain a range of non-covalent interactions.[9] Many of them are of weaker variety. Participation of polar solvent posed further difficulty in assigning their relative contributions to chiral enhancement. H-bonding, being the strongest among the various non-bonded interactions observed, definitely played key role in the chiral enhancement during crystallization. For amino alcohols, despite the wide variation in solution equilibria (4-20% *ee*), the presence of alcoholic –OH might have influenced higher enantiomeric excess after crystallization. In case of 1-phenylethylamine, the combinations of lower solubility of *S*-**3** and capability of the channels accommodating both isomers might have influenced the outcome.

2.5 Conclusions

Our previous communication showed that (*S*)-1-amino-2-propanol gets recognized in the cavity through ideal three point recognition leading to 100% *ee*. However, the relative contribution of crystallization over chiral distribution in

solution was outside the scope of that investigation. Results presented in this section revealed that solution chiral distribution of 1-phenylethylammonium is marginal (4% *ee*) while that of 1-amino-2-propanol is about 20% *ee*. The enhancement of 49% *ee* for 1-phenylethylamine could be achieved through crystallization.

In case of amino alcohols, the enhancement due to crystallization is between 80-100% *ee*. The structures contained multiple types of intra and inter-molecular non-covalent interactions. These and the participation of solvent molecules in the H-bonding posed difficulty in determining relative contribution of individual interactions towards chiral enhancement. However, amino alcohols showed considerably higher enhancement during crystallization probably owing to participation of the alcoholic –OH in the H-bonding. Understanding the mechanism of chiral recognition using non-covalent interactions is important both in terms of biology as well as resolution of chiral drugs. It is not often that one gets an opportunity to observe the recognition for a range of guests through crystallography and connect the findings with the chiral separation on the bulk. The anionic Ni(II) binuclear complex, used in the present study, provided that unique opportunity. The crystals with both enantiomers of 1-phenylethylamine (*R*-**2** and *S*-**3**) were isolated and compared with those from racemic mixture (*rac*-**4**). The morphology of the crystals and network within the lattice of *R*-**2** and *S*-**3** varied widely. The structural analysis and HPLC on the isolated amine from crystals of *rac*-**4** support single type of crystal containing a distribution of *R*- and *S*- isomer of guest cation within the channels of crystal. The chiral enhancement of *S*-isomer could be attributed to a combination of lower solubility and channel structures in the lattice.

2.6 References

1. Sahoo, S.C.; Ray, M. *Chem. Eur. J.* **2010**, *16*, 5004.
2. *Chiral Recognition in Separation Methods: Mechanisms and Applications*; Berthod, A., Ed.; Spinger: New York, **2010**. (ISBN: 978-3-642-12444-0) (b) Fiedler, D.; Leung,D. H.; Bergman, R. G.; Raymond, K. N. *Acc. Chem. Res.* **2005**, 38. (c) Hembury, G. A.; Borovkov, V. V.; Inoue, Y. *Chem. Rev.* **2008**, *108*, No. 1 (d) Zhang, X. X.; Bradshaw, J. S.; Izatt, R. M. *Chem. Rev.* **1997**, *97*, 3313. (e) Bradshaw, J. S.; Izatt, R. M.; Bordunov, A. V.; Zhu, C. Y.; Hathaway, J. K. Crown Ethers. *In Comprehensive Supramolecular Chemistry; Gokel*, G. W. Ed.; Pergamon Press: New York, **1996**; Vol. *1*, 35. (f) Gokel, G. W.; Abel, E. *In Comprehensive Supramolecular Chemistry*; Gokel, G.W. Ed.; Pergamon Press: New York, **1996**; Vol. 1, 511. (g) Nugent, T. C. In a*symmetric Reductive Amination. In Chiral Amine Synthesis. Methods, Developments and Applications*, Nugent, T. C. Ed.; Wiley-VCH: Weinheim, **2010**, 225. (h) Echegoyena, L.; Martínez-Díaz, M.V.; Mendoza, J.; Torres,T.; Vicente-Arana, M.J. *Tetrahedron.* **1992**, *48*, 9545. (i) Nugent, T. C.; Marinova, S. M. *Synthesis* **2013**, *45*, 153. (j) Kida,T.; Iwamoto, T.; Asahara, H.; Hinoue, T.; Akashi, M. *J. Am. Chem. Soc.* **2013**, *135*, 3371. (k) Sun, C.; Ren, C.; Wei, Y.; Qinb, B.; Zeng, H. *Chem. Commun*., **2013**, *49*, 5307.
3. (a) Mustranta, A.; *Appl. Microbiol. Biotech.* **1992**, *38*, 61.(b) Cheng, H.; Rogers, J. D.; Demetriades, J. L.; Holland, S.; Seibold, J; Depuy, E. *Pharmaceutical Res.*, **1994**, *11*, 824. (c) Lioyd, L.G.; Davidson, L.; Hornykiewicz,O.; *J. Pharmacol Exp. Ther.* **1975**, *195*, 453. (d) Caner,H.; Groner, E.; Levy, L.; *Drug Discovery Today*, **2004**, *9*, 105.

4. Jacques, J.; Collet. A.; Wilen, S. H. *Enantiomers, Racemates, and Resolutions*, Krieger Publishing Company, Malabar, FL, **1994**.
5. (a) Easson, L.Hz; Stedman, E. *Biochem*. J. **1933**, *27*, 1257. (b) Dalgliesh, C.E. *J. Chem. Soc.* **1952**, 3940. (c) Lochmiiller, C.H.; Souter, R.W. J. *Chromatogr.* **1975**, *113*, 283. (d) Dalgliesh, C.E. *J. Chem.Soc.* **1952**, *137*, 3940. (e) Meyer, V.R.; Rais, M. A. *Chirality* **1989**, *1*, 167. (e) Davankov, V. A.; Meyer V. R.; Rais, M. *Chirality* **1990**, *2*, 208.
6. (a) Davankov. V.A., *Chirality* **1997**, *9*, 99. (b) Berthod. A. *Anal.Chem*, **2006**,*78*, 2093.
7. (a) Haginaka, J. *J. Pharm. Biomed. Anal*. **2002**, *27*, 357. (b) Gu. bitz, G.; Schmid, M.G. *Biopharm. Drug Dispos*. **2001**, *22*, 291. (c) Amini, A. *Electrophoresis* **2001**, *22*, 3107. (d) Schurig, V. *J. Chromatogr. A* **2001**, *906*, 275. (e) Boer, T.; Zeeuw, R.A.; Jong, G.J.; Ensing, K. *Electrophoresis* **2000**, *21*, 3220. (f) Francotte, E. *Chromatography as a separationtool for the preparative resolution of racemiccompounds. In Chiral Separations: Applicationsand Technology*; Ahuja, S., Ed.; AmericanChemical Society: New York, **1996**, 271. (g) Li, B.; Haynie, D.T. *Biomacromolecules* **2004**, *5*, 1667. (h) Rmaile, H.H.; Schlenoff, J.B. *J. Am. Chem. Soc.* **2003**, *125*, 6602. (h) Xiong, R. G.; You, X. Z.; Abrahams, B. F.; Xue, Z.; Che,.C. M. *Angew. Chem*. **2001**, *113*, 4554. (i) Seo, J. S.; Whang, D.; Lee, H.; Jun, S.; Oh, I. J.; Jeon, Y.; Kim, J. K. *Nature* **2000**, *404*, 982. (j) Ishi-i, T.; Calama, M. C.; Timmerman, P.; Reinhoudt, D. N.; Shinkai, S. *Angew. Chem. Int. Ed.* **2002**, *41*, 1924. (k) Ishi-i, T.; Mateos-Timoneda, M. A.; Timmerman, P.; Calama, M. C.; Reinhoudt, D. N.; Shinkai, S. *Angew. Chem. Int. Ed.* **2003**, *42*, 2300. (d)

Fiedler, D.; Leung, D.H.; Bergman, R. G.; Raymond, K. N. *J. Am. Chem. Soc*. **2004**, *126*, 3674. (l) Reeve, T. B.; Cros, J.; Gennari, C.; Piarulli, U.; Vries J. G. *Angew. Chem. Int. Ed*. **2006**, *45*, 2449. (m) Imai, H.; Munakata, H.; Uemori, Y.; Sakura, N. *Inorg. Chem*., **2004**, *43*, 1211. (n) Tashiro, S.; Ogura, Y.; Tsuboyama, S.; Tsuboyama, K.; Shionoya M. *Inorg. Chem*. **2011**, *50*, 4. (o) Li, Z. J.; Yao, J.; Tao, Q.;Jiang, L.; Lu, T.B. *Inorg. Chem*. **2013**, *52*, 11694.

8. Conductance values were compared following (a) Geary, W. J. *Coord. Chem. Rev*. **1971**, *7*, 81. Room temperature magnetism data compared following (b) Earnshaw, A. *Introduction to Magnetochemistry*, Academic press, London, **1968**. (c) Figgis, B. N.; Lewis, *J. Prog. Inorg. Chem*. **1964**, *6*, 37.

9. (a) Nishio, M.; Hirota, M.; Umezawa, Y. 1998 The CH…π interaction; Wiley-VCH: New York (b) Desiraju, G.R.; Steiner, T.; **1999** in The weak hydrogen bond; Oxford University Press: New York (c) Desiraju, G. R. *Acc. Chem. Res* **2002**, *35,* 565.

10. Li, Z. J.; Yao, J.; Tao, Q.;Jiang, L.; Lu, T.B. *Inorg. Chem*. **2013**, *52*, 11694.

11. (a) Kinbara, K.; Hashimoto, Y.; Sukegawa, M.; Nohira, H.; Saigo, K. *J. Am. Chem. Soc*. **1996**, *118*, 3441. (b) Gernez, D. *C. R. Acad. Sci*. **1866**, *63*, 843.

Chapter- 3

Change in crystallization pathway by modifying cavity

In the previous chapter, using the binuclear Ni(II) complex with L-histidine derived reduced Schiff base ligand as host, we observed partial resolution of 1-phenylethylamine where crystallization played the dominant role.[1] Chiral separation involving crystallization is a combination of multiple factors. Differences in solution equilibrium, solubility between diastereomers and inter molecular non-covalent interactions[2], all contribute to the final outcome. Some of these factors such as solubility difference and interactions within lattice can be interconnected. Identification of these factors and their relative contribution towards the final separation can lead to modifications necessary for efficient chiral resolution. The crystal structures of diastereomers showed that H-bond between imidazole of L-histidine and carboxylate played major role in the formation of substantially different lattice architecture for the diastereomers, which in turn resulted in substantial solubility difference between diastereomers. This lead to questions: what happens if this interaction is absent? Will it affect resolution?

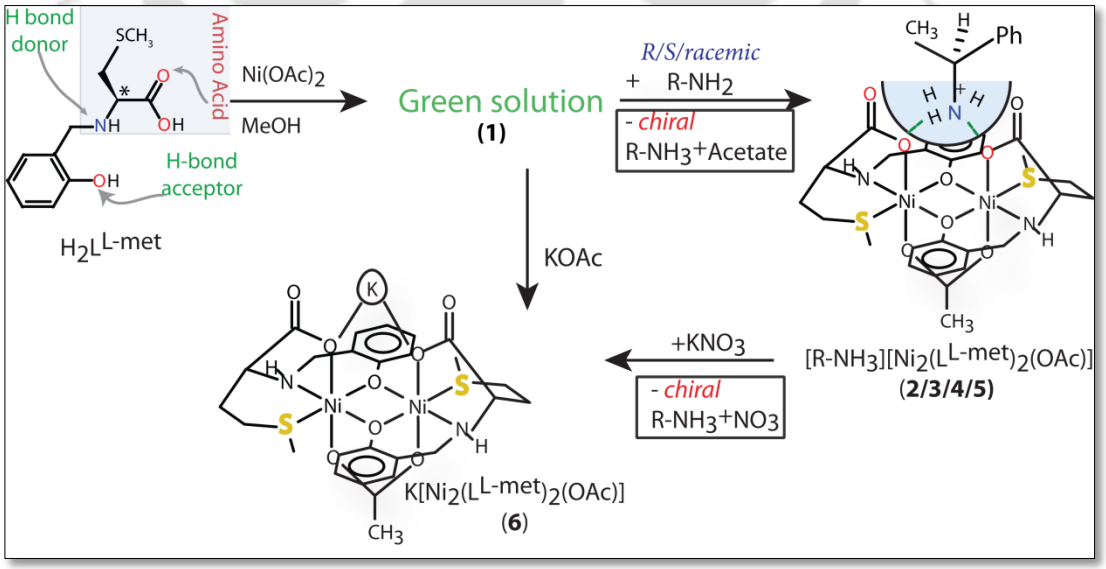

Scheme 3.1 Schematic presentation of direct synthesis of binuclear host-guest adduct from ligand $H_2L^{L\text{-met}}$ and $Ni(OAc)_2$ in presence guest amine.

Thus, in this chapter, our effort is to synthesis of a new L-methionine derived analogous system (Scheme 3.1), which lacks the imidazole group. By following the similar protocol established in Chapter 2, we would try to isolate the complexes from reaction with racemic-amine. Both the pure diastereomers using enantiopure amine in reaction will be synthesized for references purpose. We would also study on the resolution process through structural characterization of the diastereomers correlating the structural observation with that of crystallization pathway.

3.1 Material and Methods

3.1.1 Solvents and reagents

Details of the solvent purification and analytical measurements have already discussed in Chapter 2. L-methionine was purchased from Merck limited and used as received. The ligand $H_2L^{L\text{-met}}$ was prepared following reported procedures.[3]

3.1.2 Measurements

All the details of instrument used for analysis have already discussed in Chapter 2.

The crystals of complexes were mounted on glass fiber. All geometric and intensity data for the crystals were collected at room temperature using a Bruker SMART APEX CCD diffractometer equipped with a fine focus 1.75 kW sealed tube Mo-Ka (λ = 0.71073 Å) X-ray source, with increasing ω (width of 0.3º per frame) at a scan speed of either 3 or 5 s/frame. The SMART software was used for data acquisition and the SAINT software for data extraction. Absorption corrections were done using SADABS. After the initial solution and refinement with SHELXL, the final refinements were performed on WinGX environment using SHELX97. All non-hydrogen atoms in the complexes were refined anisotropically. Wherever possible, the

hydrogen atoms were located from the difference Fourier maps and were refined isotropically. Thus some of the C-H bonds will not be ideal and may vary. Some of C-C bonds have been restrained using DFIX, ISOR instruction in some complexes. Most of the hydrogen atoms attached to the solvent molecules could not be located or fixed, so the molecular weight may not match. Crystallographic data and details of refinements are listed in Table 3.1, and selected bond distances and angles for are listed in Table 3.2a. Perspective views of the complexes were shown using ORTEP.

3.2 Syntheses

Detailed synthetic procedures along with characterization data has been provided below.

3.2.1 *S*-2-(2-Hydroxybenzylamino)-4-methylsulfanylbutyric Acid. [$H_2L^{L\text{-}met}$]. A mixture of L-methionine (0.50 g, 3.35 mmol) and $LiOH.H_2O$ (0.14 g, 3.36 mmol) in methanol (dry, 15 mL) was stirred for 30 min, and salicylaldehyde (0.41 g, 3.36 mmol) in methanol was added slowly drop by drop. After the mixture was stirred for 20 min, a clear yellow color solution was obtained. The solution was treated with sodium borohydride (0.12 g, 3.35 mmol) with constant stirring upon which the solution became colorless. The solvent was evaporated using a rotary evaporator. The resulting sticky mass was dissolved in water. Clear solution was obtained, which was then acidified with dilute HCl and solution pH was maintained at 5 -7. The ligand as a white solid was precipitated out. The solid was filtered and thoroughly washed with water. The solid was dried under reduced pressure inside a desiccator. Yield 0.80 g (82%). Anal. Calcd for ($C_{12}H_{17}NO_3S$): C, 56.44; H, 6.71; N 5.48. found: C, 55.92; H, 6.74; N, 5.37. ^{1}H NMR Li_2 $L^{L\text{-}met}$ (CD_3OD, 400 MHZ. ppm): 2.06 (s, 3H, CH_3S), 2.57 (m, 2H, CH2-S), 1.97 (m, 1H, CHCHH), 1.86 (m, 1H, CHCHH), 3.19 (dd, 1H, CH),

3.83 (d, 1H, CHH-phenolate), 3.44 (d, 1H, CHH-phenolate), 6.44 (t, 1H, p-phenolate), 6.97 (m, 2H, m-phenolate), 6.65 (d, 1H, ophenolate). IR (KBr, cm^{-1}) $\upsilon(COO)_{asym}$ 1615(s); $\upsilon(COO)_{sym}$1439(m). $[\alpha]_D^{25}$ = -42° in MeOH, c = 1.00 g/100 mL, in presence of 2 equ. of $LiOH.H_2O$.

3.2.2 [$Ni^{II}(HL^{L\text{-}met})(OAc)(MeOH)$] (1). The ligand $H_2L^{L\text{-}met}$ (0.500 g, 1.96mmol) and $Ni(OAc)_2.4H_2O$ (0.487 g, 1.96mmol) were mixed in MeOH and kept stirring. Within 5 min. ligand was dissolved leaving a clear sea green solution. After 30 min of stirring a light green compound started to precipitate. After 3h stirring solution is concentrated by rotary evaporator and 10 mL acetonitrile was added for complete precipitation. The light green solid was filtered and washed with acetonitrile, dried in vacuum desiccators. Yield: 75%. The crystals could not be obtained either from methanolic or acetonitrile solution. Anal. Calcd. for $[Ni(C_{14}NSO_5H_{19})].CH_3OH$: C, 44.65; H, 5.75; N, 3.47; found C, 44.97; H, 5.10; N, 3.23; IR (KBr, cm^{-1}) $\upsilon(COO)_{asym}$ 1594(s), $\upsilon(COO)_{sym}$ 1416(m). μ_{eff}(powder, 298K); 3.26 µB. Λ_M (ohm^{-1} cm^2 mol^{-1}): 15 (MeOH) .

3.2.3 ((*S*)-1-Phenylethylammonium)[$Ni_2(L^{L\text{-}met})_2(OAc)$] (2). The ligand $H_2L^{L\text{-}met}$ (0.250 g, 0.90 mmol) and $Ni(OAc)_2.4H_2O$ (0.243 g, 0.90 mmol) were mixed in 12 mL MeOH and kept stirring. To the see green solution (*S*)-(-)-α-1-Phenylethylamine (0.285 g, 1.80 mmol) was added and stirred 3h. The resulting sea green solution was evaporated to dryness by rotary evaporator. The sticky green mass was dissolved in 6 mL acetonitrile and methanol (v/v, 1:1) in a beaker and kept it for slow evaporation in room temperature. Blue triangular shaped crystals were obtained after 2 days. The crystals were filtered, washed with acetonitrile, dried in vacuum

desiccators.Yield:80%. Anal. Calcd. for $[Ni_2(C_{34}N_3S_2O_8H_{44})].2H_2O$: C, 48.67; H, 5.77; N, 5.01; found C, 48.32; H, 5.63; N, 5.15; IR (KBr, cm^{-1}) $\upsilon(COO)_{asym}$ 1577(s), $\upsilon(COO)_{sym}$ 1478(m). μ_{eff} (powder, 298K)/Ni; 2.16 μB. Λ_M (ohm^{-1} cm^2 mol^{-1}): 80 (MeOH).

3.2.4 ((*R*)-1-Phenylethylammonium)[$Ni_2(L^{L\text{-}met})_2(OAc)$] (3): This is synthesized by following the procedure described for **1** using (*R*)-(+)-α-1-Phenylethylamine amine instead of (*S*)-(-)-α-1-Phenylethylamine. Blue hexagonal shaped crystals were obtained after 3 days. Yield: 75%. Anal. Calcd. for $[Ni_2(C_{34}N_3S_2O_8H_{44})].H_2O$: C, 49.74; H, 5.65; N, 5.12; found C, 49.59; H, 5.75; N, 5.31; IR (KBr, cm^{-1}) $\upsilon(COO)_{asym}$ 1574(s), $\upsilon(COO)_{sym}$ 1478(m). μ_{eff} (powder, 298K)/Ni; 2.70 μB. Λ_M (ohm^{-1} cm^2 mol^{-1}): 75 (MeOH).

3.2.5 (S)-1-Phenylethylammonium))[$Ni_2(L^{L\text{-}met})_2(OAc)$] (4) (*R*)-1-Phenylethylammonium)[$Ni_2(L^{L\text{-}met})_2(OAc)$] (5) from Racemic 1-Phenylethylamine: The ligand $H_2L^{L\text{-}met}$ (0.300 g, 1.17mmol) and $Ni(OAc)_2.4H_2O$ (0.291 g, 1.17mmol) were mixed in 12 mL MeOH and kept stirring. To the see green solution 1-Phenylethylamine (0.284 g, 2.35mmol) was added and stirred 3h. The resulting sea green solution was evaporated to dryness by rotary evaporator. The sticky green mass was dissolved in 6 mL acetonitrile and methanol (v/v, 1:1) in a beaker and kept it for slow evaporation in room temperature. Longer rod shaped crystals with hexagonal faces (Complex **4** and Complex **5**) were obtained. Yield: 78%.

3.2.6 K[$Ni_2(L^{L\text{-}met})_2(OAc)$] (6). The ligand $H_2L^{L\text{-}met}$ (0.250 g, 0.900mmol) and $Ni(OAc)_2.4H_2O$ ((0.243 g, 0.900mmol) were mixed in 15 mL MeOH and kept for stirring. After 30 min of stirring, to the resulting green precipitation along with green

solution, 2equi KOAc was added resulting a clear intense bluish green solution. After 1h stirring solution was concentrated to 5mL by rotary evaporator and kept for slow evaporation at room temperature. Blue block crystals were obtained after 5 days. The crystals were filtered, washed with acetonitrile, dried in vacuum. Yield: 75%.

The Crystals also were obtained from the metathesis reaction between binuclear complexes (**4**, **5**) and KNO_3. Anal. Calcd. for $K[Ni_2(C_{26}N_2S_2O_8H_{33})].6H_2O$: C, 37.67; H, 5.45; N, 3.38; found C, 37.47; H, 5.97; N, 3.89; IR (KBr, cm^{-1}) $\upsilon(COO)_{asym}$ 1574 (s), $\upsilon(COO)_{sym}$ 1480 (m). μ_{eff}(powder, 298K)/Ni; 2.67μB.

3.3 Estimation of enantiomeric separation through HPLC

Chiral amines were extracted from reaction mixture and extent of chiral separation was measured by HPLC using Chiralcel OD-H coloumn attached with UV detector at a flow-rate of 1mL /min. Hexane and isopropanol in 93:7 ratio was used as eluant. As the host-guest complexes in this Chapter are highly soluble in methanol and moderately soluble in acetonitrile, by following the previous procedure[4] from Chapter 2, extraction of bound amine from host-guest complexes could not be possible. So, the extraction procedure and organic derivative preparation (necessary for HPLC) described in Scheme 3.2 and the detailed procedures have been provided below.

3.3.1 Procedure of recovery of amine from metal complexes as crystal

The host-guest complex was dissolved in 10 mL Methanol. KNO_3 (2equ.), dissolved in minimum volume of water-methanol (1:1) was added and mixture was stirred for 6h. The solvent was evaporated to dryness. Since the sky blue mass is soluble in acetonitrile, acetone, dichloromethane and ethyl acetate, free amine was extracted from Na_2CO_3 in water-diethyl ether and the organic part was separated,

dried and evaporated to dryness. The free amine was subjected to derivatization with benzoyl chloride following procedure below (Scheme 3.2c). The derivative amide was analyzed by HPLC.

The guest amines from the crystals were also recovered by decomposition of the metal complex with dil.HCl followed by extraction of the amine from aqueous solution using ethyl acetate. The extracted amine was derivatized using the procedure described in the preceding section. HPLC results using both recovery methods were identical. However, the acidification method produces ligand fragments, which gives extra peaks in the HPLC traces.

3.3.2 Procedure of recovery of amine from amorphous metal complexes

The ligand $H_2L^{L\text{-met}}$ (0.200 g, 0.55mmol) and $Ni(OAc)_2.4H_2O$ (0.194 g, 0.55mmol) were stirred in 8 mL MeOH. After 15min. 2 equivalent of racemic mixture of 1-phenylethylamine was added to the resulting solution and stirred for 4h. The mixture was evaporated to dryness and 6 mL mixture of diethyl ether and acetonitrile (5:1) was added, a blue precipitation was obtained and filtered. From the residue free amine was recovered and derivatized by following procedure below.

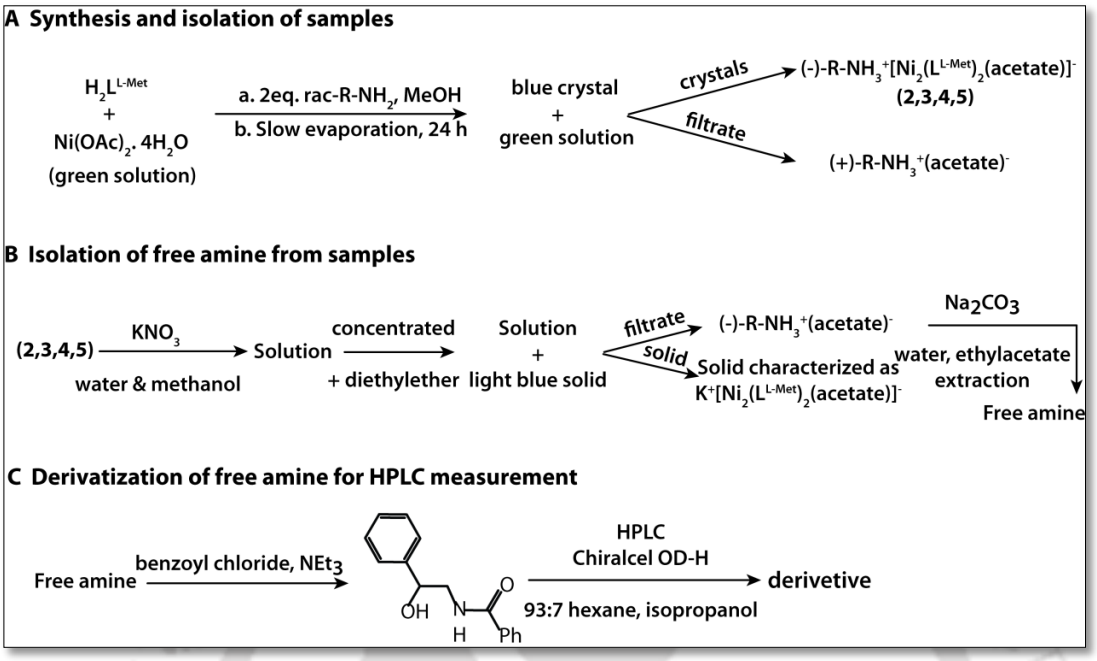

Scheme 3.2 Schematic representation of recovery of the bounded amine from host-guest complexes as either crystals or precipitations.

3.3.3 Derivatization of chiral amine With Benzoyl Chloride

By following procedure described in Chapter 2 (Section 2.3.3), we have derivatized the chiral amines recovered from host-guest complexes to corresponding amide derivative before subjecting it to HPLC run. The data of characterization of amide are identical with the previous data in Chapter 2.

3.4 Result and Discussion

3.4.1 Synthesis and characterization of monomer as chiral monobasic acid

Monomer (**1**) as green solid, was synthsized from the reaction between ligand ($H_2L^{L\text{-met}}$) and $Ni(OAc)_2.4H_2O$ in methanol and isolated as precipitation after 3h by adding acetonitrile. In spite of attaining many attempts we could not be able to obtain crystal of it.

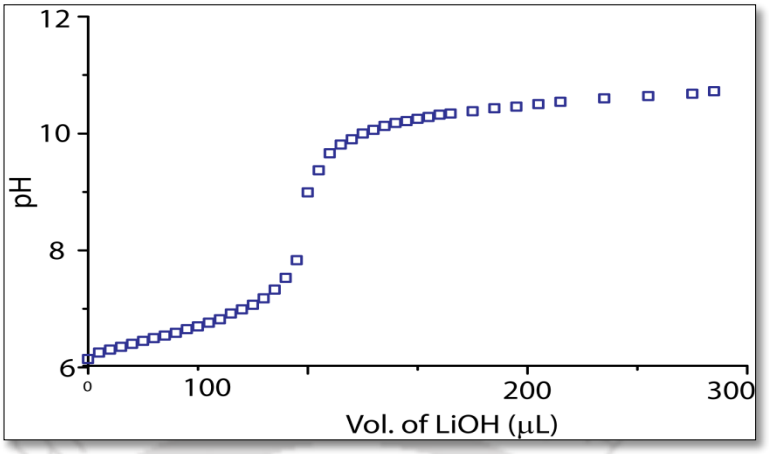

Figure 3.1 pH titration plot to determine pKa of phenolic proton in **1**.

Previously[4] we had observed that similar mononuclear Ni(II) complex with histidine derived ligand showed monobasic character which is important for the mononuclear to binuclear transformation. Thus we have performed the pH titration of the complex **1** (10mL of 1mM solution in water-methanol (v/v, 1:1)) with LiOH (1M solution in water) solution. From the plot (Figure 3.1) the pKa of the acidic proton was determined to be 6.7, which is comparable to histidine analogue's 6.6. On the basis of pH titration and other relevant analysis we assume that the green solid was monomer of Ni(II) complex having similar formulation $[Ni^{II}(HL^{L\text{-}met})(OAc)(MeOH)]$ with L-histidine analogue. The absolute structure in solid state could not be elucidated.

3.4.2 Syntheses and isolation of host-guest complexes

As the monomer behaves as monobasic weak acid, we proceed to obtain binuclear Ni(II) complexes in presence of amine as base faciliting deprotonation. Unfortunately, binuclear Ni(II) complexes with guest amine has not been crystalized out from monomer. So, Synthesis of **2** to **5** having the general formula, $(R\text{-}NH_3)[Ni_2(L^{L\text{-}met})_2(acetate)]$, where $R\text{-}NH_3^+$ were the enantiomers of 1-phenylethyl ammonium, had been carried out directly from the reaction between ligand ($H_2L^{L\text{-}met}$),

$Ni(OAc)_2.4H_2O$ and appropriate isomer of 1-phenylethylamine at room temperature. A total of three synthesis under identical conditions were carried out. In first two reactions, enantiopure (*S*)-1-phenylethylamine and (*R*)-1-phenylethylamine were used and in third reaction racemic-1-phenylethylamine was used (Scheme 3.1 & Equation 1). Crystals isolated from the first two synthesis, complex **2** and complex **3** respectively, were pure diastereomer to each other. These two serve as references. From the third reaction with racemic amine, although the isolated crystals visually resembled to each other (Figure 3.2), are found to contain both **4** and **5** upon structural characterization

$$H_2L^{L\text{-met}} + Ni(OAc)_2.4H_2O + 2\ R\text{-}NH_2 \rightarrow (R\text{-}NH_3^+)[Ni_2(L^{L\text{-met}})_2(OAc)] + (R\text{-}NH_3^+)(OAc) \quad \text{----------} \quad (1)$$

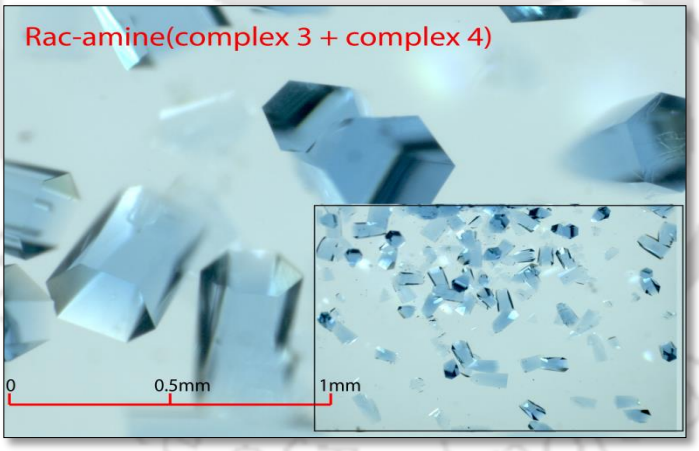

Figure 3.2 Microscopic image of crystals yielded from racemic-1-phenylethylamine (**4** and **5**).

Good quality crystals were obtained within 3 days from the acetonitrile-methanol solution, upon keeping at room temperature, with 70-80% yield. The complex **6** is obtained from the metathesis reaction between host-guest complex and KNO_3, performed for recovery of bound amine in host-guest adduct (Scheme 3.1). The complexes were also characterized using FTIR, conductance, magnetic moment. Data are commensurate with values earlier obtained for analogus complexes.[5]

3.4.3 Crystal Structure of complex 2 and complex 3

Both **2** and **3**, synthesized using enantiopure amine, were crystallized in identical space group $P3_2$ (Table 3.1) and quite similar in terms of molecular structure (Figure 3.3 & 3.4) and lattice organization (Figure 3.5). From the crystal parameters, only length of *c* axis and cell volume show some differences (Table 3.1). The asymmetric unit in both contains one anion-cation pair, ((*S or R*)-1-phenylethyl ammonium)$[Ni_2(L^{L\text{-}met})_2(OAc)]$ and two water molecules as solvent of crystallization. The geometry and the bond parameters of anionic binuclear moiety $[Ni_2(L^{L\text{-}met})_2(OAc)]^{1-}$ is almost identical in both (Table 3.2). The binuclear moiety consists of two octahedral Ni(II) centers, each ligated with one tetradentate $(L^{L\text{-}met})^{2-}$ through one amine nitrogen, one carboxylate oxygen, one thiosulfer atom, two bridging phenolate oxygen and one bridging bidentate acetate ligand (Figure 3.3a, 3.4a). Geometry around each nickel is slightly distorted from perfect octahedron as evident from the deviation of angles from ideal 90° and 180° (Table 3.2). Comparing bond lengths and angles within first coordination sphere, both Ni(II) centers of the binuclear unit are nearly identical. The chirality of the carbon centre in $(L^{L\text{-}met})^{2-}$ is *S* conformation, originated from use of L-methionine (*S*-conformation) and after coordination with metal both the coordinated amine N atoms, N1 and N1A, have *R* conformation. The chirality on the cation of **2**, is *S* conformation while same in **3** has *R* conformation as expected. They were synthesized from pure enantiomer.

The anion contains sites for the guest cation to interact. The two carboxylate oxygen from both ligands are aligned towards each-other providing a scope of H-bonding with the cationic guest. Two phenyl ring from two ligands are flanked to each other in such a way that both alignment of carboxylate oxygen and phenyl ring

forms a C_2 symmetric molecular cloven (Figure 3.3b & c, 3.4b & c). This molecular cleft felicitate guest binding though non-covalent interaction. Similar structural features were present in the histidine analogue as well.[1, 4]

The crystals contained numbers of H-bonds and other weaker interactions (Table 3.3). The direct interactions between the anion and cation include H-bonding of two NH from cation to two of the carboxylate oxygen. The third NH is H-bonded to a solvent water molecule, which in turn H-bonded to one of the terminal carboxylate oxygen. This motif is identical in both the diastereomers (Figure 3.3d & e) and was present in histidine analogue as well. The structural differences between two diastereomers are in the weaker interactions (e.g., C15-H...O2 in **2** is absent in **3**) because of change in the chirality of the cationic amine (Figure 3.3d & e). Considering the weak nature of these interactions, it is unlikely that these differences were maintained in solution. Hence, it is convenient that no chiral enhancement was observed in solution (Table 3.4).

Use of methionine instead of histidine in the ligand has affected the lattice organization (Figure 3.5). The imidazole...carboxylate (2.75 - 2.79 Å) which contributed in network formation in histidine analogue, has been replaced by a relatively weaker (2.95 - 3.01 Å) H-bond present in both **2** and **3** (Table 3.3).

The presence of -SCH_3 also reduced the involvement of bridging carboxylate oxygen in the H-bond formation. While both the oxygen participated in the H-bonding in histidine analogue, single oxygen does so in the present system. Overall, the use of methionine has reduced the differences in lattice organization between diastereomers compared to histidine analogues (Figure 3.6).

Table 3.1 Crystallographic data and refinement parameters of complexes.

	2	**3**	**4**	**5**	**6**
empirical formula	$C_{34}H_{45}N_3Ni_2O_{10}S_2$	$C_{34}H_{45}N_3Ni_2O_{10}S_2$	$C_{34}H_{45}N_3Ni_2O_{10}S_2$	$C_{34}H_{45}N_3Ni_2O_{10}S_2$	$C_{26}H_{32}K N_2 Ni_2O_{14} S_2$
fw	837.27	837.25	837.25	837.25	817.16
T (K)	296(2)	296(2)	296(2)	296(2)	296(2)
wavelength (A°)	0.71073	0.71073	0.71073	0.71073	0.71073
crystal system	Trigonal	Trigonal	Trigonal	Trigonal	Hexagonal
space group	$P3_2$	$P3_2$	$P3_2$	$P3_2$	$P6_1$
a, A°	10.7261(2)	10.70040(10)	10.71350(10)	10.6924(3)	10.5752(16)
b, A°	10.7261(2)	10.70040(10)	10.71350(10)	10.6924(3)	10.5752(16)
c, A°	30.4997(10)	31.2020(7)	30.6919(6)	31.2461(9)	55.969(18)
V, Å ^{3}	3038.86(17)	3093.95(8)	3050.82(10)	3093.7(2)	5421(3)
z/ρ	3/1.373	3/1.348	3/1.367	3/1.348	6/1.502
μ	1.087	1.067	1.082	1.067	1.336
coll.reflns	11000	7910	10708	11770	5201
indep reflns	5500	3955	5354	5885	4766
FLACK para.	0.006(6)	-0.006(12)	0.016(8)	-0.013(11)	0.07(3)
GOF	0.999	1.025	1.033	0.921	1.115
R1 [a]	0.0304	0.0397	0.0356	0.0535	0.0649
wR2 [a]	0.0622	0.0981	0.0880	0.1130	0.1267
R1[b]	0.0387	0.0450	0.0420	0.0753	0.0709
wR2[b]	0.0651	0.1008	0.0910	0.1188	0.1289

[a] $I > 2\sigma$. [b] All data

Table 3.2 Selected bond distances (Å) and angles (°) for the Complexes.

	2	**3**	**4**	**5**	**6**
Ni1 -O1	2.078(15)	2.078(3)	2.071(2)	2.078(3)	2.057(7)
Ni1-O3	2.045(16)	2.038(3)	2.041(18)	2.038(3)	2.038(6)
Ni1-O3A	2.033(16)	2.025(3)	2.026(2)	2.025(3)	2.033(8)
Ni1-$O_{acetate}$	2.031(17)	2.042(3)	2.029(17)	2.042(3)	2.055(7)
Ni1-N1	2.064(18)	2.05(4)	2.058(2)	2.05(4)	2.066(9)
Ni1-S1	2.445(8)	2.49(12)	2.445(8)	2.49(12)	2.429(3)
Ni2- O1A	2.101(16)	2.103(3)	2.102(2)	2.103(3)	2.049(7)
Ni2-O3	2.032(16)	2.025(3)	2.022 (2)	2.025(3)	2.038(7)
Ni2-O3A	2.036(15)	2.043(3)	2.038(19)	2.043(3)	2.072(6)
Ni2-O5	2.056(17)	2.042(3)	2.051(2)	2.042(3)	2.059(7)
Ni2-N1A	2.065(2)	2.055(4)	2.059(2)	2.055(4)	2.103(9)
Ni2-S1A	2.431(7)	2.45(12)	2.434(8)	2.45(12)	2.458(3)
K-O1	-	-	-	-	2.643(9)
K-O1A	-	-	-	-	2.672(7)
N1-Ni1-S1	90.39(6)	89.42(11)	90.06(6)	89.70(11)	88.9(2)
O3-Ni1-O3A	81.51(6)	81.86(12)	81.50(8)	81.93(12)	84.3(3)
N1- Ni1-O1	80.70(6)	80.69(13)	80.45(8)	80.33(14)	81.2(3)
S1-Ni1-$O_{acetate}$	89.89(5)	89.51(9)	89.93(6)	89.57(9)	92.9(2)
O1-Ni1-$O_{acetate}$	173.81(6)	175.11(13)	173.93(9)	174.95(13)	173.0(3)
N1A-Ni2-S1A	89.73(6)	88.59(12)	89.13(6)	88.37(10)	89.2(2)
O3A-Ni2-O3	81.74(6)	81.72(13)	81.69(8)	81.64(12)	83.3(3)
N1A-Ni2-O1A	80.46(7)	80.82(15)	80.58(9)	80.01(14)	81.0(3)
S1A-Ni2-O5	90.54(5)	89.59(12)	89.99(6)	88.89(12)	89.3(2)
O1A-Ni2-O5	172.45(7)	173.82(13)	173.19(9)	173.90(14)	179.2(3)

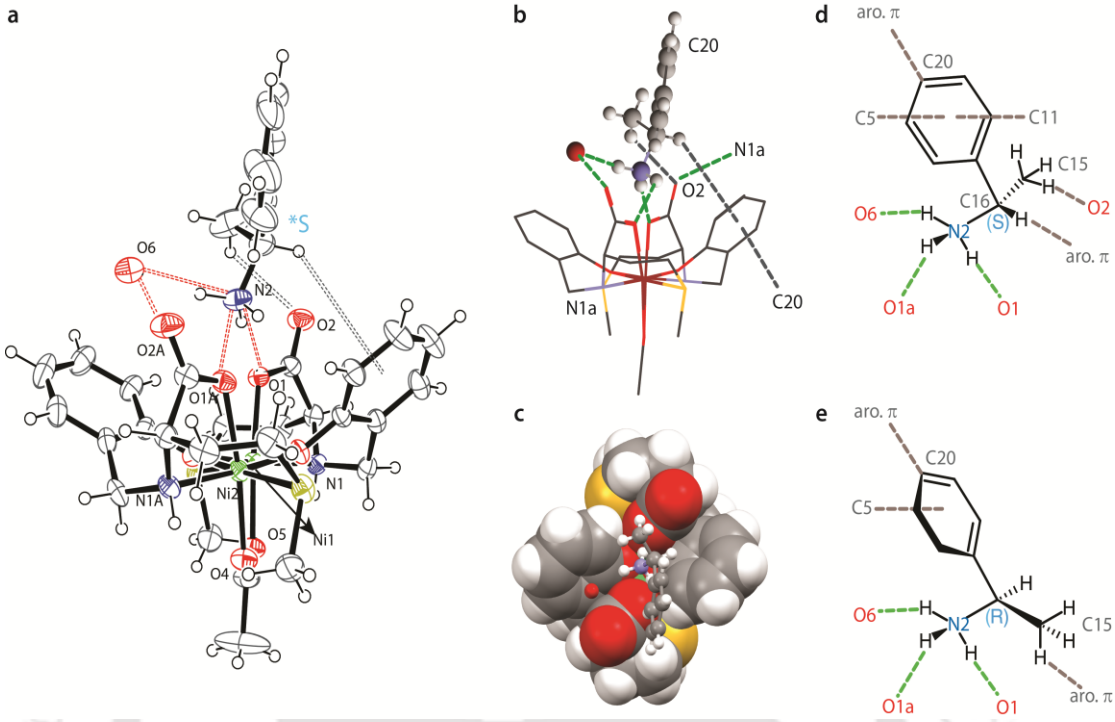

Figure 3.3 The ORTEP diagram (with 40% ellipsoid probability) (a), molecular structure of host-guest adduct (b) and space-filling model with guest amine (ball and stick) of complex **2**. Comparing major non-covalent interaction (green, H-bonding and grey, CH…π) present between guest amine, host and solvents molecules between complex **2** (*S*-amine) (d) and complex **3** (*R*-amine) (e).

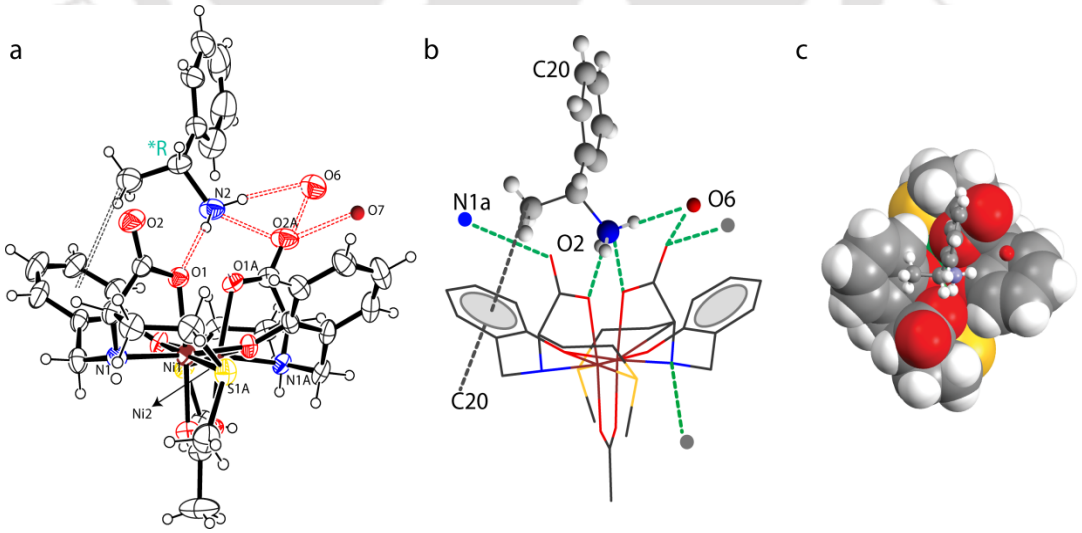

Figure 3.4 The ORTEP diagram (with 40% ellipsoid probability) (a), molecular structure of host-guest adduct (b) and space-filling model with guest amine (ball and stick) of complex **3**.

Table 3.3 Distances (Å) of H-bonding and other interactions present in complexes.

	D-H···A	D-H (Å)	H···A(Å)	D···A(Å)	DHA(°)
2	Direct Host-Guest interaction				
	N2 –H2B...O1	0.82	1.90	2.717	171
	N2 –H2C...O1A	0.88	2.33	2.853	118
	N2 –H2A...O6*	0.95	2.05	2.973	163
	C16-H16···π	0.98§	3.72§	4.3987§	127§
	Other non-covalent interactions				
	N1A –H1A...O2	0.91	2.18	2.957	143
	N1 –H1A...O6*	0.91	2.29	3.173	162
	C11A – H11A···π	0.93§	3.17§	3.882§	135§
	C20 – H20···π	0.93§	2.89§	3.801§	150§
3	Direct Host-Guest interaction				
	N2 –H2A...O1	0.89	2.08	2.846(6)	144
	N2 –H2B...O1A	0.89	1.87	2.732(5)	161
	N2 –H2C...O6*	0.89	2.19	3.036(6)	159
	C15 – H15C…π	0.961§	2.915§	3.417§	112§
	Other non-covalent interactions				
	N1A –H1A...O2	0.96	2.12	3.013	154
	N1 –H1...O6*	0.91	2.41	3.277	159
	C5 – H5Y… π	0.96§	3.14§	3.813§	129§
	C20 – H20… π	0.90§	2.51§	3.429§	167§

* Solvent Methanol/water
§ distance measured from Mercury view

3.4.4 Crystal Structure of complexes 4 and 5

The crystals isolated from racemic amine were rod shaped with hexagonal face (Figure 3.2). We randomly picked four crystals and structurally characterized all four of them. Three of them were solved with (*S*)-1-phenyethylamine as cataonic guest and one is solved with (*R*)-1-phenyethylamine These explicitly indicate crystal of complex **4** is actually crystal of complex **2** and crystal of complex **5** is actually crystal of complex **3**. Crystal parameters of **4** and **5** have been provided in Table 3.1 and bond parameter comparison has been provided in Table 3.2. The dataset of **4** and **5** were of sufficient quality (R1 value of all data 4% for **4** and 7% for **5**) and free from any major disorder (unlike histidine analogue[1]) for ascertaining chirality on the cation (Figure 3.6). Thus the crystals from racemic amine reaction produced mixture of separate crystals of both pure diastereomers. This observation is completely different

from what was observed previously in L-histidine analogue system (Scheme 3.2). In L-histidine analogue, there was only single type of crystals having both enantiomers of amine (*S*:*R* =60:40) within the channels of the crystal lattice. In molecular structure of host-guest complex, the guest amine was highly disordered in histidine analogue. No such disorder present in cationic guest amine was observed in either **4** or **5**. These observations support formation of both individual crystal of pure diastereomer in a mixture.

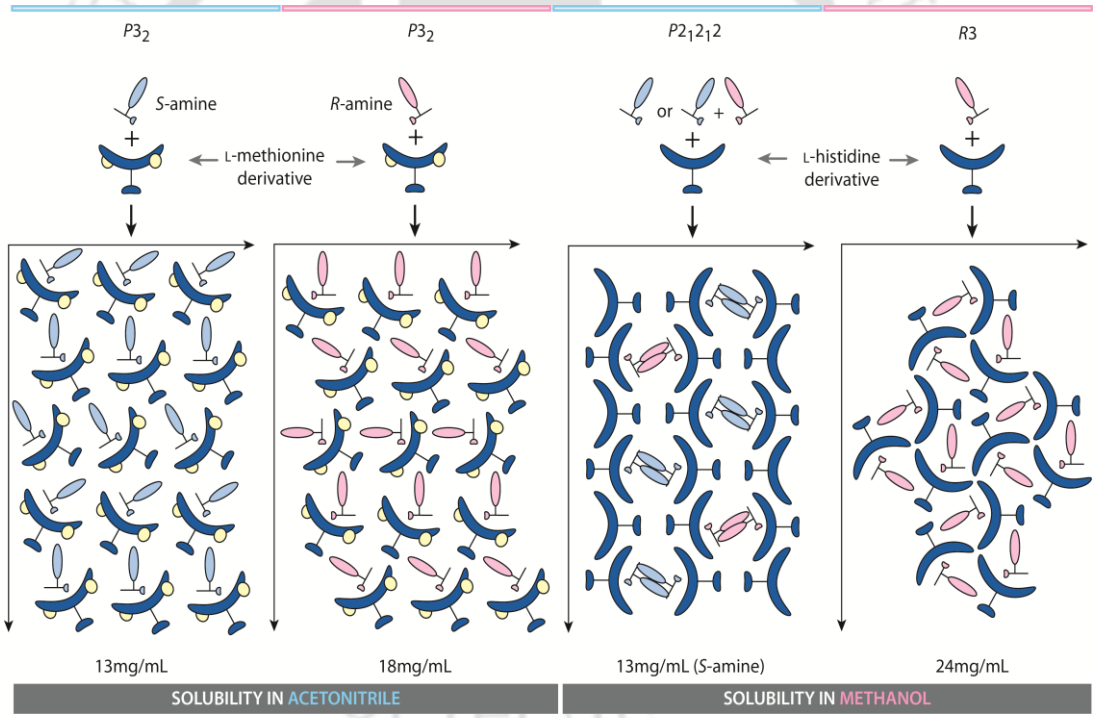

Figure 3.5 The differences and similarities between diastereomers for both the hosts are highlighted by two-dimensional cartoon representation of the crystal lattices.

3.4.5 Crystal Structure of complexes 6

The complex **6** was crystallized in space group $P6_1$. X-ray structure of **6** shows that complex contains one molecule of anionic binuclear Ni(II) entity and K^+ and four molecules of lattice water and two coordinated water molecules. K^+ ion is encapsulated in the host cavity by the coordination with carboxylate oxygen and the

two water molecule (Figure 3.7). All the bond angels and bond length are in Table 3.1 and Table 3.2.

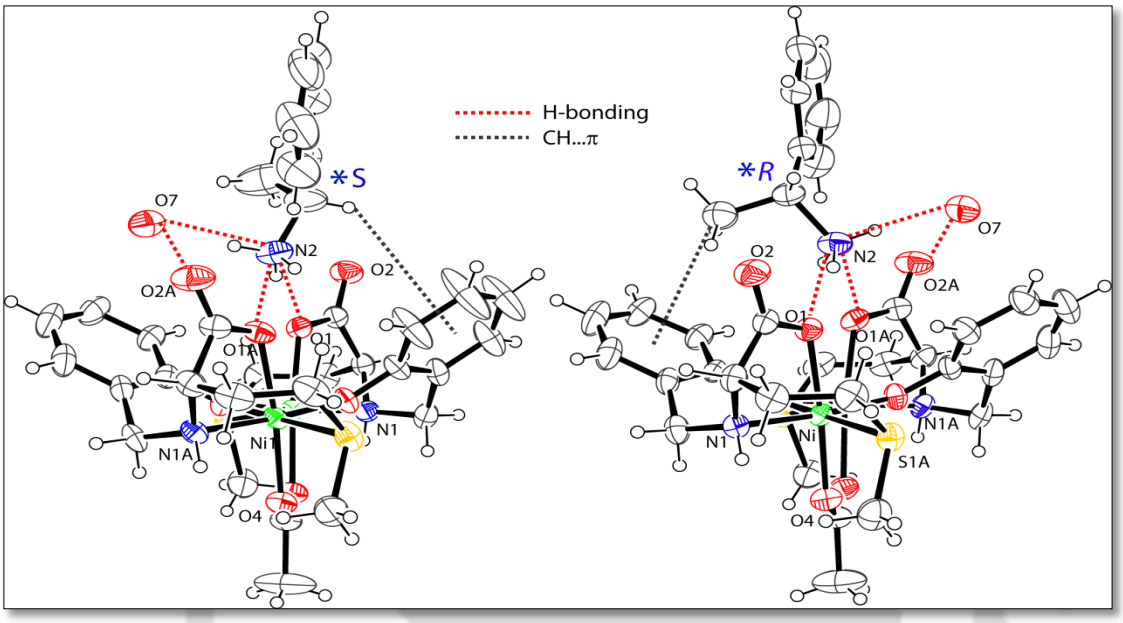

Figure 3.6 ORTEP diagram of complexes **4** and **5** obtained from reaction with racemic amine**.**

3.4.6 Chiral enahancement determined by the HPLC analysis

From our ealier report, recovery and isolation of the recognized guest amine has been accomplished by metathesis reaction with a potassium salt, as the binding constant with potassium ion is high.

The enantiomeric distribution in the bulk (all crystals) was determined using HPLC. HPLC analysis has been performed with the recovered amine from the bulk of crystals isolated from racemic amine. The result showed that chiral enhancement of 30% *ee* has been occurred after crystallization. Since we do not have any direct tool to estimate the chiral distribution in solution equilibrium, enhancement observed in amorphous solid obtained by rapid precipitation (addition of diethyl ether) can be considered as chiral enhancement in solution. The results show the ratio of chiral

distributions of both isomer is 50:50 (Table 3.4), indicating no shift in equilibrium. Thus chiral enhancement has occurred during crystallization[6] process similar to histidine analogue. Compared to this, chiral amino alcohols with histidine analogue show enhancement even in the amorphous state. The results have been tabulated in Table 3.4.

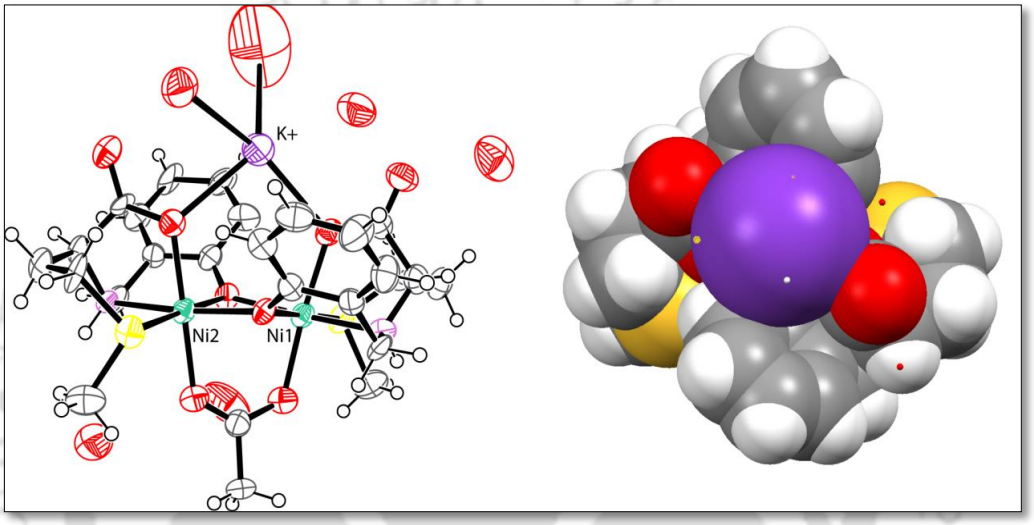

Figure 3.7 ORTEP diagram and Space-fill model of complex **6**.

Another difference between histidine and methionine derived host is that, methionine system does not show any seeding (addition of one crystal of pure diastereomer to the reaction mixture of racemic-amine during crystallization through slow evaporation) effect unlike histidine analogue.

Similar analyses are also performed on diastereomers obtained from pure amine (**2** and **3**) as well, which serve as reference. Pure diastereomers showed 98-100% *ee* as these were prepared from pure enantiomer of amine. The slightly lower % *ee* of *R*-isomer could be due to slightly higher stability of the *S*-isomer. But as the data is within 2% error (1% for individual isomer in HPLC), it is inconclusive.

Table 3.4 Chiral enhancement in bulks complexes determined by HPLC anlysis.

Guest	Isolated yield (%)	R	S	% *ee*
R-(-)-(α)-1-Phenylethylamine	70	99	1	98
S-(+)-(α)-1-Phenylethylamine	75	0	100	100
Racemic-1-Phenylethylamine	60	35	65	30
Condition: Guest isolated from amorphous precipitate[*]				
Racemic-1-Phenylethylamine	85	50	50	0

** by using diethylether and acetonitrile (3:1) for precipitation*

3.4.7 Effect of solubility difference

HPLC results showed that the observed chiral enhancement is mainly a result of crystallization. The solubility difference between diastereomers influences the nucleation of crystals and rate of the crystal growth (Scheme 3.2). The solubility of the pure diastereomers were measured and found to be lower in case *S*-isomer (13 mg/mL for S-isomer vs. 18 mg/mL for R-isomer). The difference is not as drastic as was for histidine isomer (Figure 3.4). It is likely that smaller difference allow both diastereomers to form crystals with a bias towards *S*-isomer (lower solubility). This result is attributed to the final distribution observed in HPLC results. This lower difference in solubility and similarity of the crystal lattice between two pure diastereomer probably promoted the formation of separate crystals of both pure diastereomer in a mixture in the present case (Scheme 3.2). In case of histidine analogue, along with the large solubility difference, there is also huge difference in crystal lattice between two diastereomers. One of the diastereomers has accommodating property of both isomeric amines inside the channel. These two factors perhaps facilitate a single type of crystal formation.

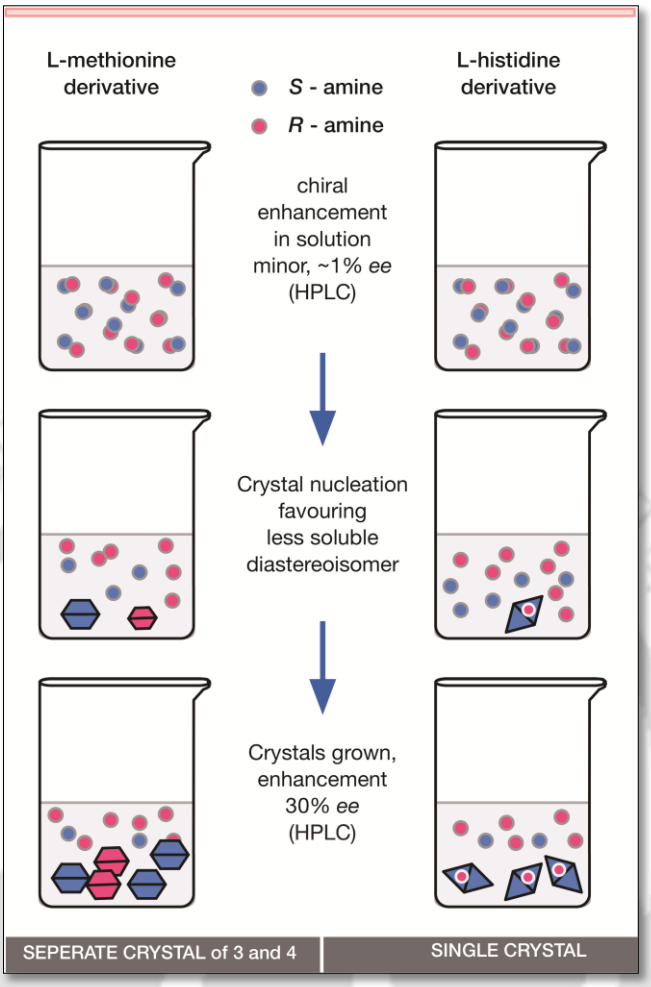

Scheme 3.2 Comparison of steps of crystallization between L-methionine and L-histidine based hosts.

3.4.8 Powder X-Ray Diffraction analysis of 2 and 3

The X-ray powder diffraction patterns were recorded for **2** (*S*-amine), **3** (*R*-amine), crystals obtained from the reaction with racemic amine (containing **4** and **5**) and a manually mixture of **2** & **3** in 65:35 ratio (Figure 3.8). The diffraction pattern, observed for the mixture of **4** and **5**, seems a combination of patterns of both **2** and **3** indicating that both are present in the crystals from racemic amine reaction. However, the pattern of physical mixture of **2** and **3** in 65:35 is identical with pattern of the crystals from racemic amine reaction, further confirming that crystals isolated from

racemic amine reaction has a 65:35 (S:R) distribution.

3.4.9 Thermogravimetric analysis of 2 and 3

Thermo-gravimetric analysis of **2** and **3** was carried out from 25 to 650 °C at 7°/min heating rate (Figure 3.9). Both TGA show similar weight loss pattern where significant weight loss starts only around 135 °C. Below 135°C, weight loss of 1.34 % for **1** and 4.0 % for 2 could be accounted for removal of less than one water molecule in **2** and two water molecules in **3** (calculated value for two waters, 4.12%).

This contradicts the crystal structures, which showed two water molecules were present as solvents of crystallization in both the case. However, crystals showed varying degree of desolvation over time. This might be the reason behind the variance. The complex decomposes above 160 °C. The elemental analysis on the crystals however supports the formula as observed in the crystal structure (two waters in each case).

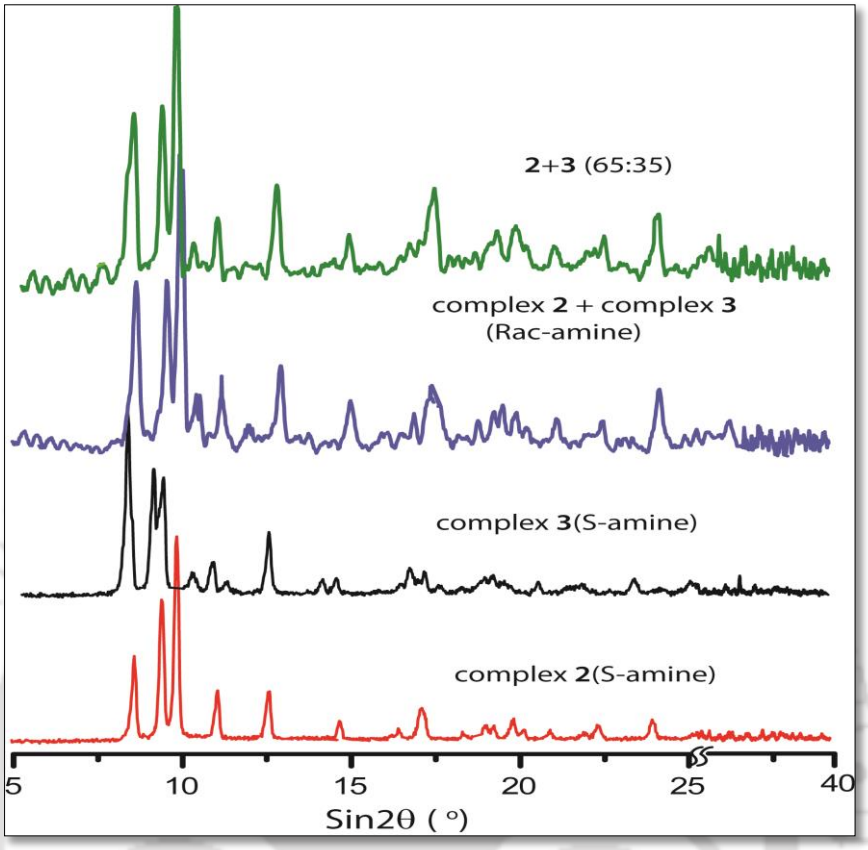

Figure 3.8 Comparison of Powder X-Ray diffraction pattern of the complexes.

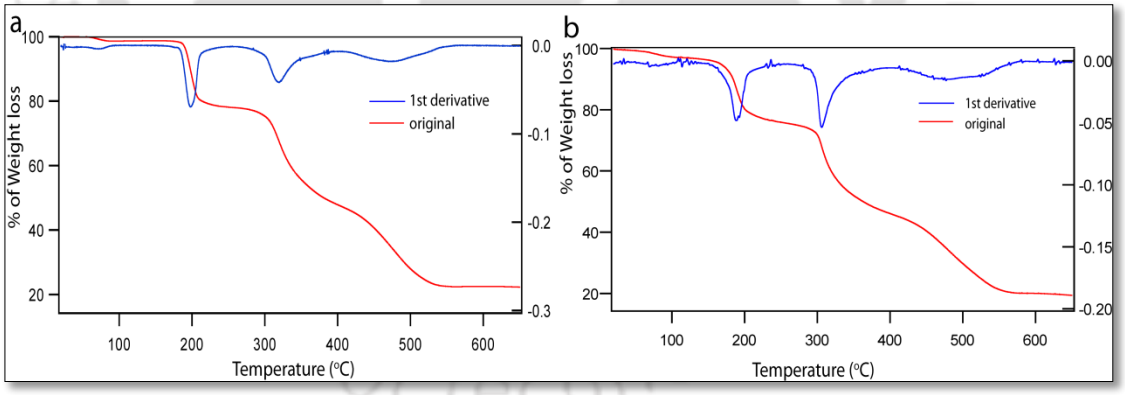

Figure 3.9 TGA plots of complex **1** (a) and complex **2** (b). Weight loss curve in red and first derivative curve in blue.

3.5 Conclusion

The L-histidine analogue with chiral amino alcohols[8] demonstrated that the combination of solution equilibrium favoring one diastereomer as well as crystallization allowed reaching ~100 % *ee*. Use of chiral amine using the same host,

where alcoholic H-bonding with host is absent, removed the advantage of chiral discrimination in solution and 30-49% *ee* occurred during crystallization. The imidazole-carboxylate H-bond was postulated as the prime factor that led to remarkable difference between the solid-state structures of diastereomers in L-histidine analogue. In the present set, use of L-methionine removed that factor. As a result we found multiple consequences on the crystallization process: (i) formation of conglomerate i.e., both diastereomers in the isolated crystals instead of a single type of crystal (Scheme 3.2) and (ii) absence of seeding effect.

Structural analysis showed that the stronger imidazole-carboxylate H-bonded (2.75-2.79 Å) network has been replaced by relatively weaker carboxylate-amine (2.95-3.01 Å) network. The different network observed between diastereomers is no longer present (Figure 3.5). This explains their comparable solubility, which led to seeding of both crystals (conglomerate), albeit with a ratio corresponding to their solubility and perhaps rate of crystallization. This led to the overall chiral enhancement observed.

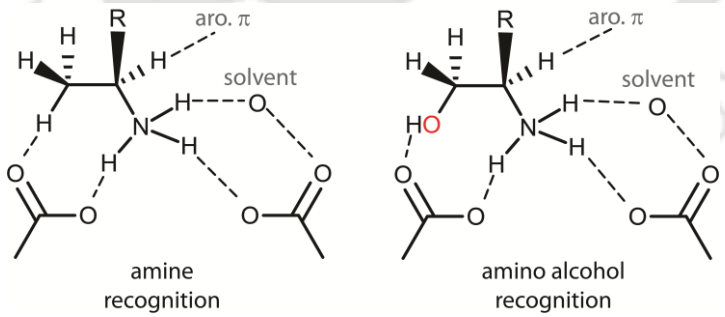

Figure 3.9 Similarity of non-covalent interaction between host and guest for (*S*)-1-phenylethylamine with methionine derived host and (*S*)-1-amino-2-propanol with histidine derived host.

Measurement of rate of crystallization is not trivial and well beyond the scope of our

facility. However, three important conclusions can be drawn from the result presented here: (i) minor perturbation in the non-covalent interactions (substituting imidazole with a thioether) can alter the crystallization path, (ii) chiral enhancement up to ~30% can occur with the present system through crystallization even if there is no significant chiral enhancement in the solution stage (Table 3.4), and (iii) chiral enhancement through crystallization is limited without stronger host-guest interaction observed in the case of amino alcohols. We have also noted a common host-guest interaction motif present in the (*S*)-1-phenylethylamine (favored diastereomer in crystalline state) with both histidine and methionine derived host and (*R*)-2-amino-1-propanol (Figure 3.9).

3.6 References

1. Das, C. R.; Sahoo, S.C.; Ray, M. *Cryst. Growth Des.* **2014**, *14*, 3958.
2. (a) Nishio, M.; Hirota, M.; Umezawa, Y. **1998.** *The CH…π interaction;* Wiley-VCH: New York. (b) Desiraju, G.R.; Steiner, T.; **1999** in *The weak hydrogen bond*; Oxford University Press: New York. (c) Desiraju, G. R. *Acc. Chem. Res* **2002**, *35*, 565.
3. Alam, Md. A.; Koner, R. R.; Das, A.; Nethaji, M.; Ray, M. *Crystal Growth & Design*, **2007**, *7*, 1818.
4. Sahoo, S.C.; Ray, M. *Chem. Eur. J.* **2010**, *16*, 5004.
5. (a) Nakamoto, K. *Infrared and Raman Spectra of Inorganic and Coordination Compounds*, Part B, John Wiley & Sons, New York. (b) Earnshaw, A. *Introduction to Magnetochemistry*, Academic Press, London, **1968**. (c) Figgis, B. N.; lewis, J. *Prog. Inorg. Chem.*, Ed. F. A. Cotton, **1964**, *6*, 37. (d) Smith, A. S.; Fraser, C. L. in *Comprehensive Cordination Chemistry II*, 1, Ed. A. B. P. Lever, vol. 1, p. 1.
6. (a) Doki, N.; Yokota, M.; Sasaki, S.; Kubota, N. *Cryst. Growth Des.*, **2004**, *4*, 1359. (b) Profir, V. M.; C. Rasmuson, A. *Cryst. Growth Des.*, **2004**, *4*, 315.

Chapter - 4

Enantiomeric Separation of Biogenic Amino alcohols

In Chapter 3, we used new L-methionine derived host for resolution of aryl amine. In spite of changing the host with L-methionine in place of L-histidine, we could achieve maximum 30% resolution of aryl amine.[1] Previously, we have observed that L-histidine derived host showed better resolution of two simple amino alcohols, 1-amino-2-propanol and 2-amino-1-propanol, than aryl amine.[2] We expected that this modified host would be efficient resolving host for amino alcohol than amine.

Thus, in this chapter, we have utilized the new L-methionine derived host for enantioselective recognition and resolution of two biogenic amino alcohols, 2-amino-1-phenylethanol (**Am1**) and 3, α-dihydroxy-phenethylamine (**Am2**) as guest (Figure 4.1) from racemic mixture. We have also checked the practical utilization of this method in chiral separation of foresaid amino alcohols.

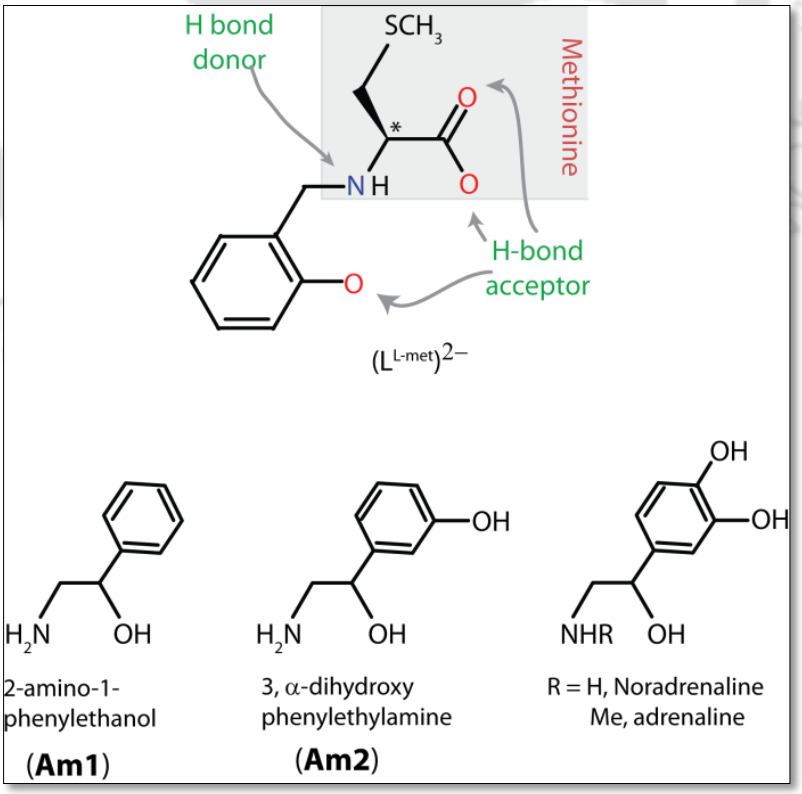

Figure 4.1 Structure of ligand used in metalloorganic host and amino alcohols as guest for chiral recognition.

The reasons of choosing these two amino alcohols are (a) 2-amino-1-phenylethanol and 3, α-dihydroxy phenethylamine, known as Norphenylephrine or meta-octopamine are naturally occurring, endogenous trace amine and play role as minor neurotransmitter in the brain.[3] (b) The (*R*)- form of both the ethanolamine are structurally related to neuro-transmitter noradrenaline and adrenaline[4] (Figure 4.1). These serve as a substrate to the enzyme phenylethanolamine N-methyl transferase[5], used commonly as building block[6] in organic and medicinal chemistry[7]. (c) There are not many reports on resolution of these two amino alcohols either using organic resolving agent or multi-step asymmetric synthesis.[8] Both are limited to small scale. So, enantiomeric separation of these biogenic alcohols using metalloorganic host still remains unexplored.

4.1 Material and Methods

4.1.1 Solvents and reagents

Details of the solvent purification and analytical measurements have been already discussed in Chapter 2. D-Metheonine, 2-Amino-1-phenylethanol and 3, α-dihydroxy-phenethylamine hydrogenchloride were purchased from Aldrich Chemical Co. Ltd. and L-Metheonine was purchased from Sisco Research Laboratories Pvt. Ltd. (SRL), India, and used as received.

4.1.2 Measurements

All the details of instrument used for analysis have already been discussed in Chapter 2. The Ligand $H_2L^{L\text{-met}}$ is synthesized by following the similar procedure described in Chapter 3.

The crystals of complexes were mounted on glass fiber and on sealed quartz tube. All geometric and intensity data for the crystals were collected at room temperature

using a Bruker SMART APEX CCD diffractometer equipped with a fine focus 1.75 kW sealed tube Mo-Ka (λ = 0.71073 Å) X-ray source, with increasing ω (width of 0.3º per frame) at a scan speed of either 3 or 5 s/frame. The SMART software was used for data acquisition and the SAINT software for data extraction. Absorption corrections were done using SADABS. After the initial solution and refinement with SHELXL, the final refinements were performed on WinGX environment using SHELX97. All non-hydrogen atoms in the complexes were refined anisotropically. Some Solvent molecules, methanol and water in few complexes were refined isotropically to avoid alert level A in checkcif. Wherever possible, the hydrogen atoms were located from the difference Fourier maps and were refined isotropically. Thus some of the C-H bonds will not be ideal and may vary. Some of C-C bonds have been restrained using DFIX instruction in some complexes. Most of the hydrogen atoms attached to the solvent molecules could not be located or fixed, so the molecular weight may not match. Crystallographic data and details of refinements are listed in Table 4.1, and selected bond distances and angles for are listed in Table 4.2a, b. Perspective views of the complexes were shown using ORTEP.

4.2 Syntheses

4.2.1 ((*R*)-2-Ammonium-1-phenylethanol))[$Ni_2(L^{L\text{-}met})_2(OAc)$](1L). The ligand $H_2L^{L\text{-}met}$ (0.150 g, 0.40mmol) and $Ni(OAc)_2.4H_2O$ (0.146 g, 0.40mmol) were stirred in 15 mL MeOH. After 15min, 2-amino-1-phenyl ethanol (0.160 g, 0.800mmol) was added to the resulting solution and stirred for 1h. The resulting blue methanolic solution was kept for slow evaporation in a beaker at room temperature. Blue rod shaped crystals were obtained after 24h. The crystals

were filtered, washed with acetonitrile, dried in vacuum. Yield:80%. Anal. Calcd. for $[Ni_2(C_{26}N_2S_2O_8H_{33})(C_8NOH_{12})].2H_2O.CH_3OH$: C, 47.34; H, 6.02; N, 4.73; found C, 47.14; H, 6.10; N, 5.22; IR (KBr, cm^{-1}) $\upsilon(COO)_{asym}$ 1595(s), $\upsilon(COO)_{sym}$1482(m), 1566(m). μ_{eff} (powder, 298K)/Ni: 2.60. Λ_M (ohm^{-1} cm^2 mol^{-1}): 35 (MeOH).

4.2.2 ((*S*)-2-Ammonium-1-phenylethanol))[$Ni_2(L^{D\text{-}met})_2(OAc)$](1D). The complex was synthesized by following the same procedure as in **1L** using the ligand $H_2L^{D\text{-}met}$ (0.150 g, 0.40mmol) instead of ligand $H_2L^{L\text{-}met}$ from 2-amino-1-phenylethanol. Blue rod shaped crystals were obtained after 48h. The crystals were filtered, washed with acetonitrile, dried in vacuum.Yield:75%. Anal. Calcd. for $[Ni_2(C_{26}N_2S_2O_8H_{33})(C_8NOH_{12})].H_2O.CH_3OH$: C, 47.34; H, 6.02; N, 4.73; found C, 48.01; H, 5.96; N, 4.97; IR (KBr, cm^{-1}) $\upsilon(COO)_{asym}$ 1590(s), $\upsilon(COO)_{sym}$1476(m) ,1563(m). μ_{eff} (powder, 298K)/Ni: 2.67. Λ_M(ohm^{-1} cm^2 mol^{-1}): 37 (MeOH).

4.2.3 ((*R*)-2-Ammonium-1-phenylethanol))[$Ni_2(L^{D\text{-}met})_2(OAc)$](1Da). The complex was synthesized by following the same procedure as in **1L** using the ligand $H_2L^{D\text{-}met}$ (0.150 g, 0.40mmol) instead of ligand $H_2L^{L\text{-}met}$ from pure (*R*)-(-)-2-amino-1-phenylethanol. A blue glassy solid was obtained after solvent evaporation. As the complex was soluble in methanol as well as acetonitrile, the complex as light blue solid was isolated by precipitation with acetonitrile and diethylether mixture (1:3) and dried in vacuum desiccator. Yield: 82%. Anal. Calcd. for $[Ni_2(C_{26}N_2S_2O_8H_{33})(C_8NOH_{12})]$: C, 49.84; H, 5.53; N, 5.12; found

C, 50.01; H, 5.56; N, 5.07; IR (KBr, cm^{-1}) $\upsilon(COO)_{asym}$1594(s), $\upsilon(COO)_{sym}$1471 (m), 1559(m). μ_{eff} (powder, 298K)/Ni: 2.64.

4.2.4 ((*R*)-3, α-dihydroxy phenethyl ammonium))$[Ni_2(L^{L\text{-}met})_2(OAc)]$(2L). The ligand $H_2L^{L\text{-}met}$ (0.150 g, 0.40mmol) and $Ni(OAc)_2.4H_2O$ (0.146 g, 0.40mmol) were stirred in 15mL MeOH. After 15min 3,α-dihydroxy phenethyl amine hydrogenchloride (0.160 g, 0.80mmol) with LiOH (0.0160 g, 0.80mmol) in 1mL MeOH was added to the resulting solution and stirred for 1h. The resulting blue methanolic solution was kept for slow evaporation in a beaker at room temperature. Blue needle shaped crystals were obtained after 48h. The crystal was filtered, washed with acetonitrile, dried in vacuum.Yield:80%. Anal. Calcd. for $[Ni_2(C_{26}N_2S_2O_8H_{33})(C_8NO_2H_{10})]$.$2CH_3OH$: C, 48.04; H, 5.94; N, 4.67; found C, 47.94; H, 6.01; N, 4.70; IR (KBr, cm^{-1}) $\upsilon(COO)_{asym}$1591(s), $\upsilon(COO)_{sym}$1481(m), 1559(m). μ_{eff} (powder, 298K)/Ni: 2.60. Λ_M (ohm^{-1} cm^2 mol^{-1}): 42 (MeOH).

4.2.5 ((*S*)-3, α-dihydroxy phenethyl ammonium)$[Ni_2(L^{D\text{-}met})_2(OAc)]$(2D). The complex was synthesized by following the same procedure as in **2L** using the ligand $H_2L^{D\text{-}met}$ (0.150 g, 0.40mmol) instead of ligand $H_2L^{L\text{-}met}$ from 3, α-dihydroxy phenethyl amine hydrogen chloride. Blue needle shaped crystals were obtained after 48h. The crystals were filtered, washed with acetonitrile, dried in vacuum.Yield:78%. Anal. Calcd. for $[Ni_2(C_{26}N_2S_2O_8H_{33})(C_8NO_2H_{12})]$.$6H_2O$: C, 43.25; H, 6.09; N, 4.45; found C, 44.01; H, 5.96; N, 4.63; IR (KBr,

cm^{-1}) $\upsilon(COO)_{asym}$1592(s), $\upsilon(COO)_{sym}$1470(m) ,1560(m). μ_{eff} (powder, 298K): 2.62. Λ_M (ohm^{-1} cm^2 mol^{-1}): 40 (MeOH).

4.3 Estimation of enantiomeric separation through HPLC.

The extraction of bound amine and preparation of organic derivative have been performed following the similar procedure described in Chapter 3. Specification of chiral column, detector, and flow rate, used in HPLC are same as in Chapter 3.

4.3.1 Procedure of recovery of amine from metal complexes as crystal

The extraction of bound amine from crystals of host-guest complexes have been performed following the similar procedure described in Chapter 3 (Section 3.3.1, Scheme 3.2).

4.3.2 Procedure of recovery of amine from amorphous metal complexes

The extraction of bound amine from amorphous of host-guest complexes have been performed following the similar procedure described in Chapter 3 (Section 3.3.2, Scheme 3.2).

4.3.3 Derivatization of chiral amine with Benzoyl Chloride

Although the derivatization of recovered amine to amide with bezoyl chloride has been accomplished by following the similar protocol described in Chapter 2, here the guest amine is different. So, the corresponding characterization data are provided here. IR (KBr, cm^{-1}): 1633(s), 3357(s). (ESI-Mass, +ve) m/z 242.105 (calc. 241.1102) ($[M+H]^+$). ^1H NMR ($CDCl_3$, 400MHz): 7.77 (2H, d, o-C_6H_5 (benzoyl)), 7.52-7.28 (8H, m, C_6H_5 (benzoyl and benzyl), 5.49 (1H, b, -N**H**), 5.92(1H, m, -C**H** (benzyl)), 3.814 & 3.453 (2H, m, -C$\mathbf{H}_2$ (methylene)), 1.35 (1H, t, -O**H**).

4.4 Result and Discussion

4.4.1 Syntheses and isolation host-guest complexes

Stirring of the ligand ($H_2L^{L\text{-met}}$), Ni(II) acetate and either guest **Am1** or **Am2** in methanol followed by slow evaporation yielded blue crystals of **1L** and **2L,** in high yields (80%) (Scheme 4.1). Similarly, use of D-methionine derived ligand, $H_2L^{D\text{-met}}$, yielded crystals of **1D** and **2D** in similar yield. Attempt to synthesize the complex **1Da,** the diastereomer of **1D**, from $H_2L^{D\text{-met}}$, Ni(II) acetate and pure *R*-isomer of **Am1** resulted either in a glassy solid from methanol (evaporation) or powder (precipitation by addition of acetonitrile-diethylether). The complex **1Da** was synthesized for comparisn purpose. The complexes were also characterized using FTIR, conductance, magnetic moment. Data are commensurate with values earlier obtained for analogus complexes.[9]

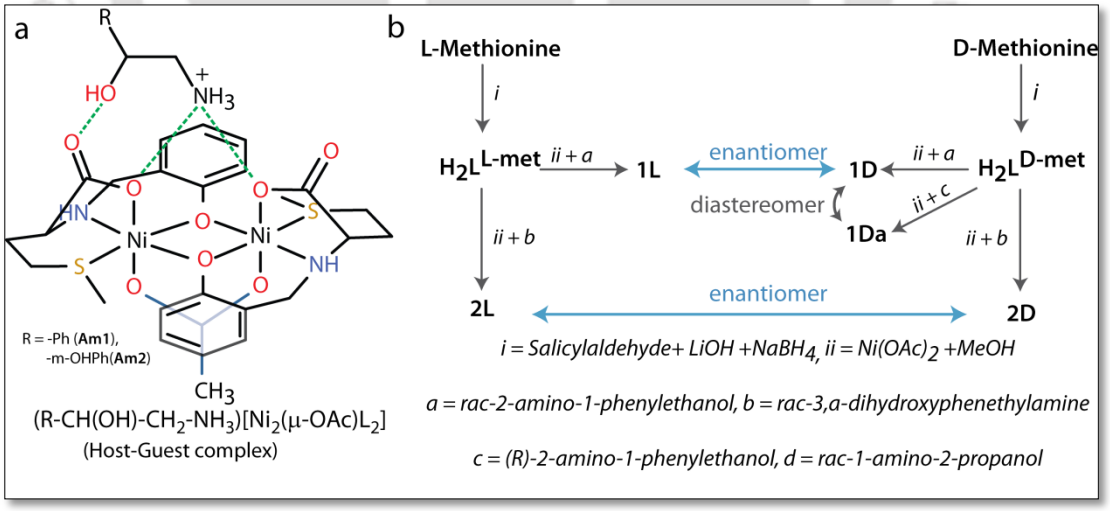

Scheme 4.1 General schematic drwaing of host-guest complex (a) and flow chart of syntheses of host-guest complexes showing the relationship of complexes with each-other (b).

Table 4.1 Crystallographic data and refinement parameters of complexes.

	IL	**1D**	**2L**	**2D**
empirical formula	C_{35} H_{50} N_3 Ni_2 O_{12} S_2	C_{35} H_{45} N_3 Ni_2 O_{12} S_2	C_{36} H_{45} N_3 Ni_2 O_{12} S_2	C_{34} H_{45} N_3 Ni_2 O_{16} S_2
fw	886.28	881.26	893.25	933.23
T (K)	296(2)	296(2)	296(2)	296(2)
wavelength (A°)	0.71073	0.71073	0.71073	0.71073
crystal system	Orthorhombic	Orthorhombic	Monoclinic	Monoclinic
space group	$P2_12_12_1$	$P2_12_12_1$	$P2_1$	$P2_1$
a, A°	10.9066(8)	10.9496(4)	11.5735(9)	11.771(3)
b, A°	17.7850(14)	17.9468(7)	10.8311(5)	10.734(4)
c, A°	20.3734(16)	20.4680(8)	16.340(11)	16.969(6)
V, Å ^{3}	3951.9(5)	4022.2(3)	2052.4(2)	2052.4(2)
z/ρ	4/1.485	4/1.455	2/1.445	2/1.478
μ	1.122	1.102	1.081	1.069
coll.reflns	7399	8016	7932	7177
indep reflns	4135	4469	6661	6321
FLACK para.	-0.07(3)	0.00(2)	-0.019(16)	-0.009(12)
GOF	1.037	1.050	1.017	1.014
R1 [a]	0.0650	0.0381	0.0474	0.0391
wR2 [a]	0.1419	0.0944	0.1151	0.0954
R1[b]	0.1211	0.0429	0.0569	0.0464
wR2[b]	0.01749	0.0978	0.1260	0.1010

[a] $I > 2\sigma$. [b] All data

4.4.2 X-Ray crystal structure of 1L and 1D

The complexes **1L** and **1D** are crystallized in same orthorhombic space group $P2_12_12_1$ (Table 4.1). Structural analysis show **1L** and **1D** are enantionmer of each other. The asymmetric unit of both the complexes consists of ammonium form of (*R*)-**Am1** and (*S*)-**Am1** in the, bound to anionic $[Ni_2(\mu\text{-acetate})(L^{L\text{-met}})_2]^-$ with three and two solvent molecules respectively. The anion has two octahedral Ni(II), each ligated with tetradentate $(L^{L\text{-met}})^{2-}$, bridging phenolate oxygen, bridging bidentate acetate ligand (Figure 4.2a & b), and thioether, a weak donor. Geometry around each nickel is slightly distorted from perfect octahedron as evident from the deviation of angles from ideal 90° and 180° (Table 4.2). The chiral carbon in $(L^{L\text{-met}})^{2-}$ has *S* conformation as L-methionine (*S*-conformation) was used during the ligand synthesis. Both the coordinated amine N atoms, N1 and N1A, have *R* conformation. This has been observed in all previous complexes with this type of ligand.

The two carboxylates oriented next to each other, flanked on both sides by the aromatic rings form a molecular cleft. Two, out of three, ammonium NH (N2) of cationic 2-amino-1-phenyl ethanol are H-bonded to this carboxylate oxygen O1 and O1A (Figure 4.2c & d). The alcoholic O6 is H-bonded to a terminal carboxylate O2. The third NH (N2), a terminal carboxylate O2A and solvent molecules form a H-bonded network. Thus the guest amine is oriented above the cleft in the binuclear complex through multiple H-bonding. Although **1L** and **1D** are pair of enantiomerss of each other, in crystal lattice the position of water molecules as solvent of crystallization remains little difference. In the crystal structures of both, the spatial orientation of host-guest brought the C15, the

carbon adjacent to the chiral centre, within 4.015 Å of the aromatic ring (C(H)...π interaction range[10] (3.36 to 4.03 Å). Although **1L** and **2L** are enantiomer to each other, because of different position of solvent molecule in lattice, minor difference of number and type of inter molecular non-covalent interactions present between two enantiomers (Figure 4.2c & d, Table 4.3). Intermolecular H-bonding between bridging carboxylate O4 and lattice water O7 form a one-dimensional column along c axis (Figure 4.4a). Guest cation lies between these parallel columns.

4.4.3 X-Ray crystal structure of 2L and 2D

Structural analysis of the complexes, **2L** and **2D** shows that both enantiomer are solved in same space group $P2_1$ (Table 4.1) with similar structure remaining the different number of solvents molecules i.e., two methanol and six water molecules respectively (Figure 4.3a & b). The molecular structure of **2L** and **2D** reveals they are enantiomers to each other having the chirality of cationic guest amine is *R* i.e., (*R*)-**Am2** and *S* i.e., (*S*)-**Am2** respectively. In both complexes, bond length, bond angle and ligation around Ni(II) metal centre in binuclear anionic moiety remain similar with **1L** (Table 4.2, Figure 4.3). The guest amino alcohol is bonded with host through similar fashion as **1L**.

Unlike **1L**, in case of **2L** and ***2D***, the guest amino alcohol is connected with other two neighbouring host through strong H-bonding. The aliphatic alcoholic oxygen O6 is taking part simultaneously in intra molecular H-bonding with terminal carboxylate O2 in same host-guest adduct and intermolecular H-bonding with coordinated nitrogen, N1 of neighbouring host. The aromatic alcoholic oxygen O7 is also H-bonded with bridged carboxylate O5 of another neighbouring host through one solvent molecule (Figure 2.3c & d). Due to the different number and type of solvent

Table 4.2 Selected bond distances (Å) and angles (°) for the Complexes.

	1L	**1D**	**2L**	**2D**
Ni1 -O1	2.0712	2.086	2.073	2.071
Ni1-O3	2.0538	2.039	2.057	2.070
Ni1-O3A	2.0371	2.038	2.046	2.016
Ni1-O4	2.0730	2.065	2.034	2.077
Ni1-N1	2.0775	2.081	2.074	2.076
Ni1-S1	2.4523	2.456	2.466	2.453
Ni2- O1A	2.0862	2.083	2.075	2.076
Ni2-O3	2.0326	2.022	2.007	2.076
Ni2-O3A	2.0519	2.030	2.045	2.039
Ni2-O5	2.0411	2.028	2.091	2.030
Ni2-N1A	2.0745	2.066	2.076	2.065
Ni2-S1A	2.4411	2.455	2.449	2.482
N1-Ni1-S1	90.58	90.6	88.94	89.71
O3-Ni1-O3A	82.37	81.41	82.61	82.74
N1- Ni1-O1	79.93	80.06	80.50	80.17
S1-Ni1-O4	90.09	91.13	90.02	89.49
O1-Ni1-O4	174.06	174.2	173.46	176.72
N1A-Ni2-S1A	89.36	89.04	89.83	88.73
O3A-Ni2-O3	82.53	82.08	83.89	82.06
N1A-Ni2-O1A	78.82	80.05	80.11	80.47
S1A-Ni2-O5	88.97	88.79	90.99	90.98
O1A-Ni2-O5	174.16	174.4	173.42	172.50

in crystal lattice between two enantiomers, inter molecular non-covalent interactions are also different (Figure 2.3c & d) remaining similar arrangement of host and guest in lattice (Figure 2.5b).

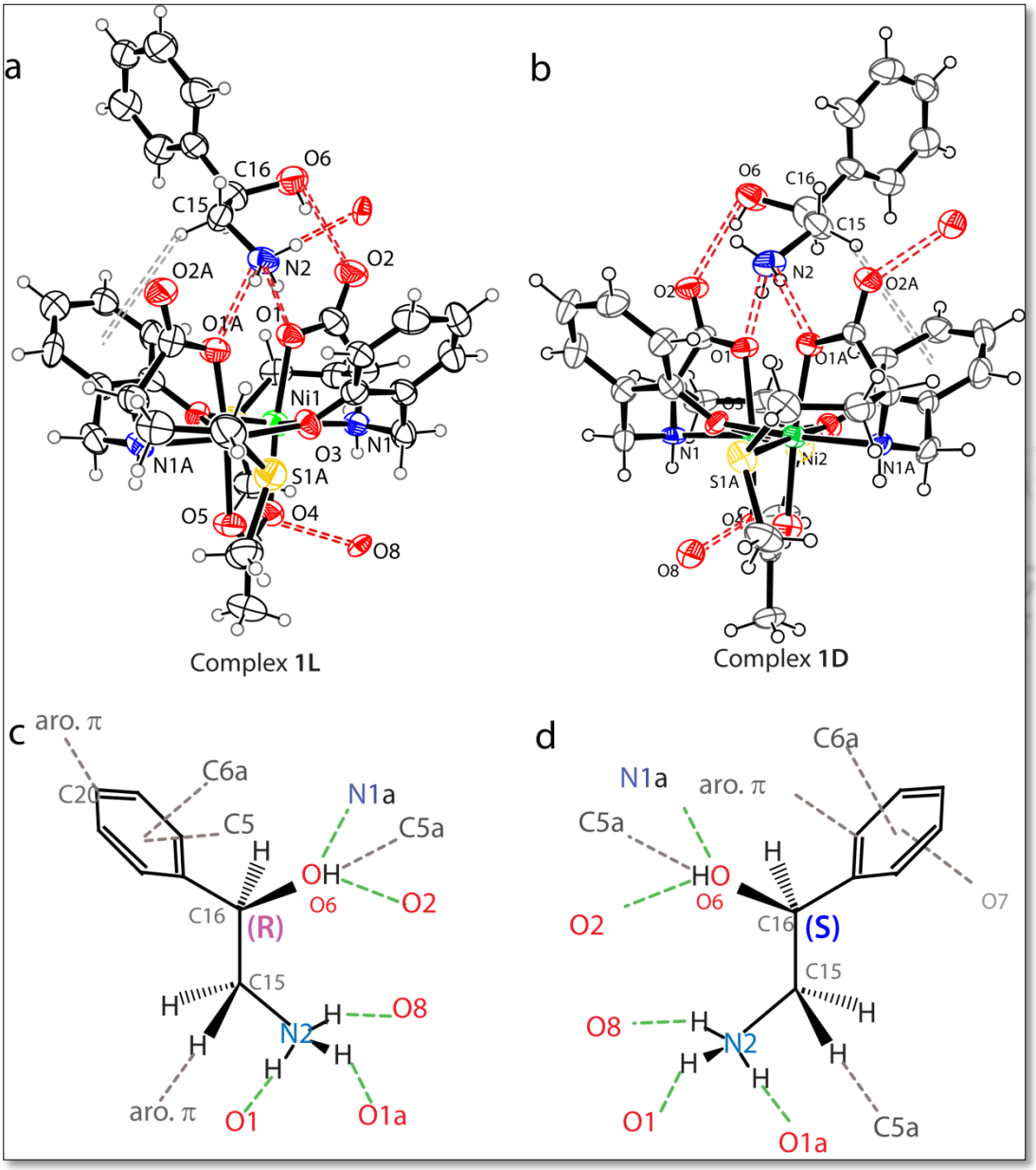

Figure 4.2 ORTEP diagram of complex **1L** and **1D** with 40% ellipsoid probability (a &b), Schematic representation of non covalent interactions between host and guest present in **1L** and **1D** showing the chirality of recognized guest amine (c & d).

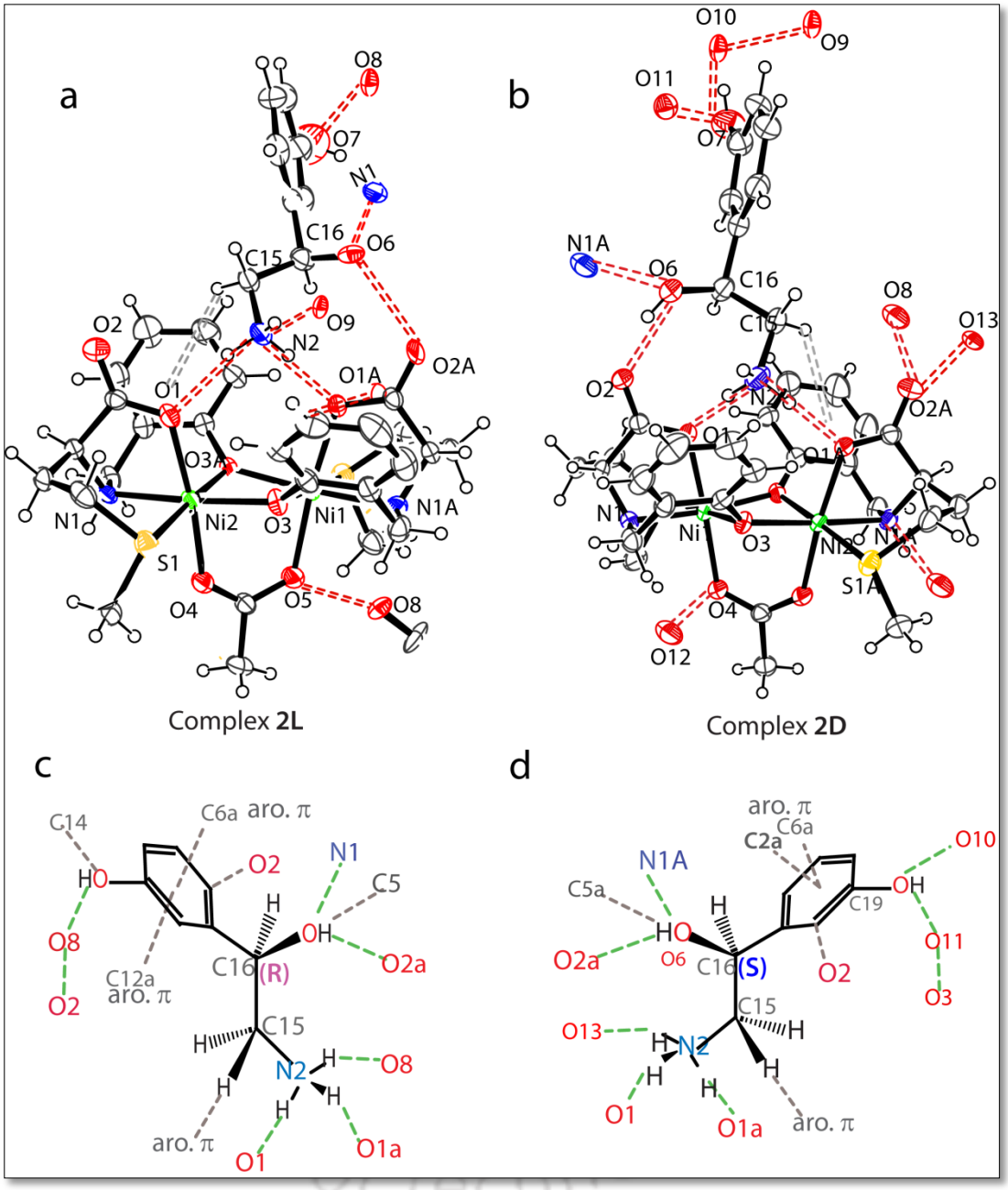

Figure 4.3 ORTEP diagram of complex **2L** and **2D** with 40% ellipsoid probability (a &b), Schematic representation of non covalent interactions between host and guest present in **2L** and **2D** showing the chirality of recognized guest amine (c & d).

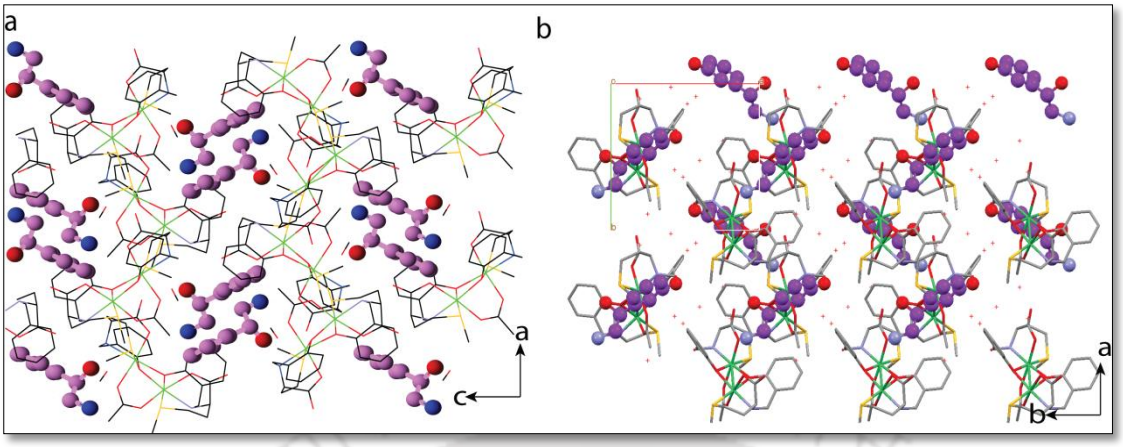

Figure 4.4 Crystal lattice of **1L** and **2L** showing the arrangentment of guest amine (in ball-Stick model, violet in colour) inside the lattice.

Table 4.3 Distances (Å) of H-bonding and other interactions present in complexes.

	D-H···A	D-H (Å)	H···A (Å)	D···A (Å)	DHA (°)		D-H···A	D-H (Å)	H···A (Å)	D···A (Å)	DHA (°)
1L	Direct Host-Guest interaction					**2L**	Direct Host-Guest interaction				
	O6– 06…O2	0.82	1.63	2.739	162		O6– H06…O2A	0.86	1.86	2.661	165
	N2--2B...O1A	0.92	1.98	2.788	146		N2 –H2C...O1	0.89	1.90	2.767	164
	N2 –H2C...O1	0.91	1.89	2.788	168		N2--H2B...O1A	0.89	1.95	2.829	170
	NH3+…. π	-	-	3.886			NH3+…. π	-	-	3.841	
	C15-H15B··· π	0.98	3.16	4.011	146		C15-H15B··· π	0.98	3.24	4.086	144
	Other non-covalent interactions						Other non-covalent interactions				
	O2A…O7			2.821			N2– H2A…O9*	0.89	2.16	2.964	150
	N2–H2A…O8	0.92	2.03	2.843	147		O7 – O8*			2.773	
	N1A-O1...O8	0.92	2.02	2.847	150		N1 – H1... O6			3.028	
	N1–H1…O2A	0.91	2.43	3.071	128		N1A-H1A... 8*			3.281	
	N1A–O1A...O6	0.91	2.27	3.115	155		O5- O8*			2.52	
	O8*--8A...O9*	0.90	2.14	2.976	157						
	O8*--H08...O7*	0.88	2.34	3.012	133						
	O4…O7*			3.011							
1D	Direct Host-Guest interaction					**2D**	Direct Host-Guest interaction				
	N2-- H2C... O1	0.89	1.87	2.760	178		N2– 2A…O1A	0.89	1.8	2.747	168
	N2--H2B... 1A	0.89	1.94	2.778	157		N2--H2B...O1A	0.89	1.89	2.775	170
	O6 – H06... O2	0.82	1.88	2.686	166		O6 – H06…O2	0.82	1.88	2.683	165
	C15 –H15A··· π	0.98	3.25	4.111	147		NH3+…. π	-	-	3.918	
	NH3+…. π	-	-	3.886			C16-H16B··· π	0.98	3.52	4.197	120
	Other non-covalent interactions						Other non-covalent interactions				
	O8* - O9*			1.934			N2- O13*			2.889	
	O2A…O7*			2.811			O13*-O9*			2.038	
	N2- H2A... O8*	0.89	2.15	2.947	148		O9*-O10*			2.898	
	O4…O7*			2.954			O9*-O8*			2.584	
	N1 – H1... O2A	0.91	2.50	3.127	126		O8*-O2A			2.855	
	N1A-H1A... O6	0.91	2.32	3.145	151		O7-O10*			2.767	
							O6- N1A			3.013	
	* solvent molecule						O13*- O2A			2.807	

4.4.4 Thermogravimetric analysis of complexes

The formulation of **1L, 1D**, **2L**, **2D** and **3L** from structure are also supported by elemental analysis. Thermogravimetric analysis (TGA) of **1L** and **1D** support the lattice solvents observed in the structure. The weight loss of 5.8% between 25-140 °C was observed as against the 5.6% calculated for two waters and one methanol (Figure 4.5a). TGA analysis for **2L** shows 8.1% weight loss between 25-140 °C and 5.8% weight loss between 160- 200 °C which could be accounted for two methanol (cald. 7.3%) and bridged acetate anion (cald. 7.1%) (Figure 4.5b). TGA analysis for **2D** shows weight loss of 7.6% for four waters (cald. 7.7%) which does not support the six number of water present in crystal (cald. 11.5%, higher than observed) (Figure 4.5c & d). This anomaly can be explained as desolvation of two water molecules as solvent for crystallization prior to experiment during drying in desiccator. After 160 °C the complexes start to decompose.

4.4.5 Powder X-Ray diffraction analysis of complexes

The purity of the bulk complexes as crystal was checked by the powder X-Ray diffraction analysis (PXRD). The diffraction pattern of **1L**, **1D**, **2L** and **2D** match well with the simulated pattern from single crystal structure (Figure 4.6). The crystallinity of complex **1D** isolated as solid by precipitation was checked by PXRD. It shows similar diffraction pattern like crystal of **1D** confirming micro crystalline nature of host-guest adduct in solution also (Figure 4.6a). Other analysis of **1Da** supports the formation of complex, PXRD show the nature of the solid as amorphous (Figure 4.6a). This indicates the significant difference in crystallinity between the diastereomers (**1D** and **1Da**) caused perhaps by the mis-fitting of guest in the cavity.

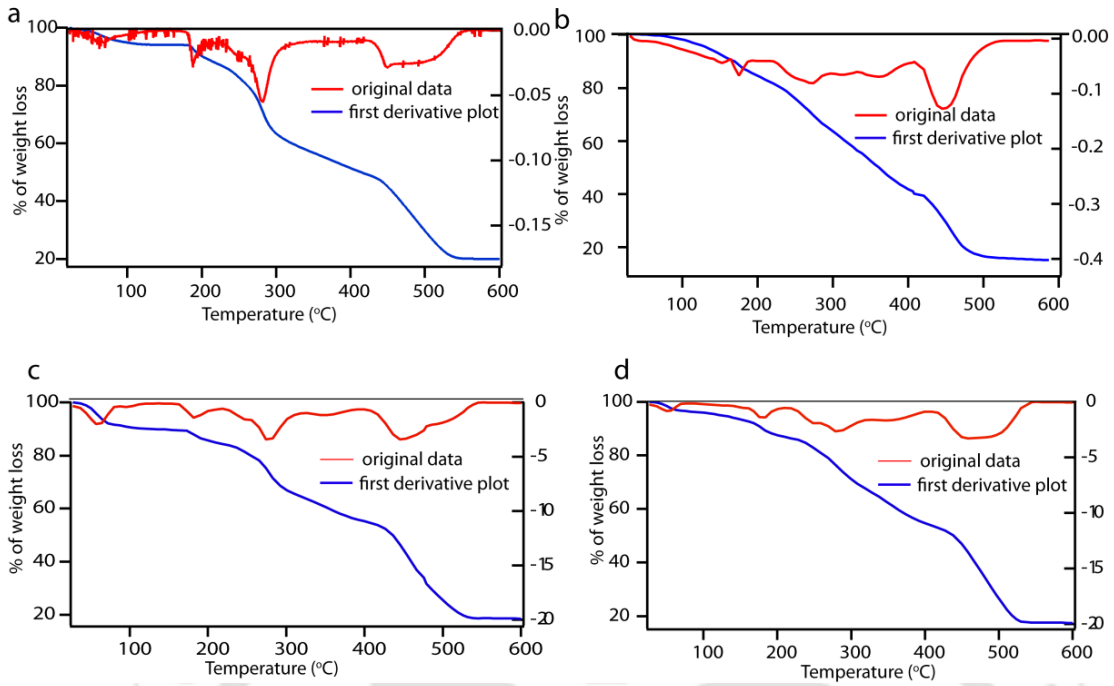

Figure 4.5 TGA plots of complex **1L** (a), complex **1D** (b), complex **2L** (c) and complex **2D** (d). Weight loss curve in blue and first derivative curve in red.

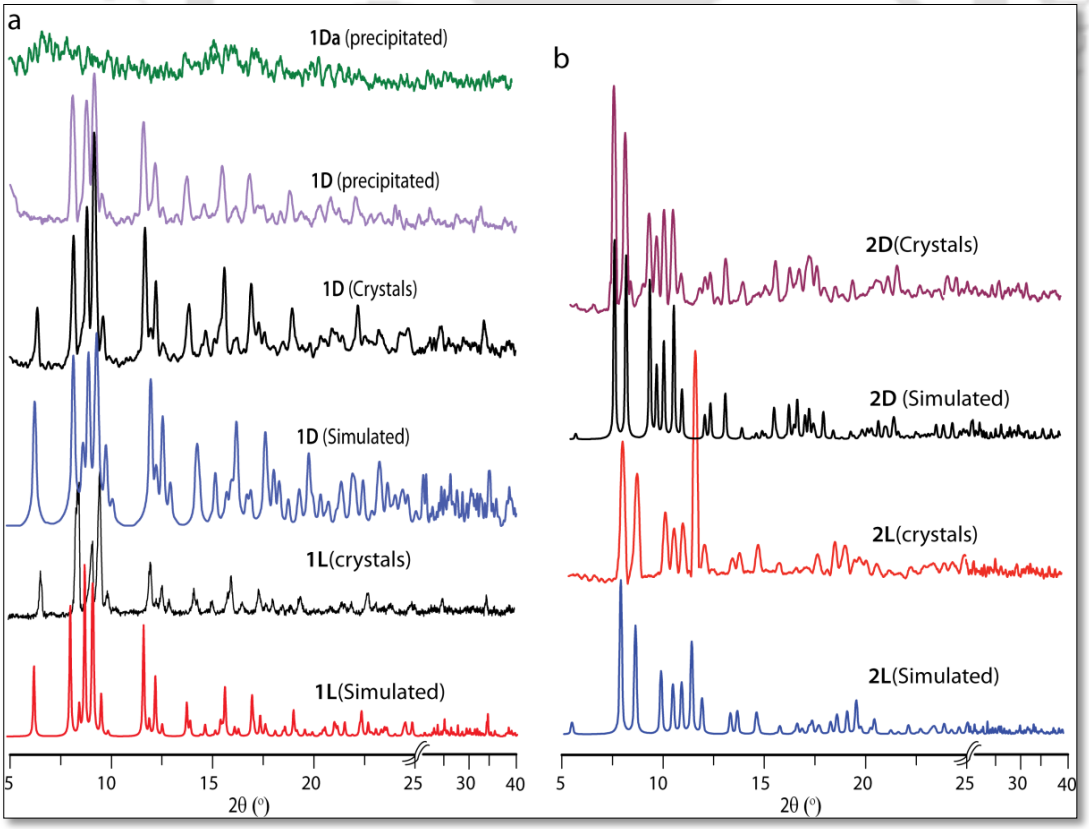

Figure 4.6 Powder X-ray Diffraction patterns of complexes **1L** & **1D** (a) and **2L** and **2D** (b).

4.4.6 Enantiomeric separation of amino alcohols estimated by HPLC analysis

From the Chapter 2, recovery and isolation of the recognized guest amine has been accomplished by metathesis reaction with a potassium salt, as the binding constant with potassium ion is high.

To estimate the content of *R* or *S*-isomer as enantiomeric excess (%*ee*) present in the bulk crystals and amorphous host-guest adduct chiral High pressure liquid chromatography (HPLC) measurements were performed with extracted amines. Results showed that (*R*)-**Am1** and (*R*)-**Am2** in the bulk of crystals of **1L** and **2L** are present in value of 92%*ee* and 94%*ee* respectively (Table 4.4).

Table 4.4 Chiral distribution of amines in bulk of crystals and amorphous precipitate determined by extracting amines and measurment using HPLC analysis.

Complex	Amines	*Isolated from crystals*				*Isolated from precipitate*			
		R	*S*	% *ee*	Yield (%)	*R*	*S*	% *ee*	Yield (%)
1L	*Am1*	96	4	92	80	87	13	74	76
1D	*Am1*	7	93	86	74	15	85	72	74
2L	*Am2*	98	2	94	80	88	12	76	72
2D	*Am2*	4	96	92	78	-	-	-	-

Reversing the chirality of Ni(II) complex using D-methionine in the ligand, the (*S*)-isomer of the amino alcohol was isolated (86%*ee*). Slight decrease in %*ee* could be due to the presence of small quantity of L-methionine in the D-methionine (Aldrich, 98%*ee*) which is opposite to higher purity level of L-methionine, usually isolated from natural sources.

Similarly, %*ee* value of respective amino alcohols present in amorphous host-guest adducts is determined by HPLC analysis. As we do not have any direct tool to measure ratio of both diastereomer in solution equilibrium before

crystallization, we estimate chiral enhancement in solution equilibrium by rapid precipitation without crystallization. The value of %*ee* in solution equilibrium is 72-76% (Table 4.4).

4.4.7 General motif of recognition between host and guest

From structural analysis of all host-guest adducts, we have noted that a common motif of host-guest interaction present between the guest (**Am1** and **Am2**) with methionine derived host (Figure 4.7a & b) like in (*S*)-1-amino-2-propanol with histidine derived host (Figure 4.7c). Other than electrostatic attraction between anionic host and cationic guest, the guest amino alcohol (**Am1** and **Am2**) is recognized by H-bonding of $-NH_3^+$ and alcoholic –OH group contributing as two point attachment and a additional C(H)…π interaction with aromatic ring acting as third point of interaction (Figure 4.7a & b).

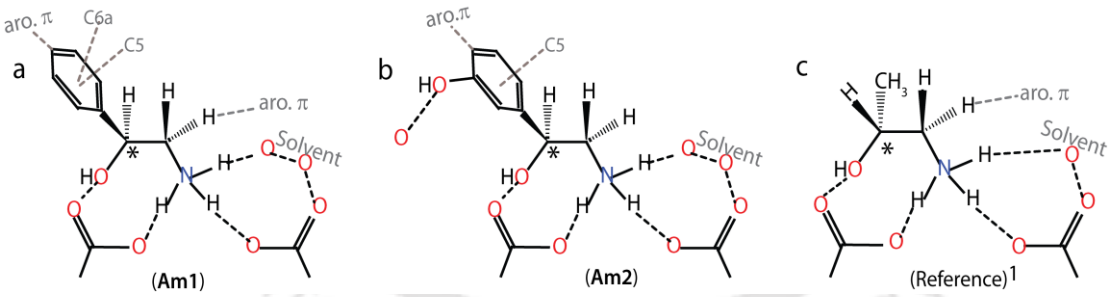

Figure 4.7 Similarity of non-covalent interaction between host and guest for guest **Am1** (a), **Am2** (b) with methionine derived host and (*S*)-1-amino-2-propanol with histidine derived host (c) as reference. [1] see Ref.2

4.4.8 Utility of this method

Whether the process can be used for resolution of the amine in preparative scale, to evaluate that, reaction was performed in larger scale. Starting from 1g of ligand and 0.568 g of racemic amine, we were able to isolate 0.144 g of the isomer (*R*, yield, 50%, 90%*ee*). The complex **1Da** was synthesized using

isolated *R*-isomer of guest **Am1** from **1L**. Considering the simplicity of the reaction from relatively cheaper ingredient, this method is not impractical. Use of di-O-p-toluoyl-tartaric acid needs fractional crystallization method, which is not necessary for the present method as the other diastereomer is not crystallized out.

4.5 Conclusions

Chiral recognition and resolution of two biologically important amino alcohols have been achieved effectively using a simple anionic binuclear Ni(II) complex as host. The host-guest complexes are structurally well characterized. Structural analysis show that like earlier, the guest amine is recognized through multiple non-covalent interactions with host. Starting from L- and D-methionine, both the enantiomer, *R* and *S*-isomer of guests, **Am1** and **Am2** could be recognized and separated respectively. With the help of HPLC analysis, % of enatiomeric excess (*ee*) is determined in bulk crystals as well as in solution. The *ee* value (72-76%) in solution is reasonable, most likely due to presence of one additional C-H...π interaction through aromatic ring in guest with neighbouring host. After crystallization, 92-96 % *ee* value is obtained indicating overall resolution is contributed by both solution enhancement and crystallization.

Practicability of this method in separation of the foresaid amino alcohols is further checked by carrying out the reaction in large scale. Compare to existing resolution methods for these amino alcohols,[8] this method can be considered as one of the efficient method in the sense of easy design, synthesis and recovery. Inherent structural rigidity of the metal complexes leads to structural characterization of most of the host-guest adducts in the present case. This helps us to compare the common

structural motifs with other amino alcohol and identify the factors responsible for the recognition in next Chapter.

4.6 References

1. Das, C. R.; Sahoo, S.C.; Ray, M. *Cryst. Growth Des.* **2014**, *14*, 3958.
2. Sahoo, S.C.; Ray, M. *Chem. Eur. J.* **2010**, *16*, 5004.
3. (a) Inwang, E. E.; Mosnaim, A. D.; Sabelli, H. C. *J. Neurochem.* **1973**, *20*, 1469. (b) Shannon, H.E.; Degregorio, C. M. *J Pharmacol Exp Ther.* **1982**, *222*, 52. (c) Danielson, T. J. Boulton, A. A.; Robertson, H. A. *Journal of Neurochemistry* **1977**, *29*, 1131.
4. (a) Ahlquist, R. P.; *Am. J. Physiol.*, **1948**, *153*, 586.(b) Nisoli, E.; Tonello, C.; Landi, M.; Carruba, M. *Mol. Pharmacol.*, **1996**, *49*, 7.
5. (a) Axelrod, J.; *Pharmacol. Rev.*, **1966**, *18*, 95. (b) Ziegler, M. G.; Bao, X.; Ken-nedy, B. P.; Joyner, A.; Enns, R. *Ann N Y Acad Sci.*, **2002**, *971*, 76.
6. (a) Evans, D. A.; Chapman, K. T.; Bisaha, J. *J. Am. Chem. Soc.*, **1988**, *110*, 1238. (b) Tietze, L. F.; Montenbruck, A.; Schneider, C. *Synlett* **1994**, *509*, 34. (c) Daicel Chemical Industries Ltd. European Patent Application No. 0 654 534 A2, 1994.
7. L. S. Goodman, A. Gilman, *Goodman and Gilman's the pharmacological basis of therapeutics*, Vol.**9** (Eds.J. G. Hardman, L. E. Limbird,); McGraw-Hill: New York, **1996**.
8. (a) Lohse, O.; Spöndlin, C. *Organic Process Research & Development* **1997**, *1*, 247. (b) Tanielyan, S. K.; Marin, N.; Alvez, G.; Augustine, R. L. *Organic Process Research & Development* **2006**, *10*, 893. (c)Taniguchi, K.; Aruga, M.; Yasutake, M. and Hirose, T. *Org. Biomol. Chem.*, **2008**, *6*, 458. (d) Yang, K.;

Li, S. Z.; Wang, Y. H.; Zhang, W. Z.; Xu, Z. H.; Zhou, X.Y.; Zhu, R.X.; Luo, J. and Wan, Q. *RSC Adv.*, **2014**, *4*, 6517.

9. (a) Nakamoto, K. *Infrared and Raman Spectra of Inorganic and Coordination Compounds*, Part B, John Wiley & Sons, New York. (b) Earnshaw, A. *Introduction to Magnetochemistry*, Academic Press, London, **1968**. (c) Figgis, B. N.; lewis, J. *Prog. Inorg. Chem.*, Ed. F. A. Cotton, **1964**, *6*, 37. (d) Smith, A. S.; Fraser, C. L. in *Comprehensive Cordination Chemistry II*, 1, Ed. A. B. P. Lever, vol. 1, p. 1.
10. (a) Nishio, M.; Hirota, M.; Umezawa, Y. **1998** *The CH…π interaction;* Wiley-VCH: New York. (b) Desiraju, G.R.; Steiner, T.; **1999** in *The weak hydrogen bond*; Oxford University Press: New York. (c) Desiraju, G. R. *Acc. Chem. Res* **2002**, *35*, 565.

Chapter - 5

Few more examples and identification of the factors

As in previous chapter, using methionine derived ligand we observed that chiral recognition of two important biogenic alcohols, **Am1** and **Am2**, could be achieved with more than 90% resolution. We decided to experiment with more amino alcohols to find out the general trend of recognition. In earlier report, using L-histidine derived ligand, chiral recognition and resolution of two amino alcohols, 1-amino-2-propanol, 2-amino-1-propanol, was achieved with 90-100% *ee*.[1]

In this chapter, we intend to study of recognition of three amino alcohols, 1-amino-2-propanol (**Am3**), 2-amino-1-propanol (**Am4**) and 2-amino-1-butanol (**Am5**), using L-methionine derived host following the same protocol from previous chapters (Figure 5.1). We then compared the structural features of all the isolated host-guest complexes.

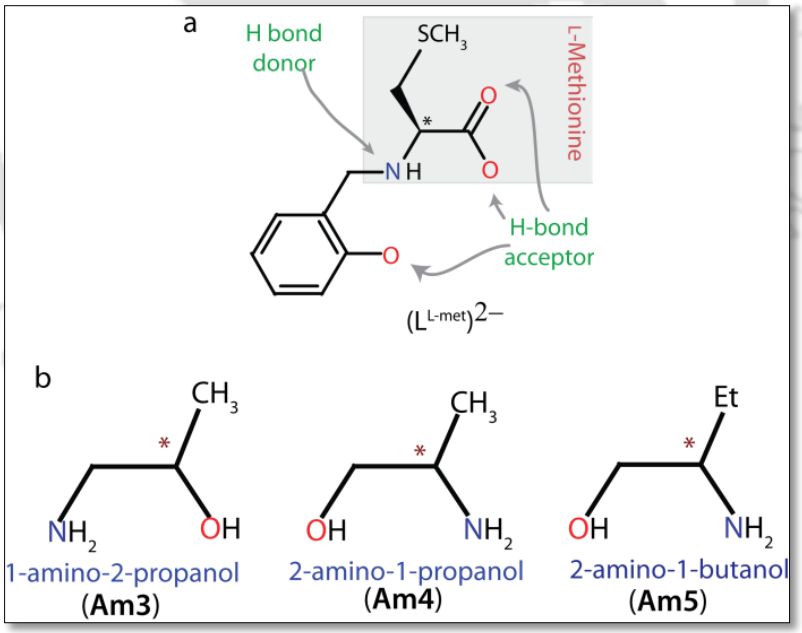

Figure 5.1 L-methionine derived ligand used in host (a) and the three amino alcohols as guest (b).

5.1 Material and Methods

5.1.1 Solvents and reagents

Details of the solvent purification and analytical measurements have already discussed in Chapter 2. 1-Amino-2-propanol, (*S*)-(+)-1-amino-2-propanol, (*R*)-(-)-1-amino-2-propanol, 2-amino-1-propanol, (*R*)-(-)-2-amino-1-propanol, (*S*)-(+)-2-amino-1-propanol, 2-amino-1-butanol, (*R*)-(-)-2-amino-1-butanol and (*S*)-(+)-2-amino-1-butanol were purchased from Aldrich Chemical Co. Ltd and used as received. The ligand $H_2L^{L\text{-met}}$ was prepared following previous procedure.[2]

5.1.2 Measurements

All the details of instrument used for analysis have already discussed in Chapter 2.

The crystals of complexes were mounted on glass fiber and on sealed quartz tube. All geometric and intensity data for the crystals were collected at room temperature using a Bruker SMART APEX CCD diffractometer equipped with a fine focus 1.75 kW sealed tube Mo-Ka (λ = 0.71073 Å) X-ray source, with increasing ω (width of 0.3º per frame) at a scan speed of either 3 or 5 s/frame. The SMART software was used for data acquisition and the SAINT software for data extraction. Absorption corrections were done using SADABS. After the initial solution and refinement with SHELXL, the final refinements were performed on WinGX environment using SHELX97. All non-hydrogen atoms in the complexes were refined anisotropically. Wherever possible, the hydrogen atoms were located from the difference Fourier maps and refined isotropically. Thus some of the C-H bonds will not be ideal and may vary. Some of C-C bonds have been restrained using DFIX, ISOR instruction in some complexes. One solvent molecule (methanol) is highly disordered in complex **2**.

Cataonic 2-amino-1-butanol in complex **4** is molded with positional disordered and treated with FVAR, PART command. Most of the hydrogen atoms attached to the solvent molecules could not be located or fixed, so the molecular weight may not match. Crystallographic data and details of refinements are listed in Table 5.1, and selected bond distances and angles are listed in Table 5.2. Perspective views of the complexes are shown using ORTEP.

5.2 Syntheses

5.2.1 ((*S*)-1-Ammonium-2-propanol)[$Ni_2(L^{L\text{-met}})_2(OAc)$] (1). The ligand $H_2L^{L\text{-met}}$ (0.200 g, 0.78mmol) and $Ni(OAc)_2.4H_2O$ (0.194 g, 0.78mmol) were mixed in 8 mL MeOH and kept stirring. After 15min, to the resulting bluish green solution racemic 1-amino-2-propanol (0.117 g, 1.56mmol) was added obtaining a blue solution. After 1h stirring, the resulting blue solution was kept for slow evaporation in room temp. Blue plate shaped crystals were obtained after 3 days. The crystals were filtered, washed with acetonitrile, dried in vacuum. Yield: 75%. Anal. Calcd. for [$Ni_2(C_{26}N_2S2O_8H_{33})(C_3NOH_{10})$].$4H_2O$: C, 41.97; H, 6.19; N, 5.06; found C, 41.47; H, 6.37; N, 5.19; IR (KBr, cm-1): $\upsilon(COO)_{asym}$ 1579 (s), $\upsilon(COO)_{sym}$ 1477 (m). μ_{eff} (powder, 298K)/Ni: 2.68 μB. Λ_M (ohm^{-1} cm^2 mol^{-1}): 31 (MeOH).

5.2.2 ((*S*)-2-Ammonium-1-propanol)[$Ni_2(L^{L\text{-met}})_2(OAc)$] (2). This is synthesized by following the same procedure as **1** using racemic 2-amino-1-propanol instead of racemic 1-amino-2-propanol. Blue plate shaped crystals were obtained after 5days by slow evaporation at room temperature from methanolic solution. The crystals were filtered, washed with acetonitrile, dried in vacuum. Yield:80%. Anal. Calcd. for [Ni_2 $(C_{26}N_2S2O_8H_{33})(C_3NOH_{10})$].$2CH_3OH.H_2O$: C, 44.32; H, 6.36; N, 5.00; found C,

45.01; H, 5.87; N, 4.99; IR (KBr, cm-1): $\upsilon(COO)_{asym}$ 1570 (s), $\upsilon(COO)_{sym}$ 1472 (m). μ_{eff} (powder, 298K)/Ni: 2.71 µB. Λ_M (ohm^{-1} cm^2 mol^{-1}): 35 (MeOH).

5.2.3 ((*R*)-2-Ammonium-1-propanol)[$Ni_2(L^{L\text{-}met})_2(OAc)$] (3). This was synthesized following the same procedure as **2** using pure (*R*)-2-amino-1-propanol instead of racemic-2-amino-1-propanol. The rod shaped crystals were obtained after 8days. The crystals were filtered, washed with acetonitrile, dried in vacuum. Yield:70%. Anal. Calcd. for $[Ni_2(C_{26}N_2S2O_8H_{33})(C_3NOH_{10})].4H_2O.CH_3OH$: C, 41.80; H, 6.43; N, 4.87; found C, 42.07; H, 6.27; N, 4.89; IR (KBr, cm-1): $\upsilon(COO)_{asym}$ 1575 (s), $\upsilon(COO)_{sym}$ 1473 (m). μ_{eff} (powder, 298K)/Ni: 2.72 µB. Λ_M (ohm^{-1} cm^2 mol^{-1}): 51 (MeOH).

5.2.4 ((*R*+*S*)-2-Ammonium-1-butanol)[$Ni_2(L^{L\text{-}met})_2(OAc)$](4). The ligand $H_2L^{L\text{-}met}$ (0.200 g, 0.78mmol) and $Ni(OAc)_2.4H_2O$ (0.194 g, 0.78mmol) were mixed in 8 mL MeOH and kept for stirring. After 15min, racemic 2-amino-1-butanol (0.139g, 1.56mmol) was added to the resulting green solution and stirred for 1h. The blue diamond shaped crystals were obtained from the methanolic solution after few days at room temperature. The crystals were filtered, washed with acetonitrile, dried in vacuum. Yield: 50%; Anal. Calcd. for $[Ni_2(C_{26}N_2S_2O_8H_{33})(C_3NOH_{10})]$ $.2H_2O$: C, 44.60; H, 6.11; N, 5.20; found C, 45.00; H, 5.87; N, 5.09; IR (KBr, cm^{-1}): $\upsilon(COO)_{asym}$ 1570 (s), υ(COO)sym 1467 (m). μ_{eff} (powder, 298K)/Ni: 2.73 µB. Λ_M (ohm^{-1} cm^2 mol^{-1}): 40 (MeOH).

5.2.5 ((*S*)-2-Ammonium-1-butanol)[$Ni_2(L^{L\text{-}met})_2(OAc)$](5). This was synthesized following the same procedure as **4** using pure (*S*)-2-amino-1-butanol instead of racemic-2-amino-1-butanol. The block shaped crystals were obtained after 2days from

4mL methanolic solution. The crystals were filtered, washed with acetonitrile, dried in vacuum.Yield:77%. Anal. Calcd. for $[Ni_2(C_{26}N_2S_2O_8H_{33})(C_4NOH_{12})].H_2O$: C, 45.61; H, 6.00; N, 5.32; found C, 45.01; H, 6.36; N, 5.63; IR (KBr, cm^{-1}) $\upsilon(COO)_{asym}$1592(s), $\upsilon(COO)_{sym}$1470(m), 1560(m). μ_{eff} (powder, 298K)/Ni: 2.70 μB; Λ_M (ohm^{-1} cm^2 mol^{-1}): 43 (MeOH).

5.2.5 ((*R*)-2-Ammonium-1-butanol)[$Ni_2(L^{L\text{-}met})_2(OAc)$](6). This was synthesized following the same procedure as **4** using pure (*R*)-2-amino-1-butanol instead of racemic-2-amino-1-butanol. A blue crystalline solid was obtained after complete evaporation of solvent. The solid was washed with acetonitrile-diethylether (v/v, 1:3), dried in vacuum. Yield: 82%. Anal. Calcd. for $[Ni_2(C_{26}N_2S_2O_8H_{33})(C_4NOH_{12})].3H_2O$: C, 43.62; H, 6.22; N, 5.09; found C, 43.42; H, 6.35; N, 5.13; IR (KBr, cm^{-1}) $\upsilon(COO)_{asym}$1582(s), $\upsilon(COO)_{sym}$1472(m), 1563(m). μ_{eff} (powder, 298K)/Ni: 2.72 μB; Λ_M (ohm^{-1} cm^2 mol^{-1}): 63 (MeOH).

5.3 Estimation of enantiomeric separation through HPLC.

Chiral amines were extracted from reaction mixture and extent of chiral separation was measured through HPLC using Chiralcel OD-H column attached with UV detector at a flow-rate of 1mL /min. Hexane and isopropanol in 93:7 ratio was used as eluant. The extraction procedure and organic derivative preparation (necessary for HPLC) were described in Chapter 3 in details.

The bound amino alcohols as ammonium have been recovered from (a) the crystal of host-guest adduct (b) amorphous solid of host-guest adduct following the similar procedure followed by derivatization with benzoyl chloride for HPLC analysis described in Chapter 3 (Section 3.3.1 – 3.3.3).

5.4 Result and Discussion

5.4.1 Syntheses and isolation host-guest complexes

Synthesis of complexes **1** to **5** having the general formula, $(R\text{-}NH_3)[Ni_2(L^{L\text{-}met})_2(OAc)]$, where $R\text{-}NH_3^+$ is the guest amino alcohols (**Am3**, **Am4**, **Am5**), has been carried out directly from the reaction between ligand ($H_2L^{L\text{-}met}$), $Ni(OAc)_2.4H_2O$ and appropriate isomer of respective amino alcohols at room temperature (Scheme 5.1).

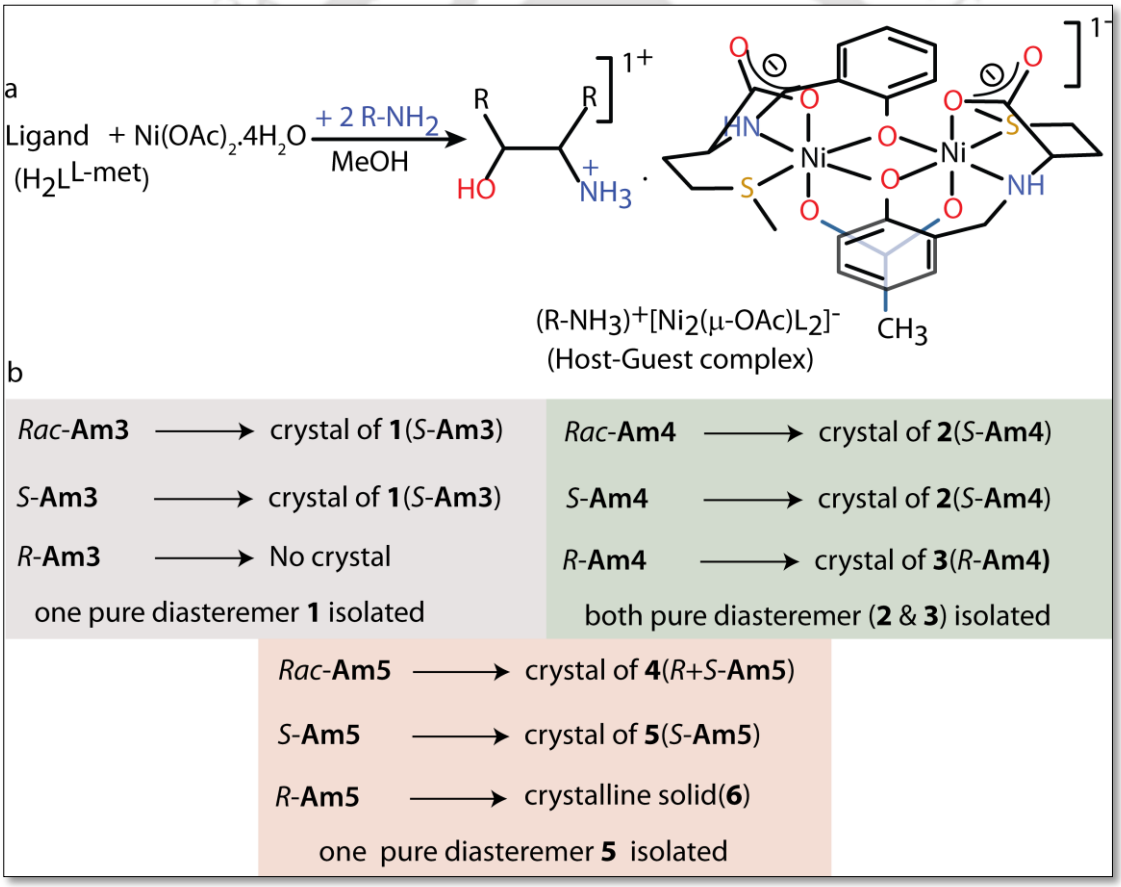

Scheme 5.1 Schematic representation of syntheses of host-guest adducts (a), the flow chart representing isolation of complexes from enatiopure amine and racemic amine (b).

The reaction of $H_2L^{L\text{-}met}$, $Ni(OAc)_2$ and the guest (**Am3**), racemic-1-amino-2-propanol or (*S*)-1-amino-2-propanol ((***S***)-**Am3**) yielded plate shaped crystals of complex **1** from the slow evaporation of methanolic solution at room temperature. To

synthesize other diastereomer from pure (*R*)-1-amino-2-propanol, ((*R*)-**Am3**) a blue glassy compound was obtained instead of crystal or crystalline solid. By following the identical protocol, from the reaction with other guest (**Am4**), racemic-2-amine-1-propanol or pure (*S*)-2-amine-1-propanol ((*S*)-**Am4**), plate shaped crystals of complex **2** were obtained. Unlike **Am3**, other diastereomer, complex **3,** with pure *R*-isomer ((*R*)-**Am4**) of **Am4** under same condition had been isolated as rod shaped crystal. Similarly, the diamond shaped crystals of complex **4** had been obtained from the reaction of ligand, Ni(II) acetate and guest, racemic -2-amino-1-butanol (**Am5)**. For synthesizing of diastereomeric pair, two separate reaction (Equation 1) had been carried out with pure *S*-isomer, ((*S*)-**Am5)** and *R*-isomer, ((*R*)-**Am5)** of **Am5** yielding blue block shaped crystals of complex **5** and a blue crystalline solid of complex **6** instead of single crystal respectively. The complexes were further characterized using FTIR, elemental analysis, magnetic susceptibility measurement and conductance. Data are commensurate with previous data.[1, 2, 3]

5.4.2 Molecular Structure of complex 1

The complex **1** is crystallized in $P3_1$ space group. In molecular structure of **1**, The asymmetric unit consists of anionic binuclear moiety $[Ni_2(L^{L\text{-}met})_2(OAc)]^{1-}$, cation of (*S*)-(-)-1-ammonium-2-propanol and four water molecules as solvent of crystallization. Like all previous complexes in Chapter 4, the anionic binuclear moiety as host is C_2 symmetric and remains similar type of octahedral geometry around Ni(II) centre from the aspects of bond length and bond angle (Table 4.2 and Figure 5.2a). The guest amine is oriented above the cleft formed by two parallel alignments of carboxylate group and two phenyl groups in the

binuclear complex and recognized by host through multiple non-covalent interactions.

Two out of three ammonium NH (N2) of cationic guest, (*S*)-**Am3** are H-bonded to this carboxylate oxygen O1 and O1A. The third NH (N2), a terminal carboxylate O2A and solvent molecules form an H-bonded network. The alcoholic O6 is H-bonded to another terminal carboxylate O2 (Figure 5.2a) and solvent molecules to form an H-bonded network. Three dimensional orientation of guest amine in cationic form brought C17, next to chiral carbon centre, in such a way that one inter molecular C(17)-H...π (4.015 Å) interaction with neighbouring host is present. Further, positions of two neighbouring host at left and right side of guest amine are such chiral carbon centre, C16(H) and next to chiral centre C15(H) are in shorter distance (3.703 Å & 3.540 Å) with C3A of one neighbouring host and C6 of another neighbouring host respectively (Figure 5.2b). Two terminal carboxylate oxygen atoms (O2 & O2A) form strong intermolecular H-bonding with N atom (N1A & N1) of amine of two neighbouring hosts (Table 5.3). Inside the crystal lattice, one water molecule shows tetrahedral H-bonding with two water and two terminal carboxylate oxygen participating in formation of one pseudo water chain intervening by guest amine (Figure 5.2c). The best compatibility of *S*-isomer of **Am3** over *R*-isomer in the aspect of well fitting and conformation inside the cleft of host may effect in formation of one diastereomer absolutely after crystallization.

The crystallographic parameter of the crystal, obtained from the reaction with (*S*)-1-amino-2-propanol is exactly same with the crystal obtained from reaction with racemic-1-amino-2-propanol. So, we have considered both the crystals as complex **1** and structural features have been discussed above.

Table 5.1. Crystallographic data and refinement parameters of complexes.

	1	**2**	**3**	**4**	**5**
empirical formula	$C_{29}H_{43}N_3Ni_2O_{13}S_2$	$C_{30.76}H_{46}N_3Ni_2O_{12.57}S_2$	$C_{30}H_{47}N_3Ni_2O_{13.71}S_2$	$C_{30}H_{34}N_3Ni_2O_{10.13}S_2$	$C_{29.77}H_{45}N_3Ni_2O_{9.04}S_2$
fw	823.16	840.40	850.57	780.18	771.00
T (K)	296(2)	296(2)	296(2)	296(2)	296(2)
wavelength (A°)	0.71073	0.71073	0.71073	0.71073	0.71073
crystal system	Trigonal	Trigonal	Trigonal	Hexagonal	Hexagonal
space group	*P3₁*	*P3₂*	*P3₁*	*P6₅*	*P6₅*
a, A°	10.6436(4)	10.6614(1)	10.6502(2)	10.6539(2)	10.6827(1)
b, A°	10.6436(4)	10.6614(1)	10.6502(2)	10.6539(2)	10.6827(1)
c, A°	28.605(3)	28.9499(8)	31.5381(9)	55.573(2)	55.3396(14)
V, Å ^{3}	2806.4(4)	2849.75(11)	3098.00(17)	5462.8(3)	5469.3(2)
z/ρ	3/1.461	3/1.469	3/ 1.368	6/1.423	6/1.405
μ	1.181	1.164	1.074	1.204	1.199
coll.reflns	12859	8222	8487	6673	4478
indep reflns	11268	7217	6693	6086	4314
FLACK para.	0.009(5)	0.024(9)	0.041(16)	0.029(16)	0.031(16)
GOF	1.001	1.029	0.989	1.110	1.143
R1 [a]	0.0292	0.0360	0.0586	0.0517	0.0365
wR2 [a]	0.0670	0.0772	0.1371	0.1144	0.0819
R1[b]	0.0366	0.0441	0.0716	0.0579	0.0389
wR2[b]	0.0698	0.0804	0.1417	0.1186	0.0828

[a] $I > 2\sigma$. [b] All data

Table 5.2 Selected bond distances (Å) and angles (°) of Complexes.

	1	**2**	**3**	**4**	**5**
Ni1 -O1	2.059	2.073	2.4285	2.0792	2.0720
Ni1-O3	2.046	2.040	2.0486	2.0395	2.0519
Ni1-O3A	2.039	2.056	2.0184	2.0448	2.0254
Ni1-O4	2.062	2.094	2.0537	2.0225	2.0295
Ni1-N1	2.084	2.068	2.0629	2.0629	2.0901
Ni1-S1	2.460	2.449	2.4285	2.4335	2.4437
Ni2- O1A	2.087	2.092	2.0760	2.0745	2.0897
Ni2-O3	2.045	2.021	2.0404	2.0282	2.0427
Ni2-O3A	2.046	2.048	2.0550	2.0372	2.0338
Ni2-O5	2.033	2.059	2.0362	2.0486	2.0250
Ni2-N1A	2.062	2.062	2.0697	2.0795	2.0631
Ni2-S1A	2.437	2.437	2.4597	2.4437	2.4349
N1-Ni1-S1	88.63	89.78	89.85	89.08	89.95
O3-Ni1-O3A	94.49	82.27	90.36	93.37	81.78
N1- Ni1-O1	80.00	80.66	79.80	80.86	79.93
S1-Ni1-O4	89.04	89.69	92.37	89.73	90.47
O1-Ni1-O4	176.89	175.46	171.53	172.45	176.01
N1A-Ni2-S1A	89.92	89.15	88.64	89.14	89.40
O3A-Ni2-O3	82.18	82.92	81.99	81.99	81.80
N1A-Ni2-O1A	80.24	80.85	88.64	80.19	80.54
S1A-Ni2-O5	90.41	90.74	87.36	90.21	88.86
O1A-Ni2-O5	169.82	171.14	176.09	176.13	172.20

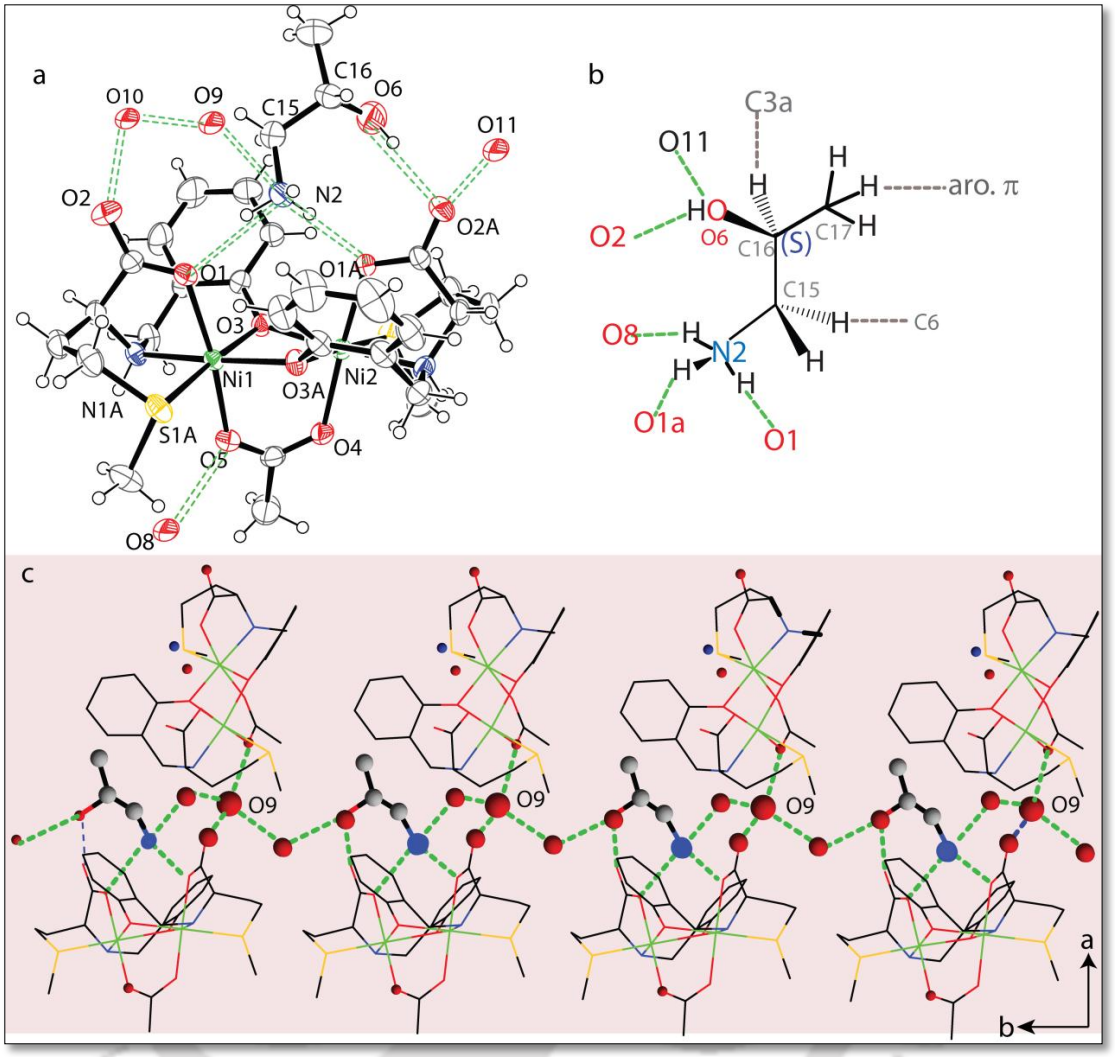

Figure 5.2 ORTEP diagram of complex **1** (a), schematic representation of recognition site of guest (*S*)-**Am3** (b) and crystal lattice of **1** (c).

5.4.3 Molecular structure of complexes 2 and 3

The complex **2** and complex **3** are solved with $P3_2$ and $P3_1$ space group respectively (Table 5.1). Upon strutural analysis, **2** and **3** are diastereomers with each other containing (*S*)-2-amino-1-propanol ((*S*)-**Am4**) and (*R*)-2-amino-1-propanol ((*R*)-**Am4**) as cationic guest in molecular structure of host-guest complex respectively.

In **2**, two NH(N2) of $-NH_3^+$ group of the guest amine (*S*)-**Am4** is strongly H-bonded with carboxylate, O1 & O1A in host and third N(H) form H-bonding with terminal carboxylate O2 by interveining one water molecule (Figure 5.3a). One

notable observation is that –OH group of guest is engaged in strong H-bonding with N(N1) and O (O4) of bridged acetate of neighbourimg host through one water molecule instead of intra-molecuar H-bonding with terminal carboxylate. Due to flexibile nature of guest, the spatial orientation of (*S*)-**Am4** may help in formation of such intermolecular H-bonding where guest amine acts as a bridge of H-bonding between two host. One side terminal carboxylate oxygen, O2 form inter-molecualr H-bonding with N1 of amine in neighbouring host.

Unlike **2**, guest amine, (*R*)-**Am4**, in **3**, is recognized by host by formation of intra molecular H-bonding through two NH of $-NH_3^+$ group with two intermediate carboxylate oxygen (O1 & O1A) and –OH group with one terminal carboxylate oxygen(O2). Further, O2 is engaged in intermolecular H-bonding with N1A of neighbouring host (Figure 5.3c).

If we consider difference in other non-covalent interactions between two diastereomers, in **2**, one extra intra-molecular C(17)-H...π interaction (3.624 Å) present with the aromatic ring which is not present in other diastereomer **3** (Figure 5.3c). The chiral carbon atom C15(H) of guest amine in **2**, is also in shorter distance (3.794 Å) with C14 of neighbouring host. These differences in non-covalent interactions may help in recognition of *S*-isomer over *R*-isomer from racemic mixture.

Like complex **1**, the crystallographic parameter of the crystal obtained from the reaction with (*S*)-2-amino-1-propanol is exactly same with the crystal obtained from reaction with pure racemic-2-amino-1-propanol. So, we have considered both the crystals as complex **2** and structural features have been discussed above.

Table 5.3 Distances (Å) of H-bonding and other interactions present in complexes.

	D-H···A	D-H (Å)	H···A (Å)	D···A (Å)	DHA (°)		D-H···A	D-H (Å)	H···A(Å)	D···A(Å)	DHA(°)
1	Direct Host-Guest interaction					**2**	Direct Host-Guest interaction				
	N2-H4A...O1	0.89	1.85	2.729	168		N2 –H3C...O1	0.89	1.87	2.754	169
	N2- H4B...O1A	0.89	1.91	2.780	166		N2 –H3B...O1A	0.89	1.99	2.803	152
	N2- H4C...O10*	0.89	2.16	2.856	134		N2 –H3A...O6	0.89	2.43	2.758	102
	O6- H9...O2	0.82	1.93	2.739	171		N2 –H3A...O8*	0.89	2.41	3.011	125
	NH_3^+…. π	-	-	3.909			NH_3^+…. π	-	-	3.850	-
	Other non-covalent interactions						C17 – H29C…π	0.96	3.33	3.989	127
	N1A -H2...O2	0.91	2.23	3.081	154		C15 – H28B…O2	0.97	2.46	3.402	160
	N1- H1...O2A	0.91	2.23	3.054	150		Other non-covalent interactions				
	C9A- H15...O1	0.93	2.57	3.239	129		N1A –H1A...O2	0.96	2.19	2.995	147
	C5A- H24C...O2	0.96	2.47	3.428	173		N1 –H1...O6*	0.91	2.26	3.051	145
	C17- H30B...O8	0.96	2.50	3.386	153		C5 – H5Y… π	0.96	3.14	3.813	129
	O2A- O9*			2.724			C20 – H20… π	0.90	2.51	3.429	167
	O6- O11*			2.888			C5A– H26C…O2	0.96	2.56	3.511	170
	O5- O8*			3.241			C3A- H19B …O2	0.97	2.53	3.371	145
3	Direct Host-Guest interaction					**4**	Direct Host-Guest interaction				
	N2 –HY...O1	0.89	1.91	2.745	154		N2A...O1	-	-	2.854	-
	N2 –HZ...O1A	0.89	1.94	2.796	161		N2A…O1A	-	-	2.642	-
	N2 –HX...O7	0.89	2.09	2.897	150		N2B...O1	-	-	2.758	-
	O6- H6...O2A	0.82	1.87	2.698	169		N2B...O1A	-	-	2.837	-
	NH3+…. π	-	-	3.982			O6A...O2A	-	-	2.738	-
	Other non-covalent interactions						O6B...O2				
	N1A -H2...O2A	0.91	2.19	2.979	144		Other non-covalent interactions				
	O6- O12*	-	-	2.810	-		N1A –H4...O2A	0.91	2.20	3.030	144
	O2- O7*	-	-	2.856	-		O6A...O8*	-	-	3.008	-
	O2- O9*	-	-	2.702	-		O6B...O8*	-	-	2.998	-
5	Direct Host-Guest interaction						Other non-covalent interactions				
	N2 –H2A...O1	0.89	1.85	2.713	163		N1A –H1A...O2	0.91	2.24	3.049	149
	N2 –H2B...O1A	0.89	1.89	2.756	164		N1 –H1...O2A	0.91	2.38	3.236	158
	O6…O2	-	-	2.709	-		C6A…O2			3.479	
	NH_3^+…. π	-	-	4.035			C5A…O2			3.516	
							C5…O2A			3.333	

* solvent molecule

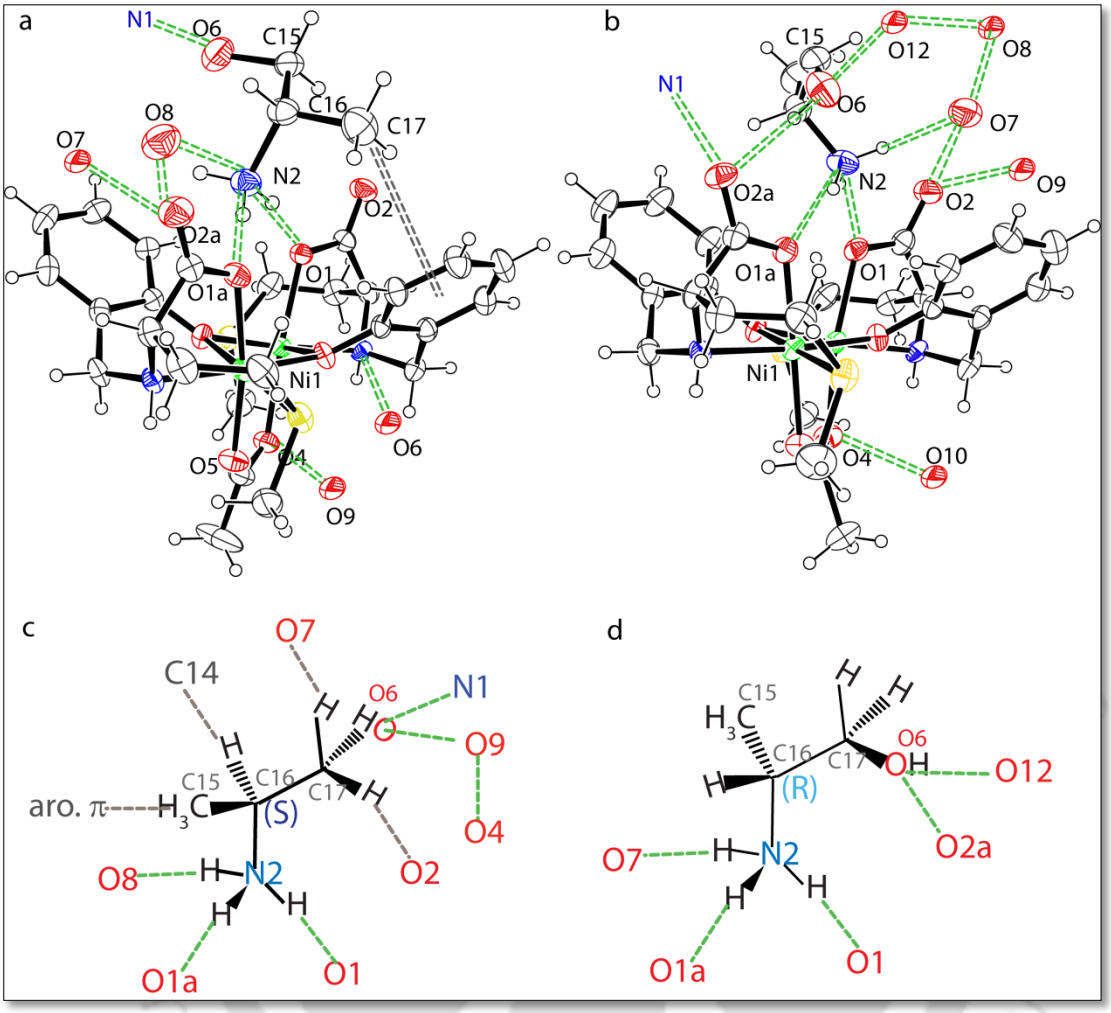

Figure 5.3 ORTEP diagram of complex **2** and **3** with 40% ellipsoid probability (a, b) and Schematic representation of recognition site of guest (*S*)-**Am3** and (*R*)-**Am3** (b, c).

5.4.4 Molecular structure of complexes 4 and 5

Structural analysis reveals that both the complex **4** and **5** are crystalized in $P6_5$ space group (Table 5.2). Like all previous complexes, the asymetric unit of both consist of anionic binuclear moiety $[Ni_2(L^{L\text{-}met})_2(OAc)]^{1-}$, cationic guest amine in ammonium form and few solvent molecule as solvent of crystalization. In the molucular structure of complex **4** obtained from the reaction with racemic 2-amino-1-butanol (Section 5.4.1), the guest amine, **Am5** is highly positional disordered remaining other parts are as it was. The disordered cation was modeled and refined

using PART and free variable (FVAR) options. The model fits well with 55:45 ratio of *S* and *R* enantiomer of the chiral cation respectively (Figure 5.4b) as observed in case of guest 1-phenylethyl amine described in Chapter 2 (Section 2.4.5).[4] Both isomer of disorder amine is H-bonded with one host through–NH_3^+ and –OH group with carboxylate oxygen of host (Figure 5.4c & d). One side inter-molecular H-bonding between terminal carboxylate O2 and N1 of amine in neighboring host is also observed.

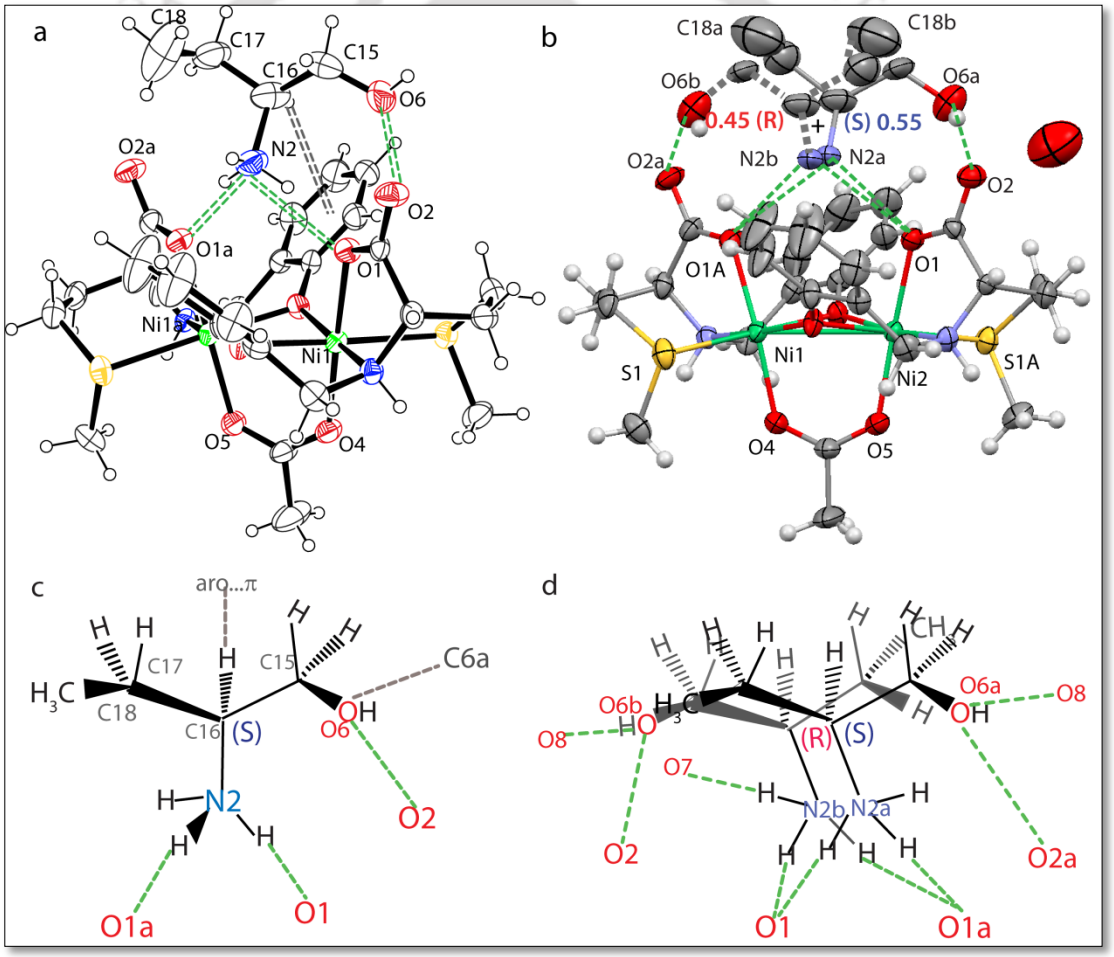

Figure 5.4 ORTEP diagram of complex **4** and **5** with 40% ellipsoid probability (some solvent molecules removed for clarity (a, b) and Schematic representation of recognition site of guest (*S*)-**Am3** and (*R*)-**Am3** (c, d).

In the pure diastereomer **5**, (*S*)-**Am5** is recognized by H-bonding of two groups, –NH_3^+ and –OH around chiral carbon centre, with carboxylate oxygen in host. An additional very weak C(18)-H...π interaction (4.120 Å) with aromatic ring of another host is present as third point of interaction around chiral carbon centre (Figure 5.4a & c). From syntheses section we observed other pure diastereomer **6** with *R*-isomer could be isolated as crystalline solid instead of crystal. So, the structural characterization and comparison of complex **6** is now out of our scope.

5.4.5 Powder X-Ray diffraction analysis

Along with other characterizations, the complexes are futher characterized by Powder X-Ray diffraction experiment (Figure 5.5). The experimental diffraction pattern for complex **1** match with the simulated pattern (obtained from single crystal

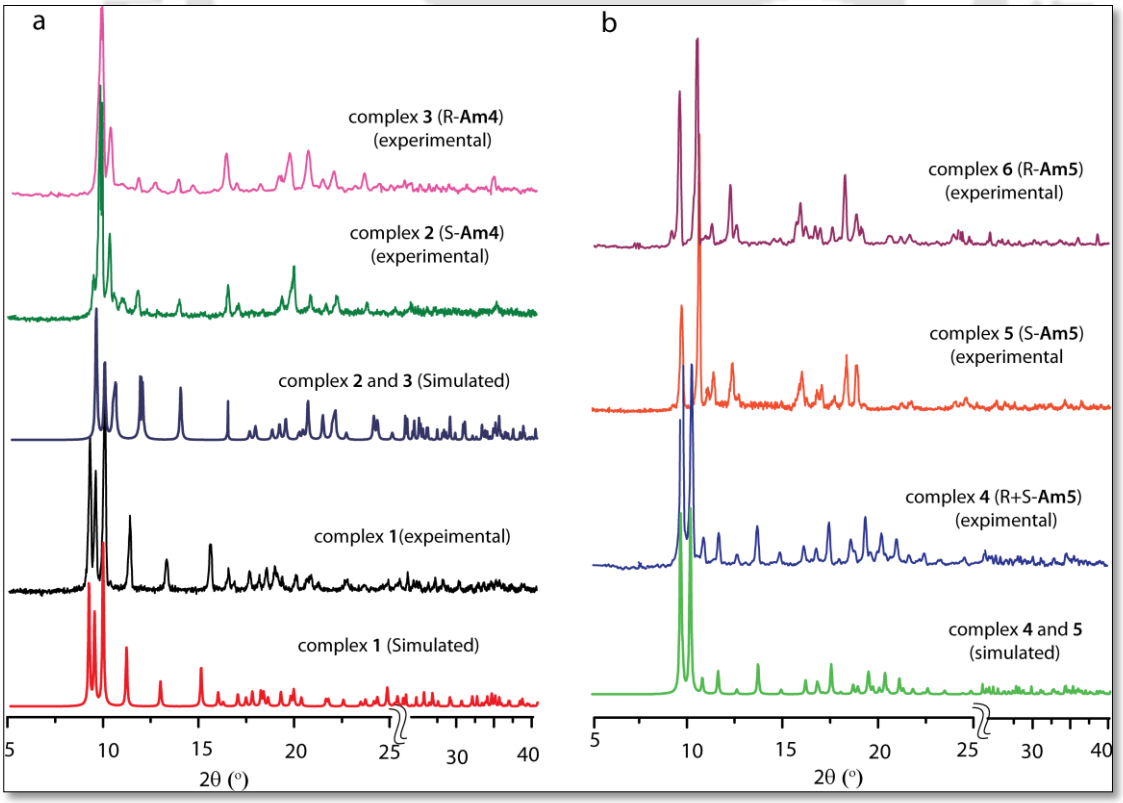

Figure 5.5 Powder X-ray Diffraction patterns of complexes (corresponding naming with respect to complex given).

X-ray diffraction using Mercury software) with good agreement. The diffraction pattern of both diastereomers with guest **Am4**, complex **2** and **3** are almost similar with each other remaning different from the simulated pattern in terms of position and intensity of peak. In case of guest **Am5**, single crystal of only one pure diastereomer with (*S*)-**Am5**, complex **5**, is obtained, where as other diastereomer with pure (*R*)-**Am5**, complex **6**, could be obtained as crystalline solid instead of single crystal even after attaining many attempts. So, with the help of PXRD experiment, crystaline nature of complex **6** is checked and compared with complex **5** showing almost similar diffraction pattern. Diffraction pattern of complex **4**, crystals isolated from racemic-**Am5**, is different from complex **5** and **6**, but quite match with simulated pattern (Figure 5.5b).

5.4.6 Chiral enahancement determined by the HPLC

By following the similar protocol for recovery of bound amine from host-guest complexes described in Chapter 3, the recovered guest amino alcohols from all complexes in either crystals or amorphous solid, are derivatized with benzoyl alcohol to amide for HPLC run to estimate the ratio of distribution of *R* and *S* isomer in bulk crystals or bulk precipitation i.e., enantiomeric excess (*ee*) value. %*ee* values obtained from rapid precipitation of complexes without crystallization are considered as chiral distribution present in the solution as in Chapter 4. The recovered amine from complex **3**, **5** and **6**, obtained from the reaction with enantiopure guest, serve as reference. HPLC results show that, in case of guest **Am3**, 98% *ee* of *S*-isomer present in bulk crystals whereas in solution equilibrium, chiral enhancement is only 20% of *S*-isomer (Table 5.4). From the bulk crystals of complex **2** and complex **4**, 70% *ee* of (*S*)-**Am4**

and 68% *ee* of (*S*)-**Am5** are observed. Chiral enhancement in solution remains 16% *ee* and 24% *ee* respectively which are comparable with **1**.

Table 5.4 Determination of % *ee* of amine present in either bulk crystals or amorphous solid by HPLC analysis.

Guest	% *ee*	R	S	Isolated yield (%)
Condition: Guest isolated from crystals				
*Rac-**Am3***	98	1	99	75
*Rac-**Am4***	70[2]	15	85	45
*Rac-**Am5***	68[2]	14	86	48
Condition: Guest isolated from amorphous precipitation				
*Rac-**Am3***	20	40	60	65
*Rac-**Am4***	16	42	58	57
*Rac-**Am5***	24	38	62	64

Thus, these indicate one diastereomer remains preferably in higher amount in solution, which is eventually recognized after crystallization showing high %*ee* (68-100%).

5.4.7 Comparison of crystal lattice and the solubility difference

HPLC results showed that the observed chiral enhancement is a result of both chiral enhancement in solution equilibrium and crystallization. From the structural analysis we observed that in case of guest **Am3**, *S*-isomer is recognized. Isolation of other pure diastereomer with pure *R*-isomer even as amorphous solid also could not be possible. *S*-isomer of **Am3** inside the cleft of host is more compatible than *R*-isomer so that high solubility difference between two diastereomer results formation of one diastereomer absolutely after crystallization.

From Chapter 2 and Chapter 3, we knew that along with the number of non-covalent interactions, special arrangement inside the crystal lattice of host-guest complex effects in solubility difference between two pure diastereomers. In case of

guest **Am4**, both the pure diastereomers from pure *S* and *R* isomer are isolated as crystals and from racemic-**Am4**, *S*-isomer is recognized. The structural analysis of both diastereomers unveils minor difference in crystal lattice between two diastereomers (Figure 5.6) resulting minor solubility difference between complex **2** and **3**. Upon checking, diastereomer with (*S*)-**Am4** is less soluble (23 mg/mL in acetonitrile) than the diastereomer with (*R*)-**Am4** (29 mg/mL). So, during crystallization process of the solution with racemic **Am4**, less soluble diastereomer **2** starts nucleation first and once nucleation starts, seeding became faster. Consequently, separate crystals of pure diastereomer, **2** and **3**, remain with 85:15 ratios after crystallization in bulk crystals which was confirmed by HPLC run.

As, in case of guest **Am5**, only one pure diastereomer with (*S*)-**Am5** is crystallized out, other diastereomer with pure (*R*)-**Am5** is isolated as crystalline solid instead of crystal, we could not be able to compare the crystal lattice between two diastereomer other than PXRD and solubility measurement. Solubility of **6** with (*R*)-**Am5** is much higher (36 mg/mL in acetonitrile) than solubility of **5** with (*S*)-**Am5 (**14 mg/mL in acetonitrile). Molecular structure of complex **4**, obtained from racemic-**Am5**, contain both *S* and *R* isomer. Due to positional disorder of cationic guest, major difference occurs in crystal lattice between **4** and **5**, (Figure 5.6) reflecting the higher solubility difference (for **4**: 32 mg/mL, **5**: 22 mg/mL in acetonitrile).

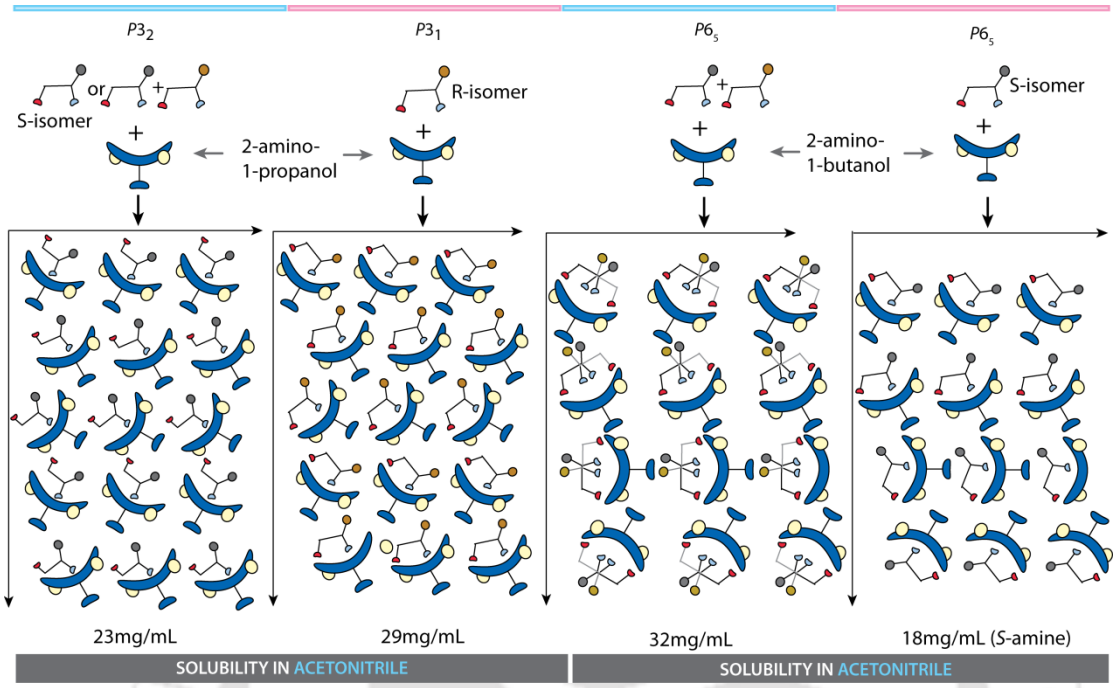

Figure 5.6 two-dimensional cartoon representation of the crystal lattices showing the differences and similarities between pure or racemic diastereomers obtained for two guest **Am4** and **Am5**.

5.5 Conclusions

In this chapter, we have attempted to rationalize effect of modification in the host using methionine derived ligand on the recognition behaviour of few amino alcohols which were already recognized by using histidine derived ligand. The major findings of this section are: (a) Indeed, recognition of amino alcohol is better than aryl amine. Due to the presence of –OH group in guest amino alcohol capable of strong H-bonding (Figure 5.7a & b), one diastereomer (lower energy) remains in solution preferably which is eventually recognized after crystallization. (b) In amino alcohols which are substituted with phenyl ring, because of the presence of one extra non-covalent C(H)...π with aromatic ring, chiral enhancement (>70% *ee*) in solution equilibrium is higher than the chiral enhancement (14 -24% *ee*) of amino alcohol which are not substituted with phenyl ring (Figure 5.7b & c).

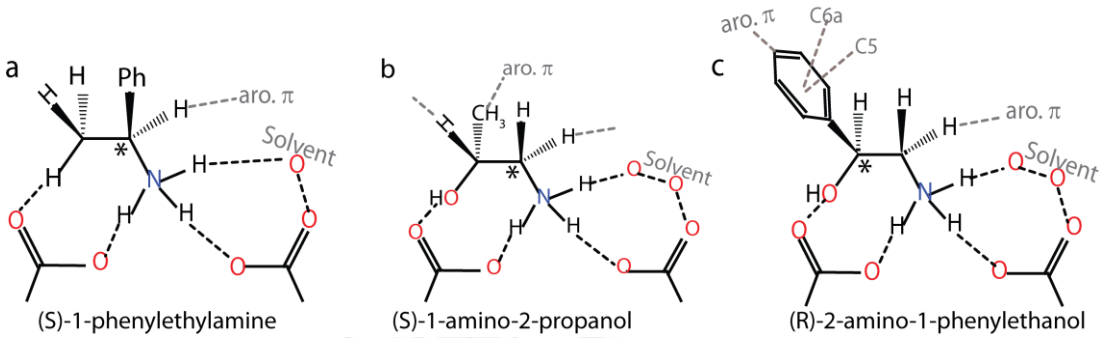

Figure 5.7 Recognition of amine and amino alcohols with methionine derived host

Other findings of this section are that (a) in case of 1-amino-2-propanol, *S*-isomer is recognized with comparable % of resolution (98% *ee*) to the earlier result (100% *ee*) remaining similar recognition site with anionic host (b) by changing the host, from racemic 2-amino-1-propanol, *S*-isomer is recognized over *R*-isomer with 70% *ee*. Structural analysis showed the recognition sites of guest are also changed from histidine analogue to methionine analouge. In histidine derived host, *R*-isomer guest amino alcohol was recognized over *S*-isomer from racemic mixture by H-bonding through $–NH_3^+$ and –OH with same host. But in case of methionine derived host, spatial orientation of guest is such that is $–NH_3^+$ and –OH group is not H-bonded with same host.

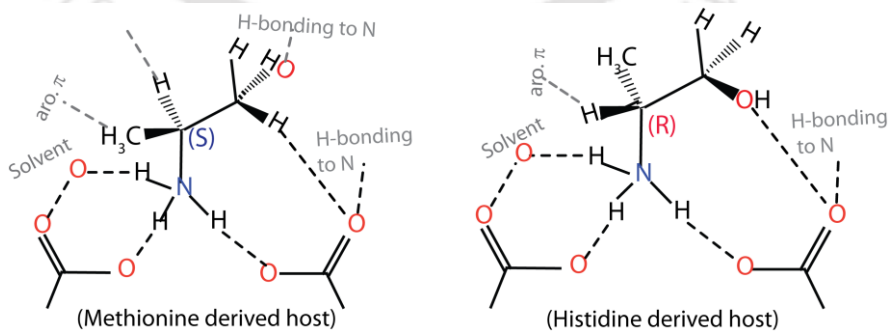

Figure 5.8 Similarity and difference in recognition of 2-amino-1-propanol with methionine and histidine derived ligand (recognized chirality was shown).

Also, there are other mere difference in other non-covalent interactions. These differences might have effected in the recognition of *S*-isomer over *R*-isomer from racemic mixture (Figure 5.8) (c) Although 2-amino-1-butanol is one higher carbon analogue of 2-amino-1-propanol, recognition behaviour through non-covalent interactions has been changed significantly, most likely, because of presence of bulkier –Et group instead of -Me group attached with chiral carbon.

5.6 References

1. Sahoo, S.C.; Ray, M. *Chem. Eur. J.* **2010**, *16*, 5004.
2. Alam, Md. A.; Koner, R. R.; Das, A.; Nethaji, M.; Ray, M. *Crystal Growth & Design*, **2007**, *7*, 1818.
3. (a) Nakamoto, K. *Infrared and Raman Spectra of Inorganic and Coordination Compounds*, Part B, John Wiley & Sons, New York. (b) Earnshaw, A. *Introduction to Magnetochemistry*, Academic Press, London, **1968**. (c) Figgis, B. N.; lewis, J. *Prog. Inorg. Chem.*, Ed. F. A. Cotton, **1964**, *6*, 37. (d) Smith, A. S.; Fraser, C. L. in *Comprehensive Cordination Chemistry II*, 1, Ed. A. B. P. Lever, vol. 1, p. 1.
4. (a) Das, C. R.; Sahoo, S.C.; Ray, M. *Cryst. Growth Des.* **2014**, *14*, 3958. (b) Li, Z. J.; Yao, J.; Tao, Q.;Jiang, L.; Lu, T.B. *Inorg. Chem.* **2013**, *52*, 11694.

FINDINGS OF THE THESIS

The work in this thesis stems from earlier observation on chiral recognition of two amino alcohol by formation of host-guest adduct of anionic binuclear Ni(II) host and cationic guest amine.[i] The guest amino alcohol was recognized through multiple non-covalent interactions. In literature, up-to our best knowledge, this was the first example for chiral recognition using such rigid inorganic chiral anionic host of amine and amino alcohols in ammonium form. But these two examples were not sufficient in understanding of the recognition process properly. Thus, we thought it is worth extending for other examples by systematic change in guest and host.

Therefore, at first we have put emphasize on recognition and separation of aryl amine instead of amino alcohol, lacking –OH group, capable of strong H-bonding using two Ni(II) metalloorganic host with L-histidine by isolation and structural characterization of host-guests adducts obtained from pure and racemic-amine. Then we have modified the host using L-methionine derived ligand in place of L-histidine. The results are described in Chapter 2 and Chapter 3. It is shown that recognition of guest by both host followed a general motif of interactions. Both the pure diastereomers structurally differs from each other only by presence/absence of very weak interaction e.g., CH…π, C-H…O etc. Being very weak in energy, estimation of individual contribution of each non-covalent interaction was difficult. To gain the essence of such interactions to some extend we intended to expand our experiment for few amino alcohol as guest having substituted aromatic ring which has scope for π…π or CH…π interaction with host. For that purpose, we had chosen two amino

alcohol, 2-amino-1-phenyethanol and norphenylephrine. These are also biologically important, endogenous trace amine, used as sympathomimetic drug.[ii] Along with successful resolution of two foresaid amino alcohol, recognition motif between host and guest was elucidated by structural analysis which is described in Chapter 4. Further, to compare (similarities and differences of recognition and resolution) with earlier observed result of L-histidine host, L-methionine host was utilized for recognition of three amino alcohols and the details are illustrated in Chapter 5. In the step wise proceeding, we ascertain some factors in recognition process which are mainly attributed to varied percentage of chiral resolution of amine and amino alcohols. These are discussed bellow as outcome of this thesis.

Amine vs. amino alcohols

Overall recognition and resolution of amino alcohols are better than aryl amine. Structural characterization of host-guest adducts showed that recognition of amino alcohol has occurred through two strong H-bonding of ammonium $-NH_3^+$ and -OH group as two point attachment and one weak interaction of C-H units by the host showing three point recognition. As 1-phenylethylamine is losing of one strong H-bonding interaction site, the recognition of amine was not happened properly through three point recognition with host. In the absence of an alcoholic group, less than three point of interaction reduced the energy difference between two diastereomers. As a result, both the diastereomers could be isolated as pure diastereomer from the reaction with pure amine as well as with racemic-amine (in L-methionine host). In amino alcohols, most of the cases only one diastereomer could be isolated from racemic amine, while other one could not be isolated as solid also even from pure amine.

Thus, the numbers of interaction site effects on chiral enhancement which is discussed in next section.

Solution enhancement vs. crystallization

In general, chiral enhancement is contributed by both solution enhancement as well as crystallization. Solution enhancement has been estimated by forced precipitation of host-guest adducts followed by isolation of guest and subsequent HPLC experiments. (i) In 1-phenylethylamine, using both hosts, the solution enhancement was negligible (0-4% *ee*). Thus the enhancement of 30% *ee*, observed after crystallization was primarily occurred during crystallization (Scheme 1). (ii) In amino alcohols, solution enhancement is widely varied between 14-70% *ee*. Curiously, two amino alcohols with phenyl ring showed much higher solution enhancement (70% *ee*) than the three amino alcohols without phenyl ring (15-25% *ee*). However, all amino alcohols showed higher enhancement of 68-100% *ee* after crystallization compared to 1-phenylethylamine. Thus in case of amino alcohols, both solution enhancement and crystallization contributed to the final observed enhancement.

Solubility of diastereomers vs. chiral enhancement

Diastereomer solubility must have played an important role in chiral enhancement during crystallization. Three out of five amino alcohols, very high solubility of one of the diastereomer prevented its isolation as solid, even when attempted with pure enantiomer. With 1-phenylethylamine, using both host and 2-amino-1-propanol with methionine derived host, both diastereomers could be isolated and crystallized using pure enantiomer of the guest. Solubility of diastereomer pairs was measured and compared. When these were tested with racemic guest, the isolated host-guest adduct showed chiral enhancement of the diastereomer having the lower solubility. Thus in

almost all the case, diastereomer with lower solubility determined the chirality of the isolated amine.

Lattice organization vs. solubility

Connecting solubility with the lattice organization is somewhat possible considering wherever isolation of both pure diastereomers was possible. First one is 1-phenylethylamine with histidine host. The pure diastereomers obtained from *R*-amine and *S*-amine were crystallized in very different space group *R3* and $P2_12_12$ respectively. In the crystal lattice of diastereomer with *R*-amine, three molecules of host-guest adducts form a very compact triangular assembly through one strong inter-molecular H-bonding between imidazole N and carboxylate oxygen and one CH…π interaction. Whereas, two inter-molecular H-bonding between imidazole and carboxylate form 2D network having one dimensional channel along c-axis inside of crystal lattice of other diastereomer. This drastic difference in crystal lattice might be responsible for the huge solubility difference, almost double between two diastereomers. In case of methinine host for same amine, both the pure diastereomer had been crystallized out in same space group with similar host-guest organization in crystal lattice. The minor difference of crystal lattice resulted mere solubility difference between two diastereomer. Similar observation was found in recognition of 2-aminio-1-propanol by methionine derived host.

Amino alcohols with phenyl ring vs amino alcohols with phenyl ring

In amino alcohols which are substituted with phenyl ring, because of the presence of one extra intermolecular non-covalent C(H)...π interaction between aromatic ring and neighbouring host, chiral enhancement (>70% *ee*) in solution equilibrium is

higher than the chiral enhancement (14 -24% *ee*) of amino alcohol which are not substituted with phenyl ring. This might increased the rate of crystallization of less soluble diastereomer over other.

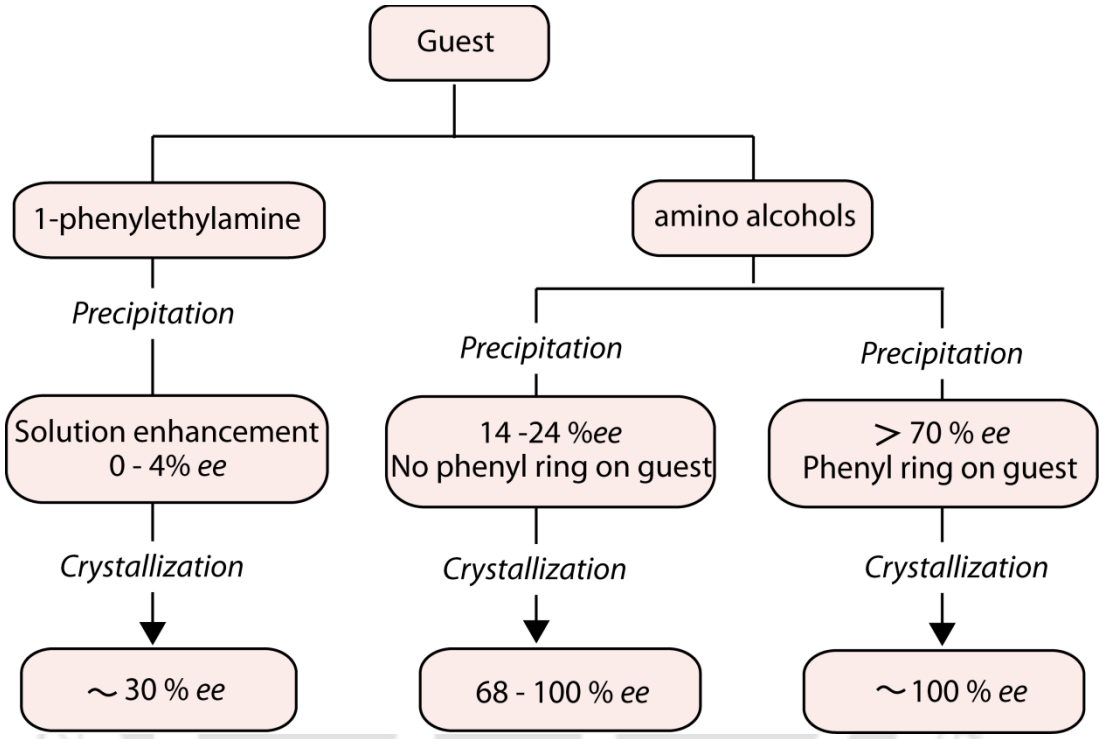

Scheme 1. Schematic representation of observations on chiral enhancement of amine and amino alcohols by two binuclear hosts.

Common interaction motifs

The enhancement during crystallization and solubility difference are presumably connected with inter-molecular networks formed in the crystals through non-covalent interactions. There are plenty of these present in each of these crystals. As the energy of stabilization of most of these interactions varies within a narrow range of 0.6 to 8 kcal/mole (on the higher side; OH...O, 5 - 7Kcal/mol, NH...O, 3 - 5Kcal/mole, rest of the interactions 0.6 - 2Kcal/mol), it is difficult to quantify and pinpoint the individual contribution to either solubility or chirality. However, comparison of host-guest

interactions in all the structure showed recurrence of similar pattern of recognition, where all four oxygen of the two carboxylate and at least one of the aromatic rings of the host is utilized for recognition of the guest (Figure 1). We categorized into three types. This is true for both the binuclear host. Out of fourteen structurally characterized host-guest complexes, six complexes have Type-I motif, six have Type-II motif and two complexes follow Type-III motif.

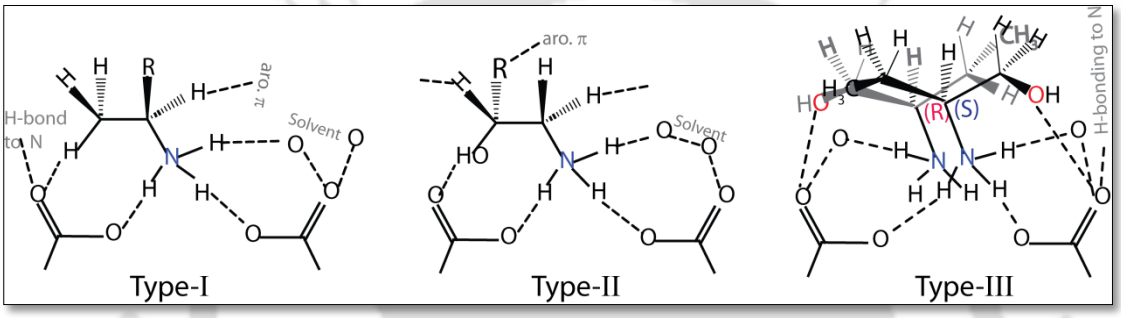

Figure 1. General motif of interactions present in host-guest complexes during recognition of guest amine and amino alcohol by two host.

Position of chiral centre in guest

In the thesis work, the amino alcohols were chosen to have chiral centre either near amine or near alcohol group. Curiously we observed, amino alcohols with chiral centre near alcohol group, seemed to show consistently better resolution (98-100% *ee*) compared to the ones with chiral centre near amine (68-90% *ee*). However, number of examples is still few thus difficult to make a generalization. This was just an observation.

---

[i] Sahoo, S.C.; Ray, M. *Chem. Eur. J.* **2010**, *16*, 5004

[ii] (a) Danielson, T. J. Boulton, A. A.; Robertson, H. A. *Journal of Neurochemistry* **1977**, *29*, 1131 (b) Macdonald, F. *Dictionary of Pharmacological Agents*. **1997**, CRC Press. p. 104.

List of Publications

1. Das, C. R.; Sahoo, S. C.; Ray, M., Chiral recognition and partial resolution of 1-Phenylethylamine through non-covalent interactions using binuclear Ni(II) complex as host. *Crystal Growth & Design* **2014**, *14*, 3958.

Manuscript to be submitted

2. Das, C. R.; Ray, M., Substitution of L-Histidine with L-Methionine in the Metalloorganic Host Causes Significant Changes in Crystallization Pathway during Chiral Resolution of 1-Phenylethylamine. *(resubmitted)*
3. Das, C. R.; Ray, M., Enantiomeric Separation of Biogenic amino alcohol Using Metalloorganic host. *(resubmitted)*
4. Das, C. R.; Ray, M., Findining the Factors Affecting the chiral Enhancement during Separation of Amine and Amino alcohols by Ni(II) Metalloorganic Host. *(manuscript Prepared)*